Dynamics and Control of Electric Power Systems

Lecture 227-0528-00, ITET ETH

Göran Andersson
EEH - Power Systems Laboratory
ETH Zürich

February 2012

Eidgenössische Technische Hochschule Zürich
Swiss Federal Institute of Technology Zurich

Contents

Preface

These lectures notes are intended to be used in the lecture *Dynamics and Control of Power Systems (Systemdynamik und Leittechnik der elektrischen Energieversorgung)* (Lecture 227-0528-00, D-ITET, ETH Zürich) given at ETH Zürich in the Master Programme of Electrical Engineering and Information Technology.

The main topic covered is frequency control in power systems. The needed models are derived and the primary and secondary frequency control are studied. A detailed model of the synchronous machine, based on Park's transformation, is also included. The excitation and voltage control of synchronous machines are briefly described. An overview of load models is also given.

Zürich, February 2012

Göran Andersson

1
Introduction

In this chapter a general introduction to power systems control is given. Some basic results from control theory are reviewed, and an overview of the use of different kinds of power plants in a system is given.

The main topics of these lectures will be

- Power system dynamics
- Power system control
- Security and operational efficiency.

In order to study and discuss these issues the following tools are needed

- Control theory (particularly for linear systems)
- Modelling
- Simulation
- Communication technology.

The studied system comprises the subsystems *Electricity Generation, Transmission, Distribution, and Consumption (Loads)*, and the associated control system has a hierarchic structure. This means that the control system consists of a number of nested control loops that control or regulate different quantities in the system. In general the control loops on lower system levels, e.g. locally in a generator, are characterized by smaller time constants than the control loops active on a higher system level. As an example, the *Automatic Voltage Regulator* (AVR), which regulates the voltage of the generator terminals to the reference (set) value, responds typically in a time scale of a second or less, while the *Secondary Voltage Control*, which determines the reference values of the voltage controlling devices, among which the generators, operates in a time scale of tens of seconds or minutes. That means that these two control loops are virtually de-coupled. This is also generally true for other controls in the systems, resulting in a number of de-coupled control loops operating in different time scales. A schematic diagram showing the different time scales is shown in Figure 1.1.

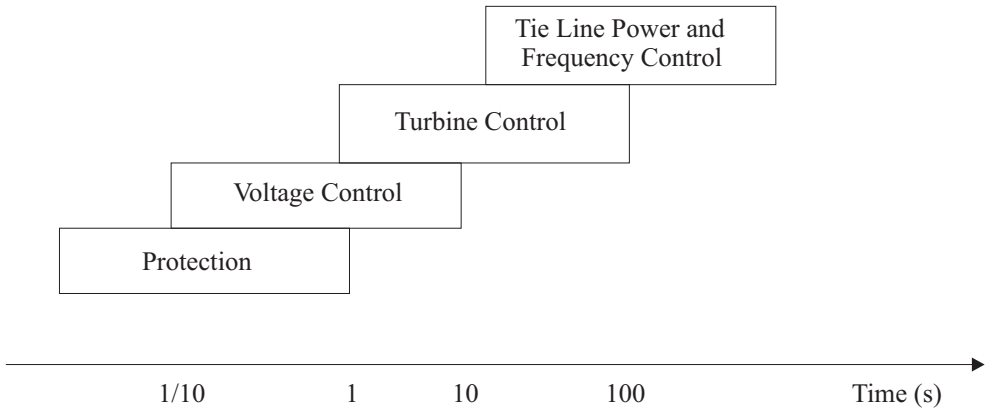

Figure 1.1. Schematic diagram of different time scales of power system controls.

The overall control system is very complex, but due to the de-coupling it is in most cases possible to study the different control loops individually. This facilitates the task, and with appropriate simplifications one can quite often use classical standard control theory methods to analyse these controllers. For a more detailed analysis, one usually has to resort to computer simulations.

A characteristic of a power system is that the load, i.e. the electric power consumption, varies significantly over the day and over the year. This consumption is normally uncontrolled. Furthermore, since substantial parts of the system are exposed to external disturbances, the possibility that lines etc. could be disconnected due to faults must be taken into account. The task of the different control systems of the power system is to keep the power system within acceptable operating limits such that security is maintained and that the quality of supply, e.g. voltage magnitudes and frequency, is within specified limits. In addition, the system should be operated in an economically efficient way. This has resulted in a hierarchical control system structure as shown in Figure 1.2.

1.1 Control Theory Basics - A Review

The de-coupled control loops described above can be analyzed by standard methods from the control theory. Just to refresh some of these concepts, and to explain the notation to be used, a very short review is given here.

1.1.1 Simple Control Loop

The control system in Figure 1.3 is considered. In this figure the block $G(s)$ represents the controlled plant and also possible controllers. From this figure

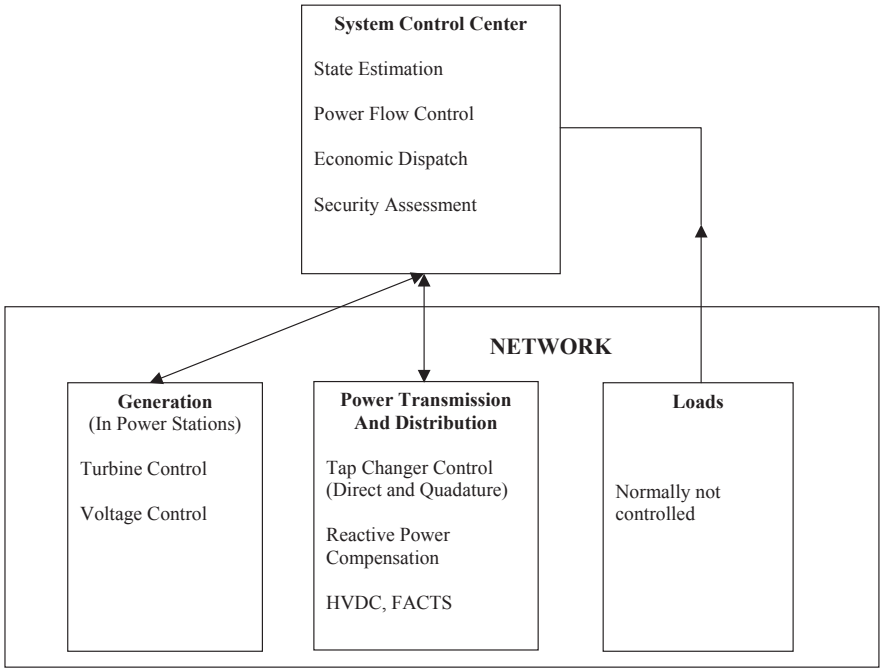

Figure 1.2. The structure of the hierarchical control systems of a power system.

the following quantities are defined[1]:

- $r(t)$ = Reference (set) value (input)
- $e(t)$ = Control error
- $y(t)$ = Controlled quantity (output)
- $v(t)$ = Disturbance

Normally the controller is designed assuming that the disturbance is equal to zero, but to verify the robustness of the controller realistic values of v must be considered.

In principle two different problems are solved in control theory:

1. Regulating problem
2. Tracking problem

[1]Here the quantities in the time domain are denoted by small letters, while the Laplace transformed corresponding quantities are denoted by capital letters. In the following this convention is not always adhered to, but it should be clear from the context if the quantity is expressed in the time or the s domain.

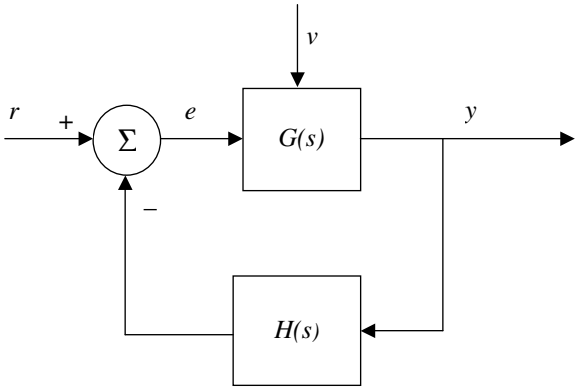

Figure 1.3. Simple control system with control signals.

In the regulating problem, the reference value r is normally kept constant and the task is to keep the output close to the reference value even if disturbances occur in the system. This is the most common problem in power systems, where the voltage, frequency, and other quantities should be kept at the desired values irrespective of load variations, line switchings, etc.

In the tracking problem the task is to control the system so that the output y follows the time variation of the input r as good as possible. This is sometimes also called the servo problem.

The transfer function from the input, R, to the output, Y, is given by (in Laplace transformed quantities)

$$F(s) = \frac{Y(s)}{R(s)} = \frac{C(s)}{R(s)} = \frac{G(s)}{1 + G(s)H(s)} \tag{1.1}$$

In many applications one is not primarily interested in the detailed time response of a quantity after a disturbance, but rather the value directly after the disturbance or the stationary value when all transients have decayed. Then the two following properties of the Laplace transform are important:

$$g(t \to 0+) = \lim_{s\to\infty} sG(s) \tag{1.2}$$

and

$$g(t \to \infty) = \lim_{s\to 0} sG(s) \tag{1.3}$$

where G is the Laplace transform of g. If the input is a step function, Laplace transform $= 1/s$, and $F(s)$ is the transfer function, the initial and stationary response of the output would be

$$y(t \to 0+) = \lim_{s\to\infty} F(s) \tag{1.4}$$

and

$$y(t \to \infty) = \lim_{s\to 0} F(s) \tag{1.5}$$

1.1.2 State Space Formulation

A linear and time-invariant controlled system is defined by the equations

$$\begin{cases} \dot{x} &= Ax + Bu \\ y &= Cx + Du \end{cases} \tag{1.6}$$

The vector $x = (x_1\ x_2\ \ldots x_n)^T$ contains the states of the system, which uniquely describe the system. The vector u has the inputs as components, and the vector y contains the outputs as components. The matrix A, of dimension $n \times n$, is the system matrix of the uncontrolled system. The matrices B, C, and D depend on the design of the controller and the available outputs. In most realistic cases $D = 0$, which means that there is zero feedthrough, and the system is said to be strictly proper. The matrices A and B define which states are controllable, and the matrices A and C define which states are observable. A controller using the outputs as feedback signals can be written as $u = -Ky = -KCx$, assuming $D = 0$, where the matrix K defines the feedback control, the controlled system becomes

$$\dot{x} = (A - BKC)x \tag{1.7}$$

1.2 Control of Electric Power Systems

1.2.1 General considerations

The overall control task in an electric power system is to maintain the balance between the electric power produced by the generators and the power consumed by the loads, including the network losses, at all time instants. If this balance is not kept, this will lead to frequency deviations that if too large will have serious impacts on the system operation. A complication is that the electric power consumption varies both in the short and in the long time scales. In the long time scale, over the year, the peak loads of a day are in countries with cold and dark winters higher in the winter, so called winter peak, while countries with very hot summers usually have their peak loads in summer time, summer peak. Examples of the former are most European countries, and of the latter Western and Southern USA. The consumption varies also over the day as shown in Figure 1.4. Also in the short run the load fluctuates around the slower variations shown in Figure 1.4, so called spontaneous load variations.

In addition to keeping the above mentioned balance, the delivered electricity must conform to certain quality criteria. This means that the *voltage magnitude*, *frequency*, and *wave shape* must be controlled within specified limits.

If a change in the load occurs, this is in the first step compensated by the kinetic energy stored in the rotating parts, rotor and turbines, of the

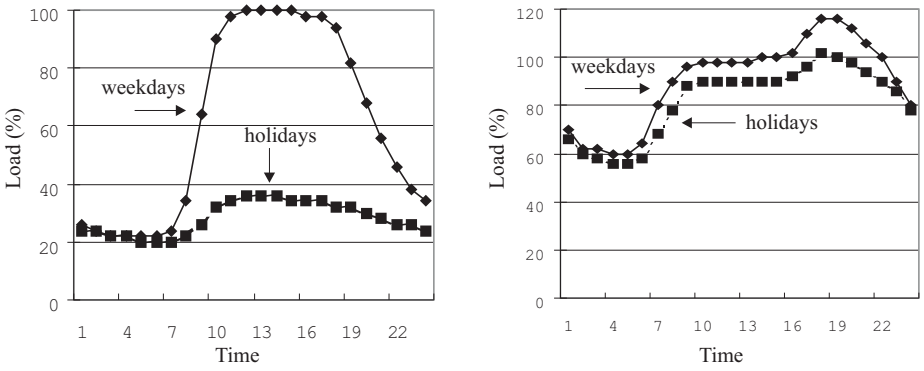

Figure 1.4. Typical load variations over a day. Left: Commercial load.; Right: Residential load.

generators resulting in a frequency change. If this frequency change is too large, the power supplied from the generators must be changed, which is done through the *frequency control* of the generators in operation. An unbalance in the generated and consumed power could also occur as a consequence of that a generating unit is tripped due to a fault. The task of the frequency control is to keep the frequency deviations within acceptable limits during these events.

To cope with the larger variations over the day and over the year generating units must be switched in and off according to needs. Plans regarding which units should be on line during a day are done beforehand based on *load forecasts*[2]. Such a plan is called *unit commitment*. When making such a plan, economic factors are essential, but also the time it takes to bring a generator on-line from a state of standstill. For hydro units and gas turbines this time is typically of the order of some minutes, while for thermal power plants, conventional or nuclear, it usually takes several hours to get the unit operational. This has an impact on the unit commitment and on the planning of reserves in the system[3].

Depending on how fast power plants can be dispatched, they are classified as peak load, intermediate load, or base load power plants. This classification is based on the time it takes to activate the plants and on the

[2]With the methods available today one can make a load forecast a day ahead which normally has an error that is less than a few percent.

[3]In a system where only one company is responsible for the power generation, the unit commitment was made in such a way that the generating costs were minimized. If several power producers are competing on the market, liberalized electricity market, the situation is more complex. The competing companies are then bidding into different markets, pool, bi-lateral, etc, and a simple cost minimizing strategy could not be applied. But also in these cases a unit commitment must be made, but according to other principles.

fuel costs and is usually done as below[4]. The classification is not unique and might vary slightly from system to system.

- **Peak load units**, operational time 1000–2000 h/a
  - Hydro power plants with storage
  - Pumped storage hydro power plants
  - Gas turbine power plants
- **Intermediate load units**, operational time 3000–4000 h/a
  - Fossil fuel thermal power plants
  - Bio mass thermal power plants
- **Base load units**, operational time 5000–6000 h/a
  - Run of river hydro power plants
  - Nuclear power plants

In Figure 1.5 the use of different power plants is shown in a load duration curve representing one year's operation.

The overall goal of the unit commitment and the economic dispatch is the

- Minimization of costs over the year
- Minimization of fuel costs and start/stop costs

[4]The fuel costs should here be interpreted more as the "value" of the fuel. For a hydro power plant the "fuel" has of course no cost *per se*. But if the hydro plant has a storage with limited capacity, it is obvious that the power plant should be used during high load conditions when generating capacity is scarce. This means that the "water value" is high, which can be interpreted as a high fuel cost.

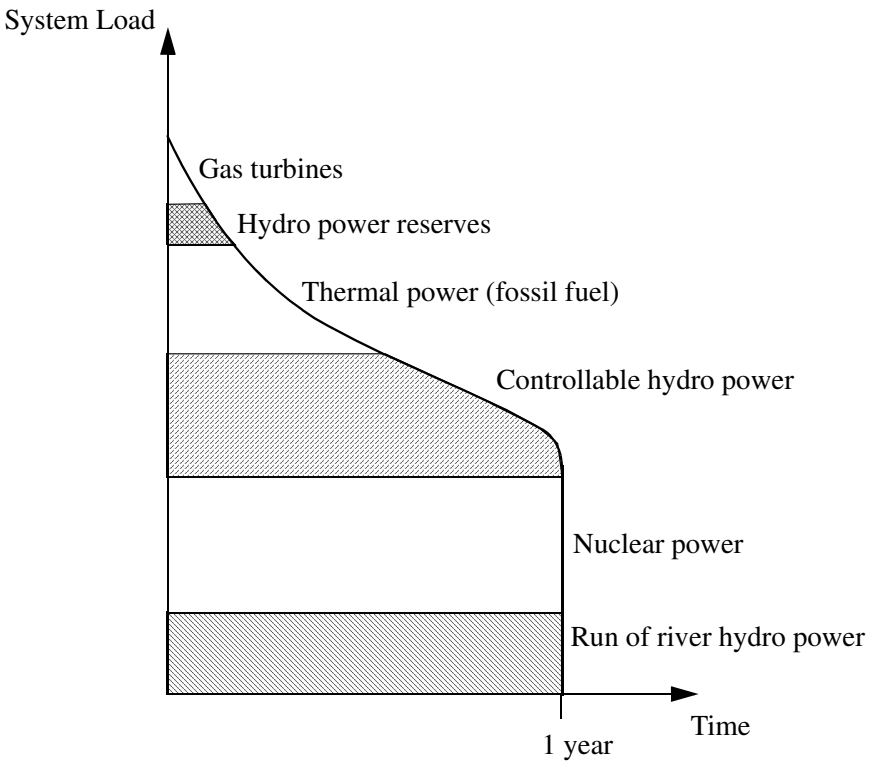

Figure 1.5. Duration curve showing the use of different kinds of power plants.

2
Frequency Dynamics in Electric Power Systems

In this chapter, the basic dynamic frequency model for a large power system is introduced. It is based on the swing equation for the set of synchronous machines in the system. Certain simplifications lead to a description of the dominant frequency dynamics by only one differential equation which can be used for the design of controllers. Also of interest is the frequency dependency of the load in the system, which has a stabilizing effect on the frequency. Note that no control equipment is present yet in the models presented in this chapter: the system is shown in "open loop" in order to understand the principal dynamic behaviour. Control methods are presented in the subsequent chapters.

2.1 Dynamic Model of the System Frequency

In order to design a frequency control methodology for power systems, the elementary dynamic characteristics of the system frequency have to be understood. For this purpose, a simplified model of a power system with several generators (synchronous machines) will be derived in the sequel. The nominal frequency is assumed to be 50 Hz as in the ENTSO-E Continental Europe system (former UCTE). Generally, deviations from this desired value arise due to imbalances between the instantaneous generation and consumption of electric power, which has an accelerating or decelerating effect on the synchronous machines.

2.1.1 Dynamics of the Generators

After a disturbance in the system, like a loss of generation, the frequency in different parts of a large power system will vary similar to the exemplary illustration shown in Figure 2.1. The frequencies of the different machines can be regarded as comparatively small variations over an average frequency in the system. This average frequency, called the system frequency, is the frequency that can be defined for the so–called centre of inertia (COI) of the system.

We want to derive a model that is valid for reasonable frequency deviations. For this purpose, the exact version of the swing equation will be used

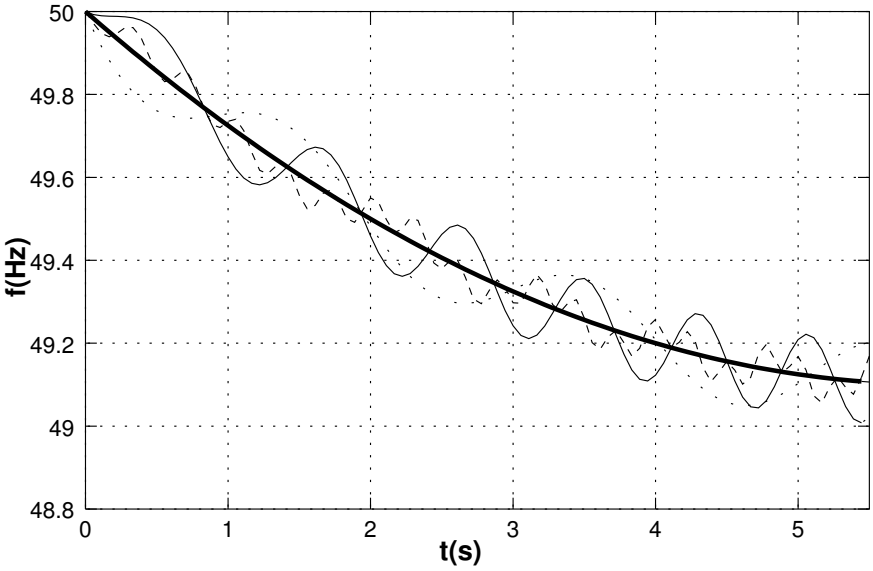

Figure 2.1. The frequency in different locations in an electric power system after a disturbance. The thicker solid curve indicates the average system frequency. Other curves depict the frequency of individual generators.

to describe the dynamic behaviour of generator i:

$$\dot{\omega}_i = \frac{\omega_0}{2H_i}(T_{mi}(p.u.) - T_{ei}(p.u.)) \ , \tag{2.1}$$

with the usual notation. The indices m and e denote mechanical (turbine) and electrical quantities respectively. ω_i is the absolute value of the rotor angular frequency of generator i. The initial condition for eq. (2.1), the pre-disturbance frequency, is normally the nominal frequency $\omega_i(t_0) = \omega_0$. Of main interest is usually the angular frequency deviation $\Delta\omega_i$:

$$\Delta\omega_i = \omega_i - \omega_0 \ \ . \tag{2.2}$$

By deriving eq. (2.2) with respect to the time, one obtains $\Delta\dot{\omega}_i = \dot{\omega}_i$. Note that for rotor oscillations the frequency of $\Delta\omega_i$ is often of interest, while the amplitude of $\Delta\omega_i$ is the main concern in frequency control. Also note that for the initial condition $\Delta\omega_i(t_0) = 0$ holds if eq. (2.1) is formulated for $\Delta\omega$.

In order to convert the torques in eq. (2.1) to power values, the relation $P(p.u.) = T(p.u.)\frac{\omega}{\omega_0}$ is used, which yields:

$$\Delta\dot{\omega}_i = \frac{\omega_0^2}{2H_i\omega_i}(P_{mi}(p.u.) - P_{ei}(p.u.)) \ , \tag{2.3}$$

The power can also be expressed in SI–units (e.g. in MW instead of p.u.) by multiplication with the power base S_{Bi}, which represents the rated power of

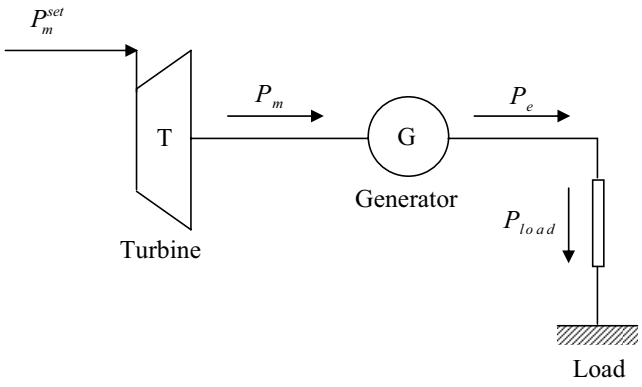

Figure 2.2. Simplified representation of a power system consisting of a single generator connected to the same bus as the load.

the generator i. Furthermore, eq. (2.3) can be rewritten such that the unit on both sides is MW:

$$\frac{2H_i S_{Bi}}{\omega_0}\Delta\dot{\omega}_i = \frac{\omega_0}{\omega_i}(P_{mi} - P_{ei}) \ . \tag{2.4}$$

Note that this is still the exact version of the swing equation, which is nonlinear. For further details on different formulations of the swing equation, please refer to Appendix A. Now, the goal is to derive the differential equation for the entire system containing n generators. In a highly meshed system, all units can be assumed to be connected to the same bus, representing the centre of inertia of the system. With further simplifications, they can even be condensed into one single unit. An illustration of this modelling is depicted in Figure 2.2. A summation of all the equations (2.4) for the n generators in the system yields

$$2\sum_{i=1}^{n} H_i S_{Bi}\frac{1}{\omega_0}\Delta\dot{\omega}_i = \sum_{i=1}^{n}\frac{\omega_0}{\omega_i}(P_{mi} - P_{ei}) \ . \tag{2.5}$$

Because of the strong coupling of the generation units, $\omega_i = \omega$ can be as-

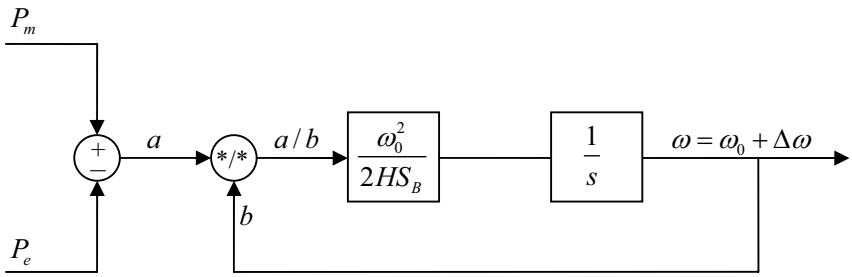

Figure 2.3. Block diagram of nonlinear frequency dynamics as in eq. (2.11).

sumed for all i. By defining the quantities

$$\omega = \frac{\sum_i H_i \omega_i}{\sum H_i} \qquad \text{Centre of Inertia frequency} \tag{2.6}$$

$$S_B = \sum_i S_{Bi} \qquad \text{Total rating,} \tag{2.7}$$

$$H = \frac{\sum_i H_i S_{Bi}}{\sum_i S_{Bi}} \qquad \text{Total inertia constant,} \tag{2.8}$$

$$P_m = \sum_i P_{mi} \qquad \text{Total mechanical power,} \tag{2.9}$$

$$P_e = \sum_i P_{ei} \qquad \text{Total electrical power,} \tag{2.10}$$

the principal frequency dynamics of the system can be described by the nonlinear differential equation

$$\Delta\dot{\omega} = \frac{\omega_0^2}{2HS_B\omega}(P_m - P_e) \ . \tag{2.11}$$

Eq. (2.11) is illustrated as a block diagram in Figure 2.3. For the frequency ω in the centre of inertia holds as well

$$\omega = \omega_0 + \Delta\omega \ . \tag{2.12}$$

In order to obtain a linear approximation of eq. (2.11), $\omega = \omega_0$ can be assumed for the right-hand side. This is a valid assumption for realistic frequency deviations in power systems. This yields

$$\Delta\dot{\omega} = \frac{\omega_0}{2HS_B}(P_m - P_e) \ . \tag{2.13}$$

The dynamics can also be expressed in terms of frequency instead of angular frequency. Because of $\omega = 2\pi f$ and $\dot{\omega} = 2\pi\dot{f}$ follows

$$\Delta\dot{f} = \frac{f_0}{2HS_B}(P_m - P_e) \ . \tag{2.14}$$

A very simple and useful model can be derived if some more assumptions are made. The overall goal of our analysis is to derive an expression that gives the variation of $\Delta\omega$ after a disturbance of the balance between P_m and P_e. Therefore, we define

$$P_m = \sum_i P_{mi} = P_{m0} + \Delta P_m \quad , \tag{2.15}$$

where P_{m0} denotes the mechanical power produced by the generators in steady state and ΔP_m denotes a deviation from that value. The total generated power is consumed by the loads and the transmission system losses, i.e.

$$P_e = \sum_i P_{ei} = P_{load} + P_{loss} \quad , \tag{2.16}$$

which can, in the same way as in eq. (2.15), be written as

$$P_e = P_{e0} + \Delta P_{load} + \Delta P_{loss} \tag{2.17}$$

with

$$P_{e0} = P_{load0} + P_{loss0} \quad . \tag{2.18}$$

If the system is in equilibrium prior to the disturbance,

$$P_{m0} = P_{e0} \tag{2.19}$$

and

$$P_{m0} = P_{load0} + P_{loss0} \tag{2.20}$$

are valid. Furthermore, the transmission losses after and before the disturbance are assumed to be equal, i.e.

$$\Delta P_{loss} = 0 \quad . \tag{2.21}$$

If neither the disturbance nor the oscillations in the transmission system are too large, these approximations are reasonable. Using eqs. (2.15) – (2.21), eq. (2.13) can now be written as

$$\Delta\dot{\omega} = \frac{\omega_0}{2HS_B}(\Delta P_m - \Delta P_{load}) \quad , \tag{2.22}$$

or equivalently

$$\Delta\dot{f} = \frac{f_0}{2HS_B}(\Delta P_m - \Delta P_{load}) \quad . \tag{2.23}$$

Eq. (2.23) can be represented by the block diagram in Figure 2.4.

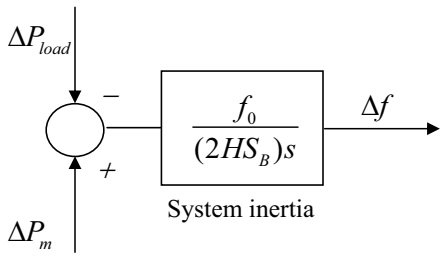

Figure 2.4. Linearized model of the power system frequency dynamics.

2.1.2 Frequency Dependency of the Loads

Loads are either frequency-dependent or frequency-independent. In real power systems, a frequency dependency of the aggregated system load is clearly observable. This has a stabilizing effect on the system frequency f, as will be shown in the sequel. Apart from a component depending directly on f, large rotating motor loads cause an additional contribution depending on $\dot{f}$. This is due to the fact that kinetic energy can be stored in the rotating masses of the motors.
A load model that captures both effects is given by

$$P_{load}^{f} - P_{load}^{f_0} = \Delta P_{load}^{f} = K_l \Delta f + g(\Delta \dot{f}) \tag{2.24}$$

where

- $P_{load}^{f_0}$: Load power when $f = f_0$,
- K_l: Frequency dependency,
- $g(\Delta \dot{f})$: Function that models the loads with rotating masses.

The function $g(\Delta \dot{f})$ will now be derived. The rotating masses have the following kinetic energy:

$$W(f) = \frac{1}{2} J (2\pi f)^2 \tag{2.25}$$

The change in the kinetic energy, which is equal to the power P_M consumed by the motor, is given by

$$P_M = \frac{dW}{dt} \tag{2.26}$$

and

$$\Delta P_M = \frac{d\Delta W}{dt} \quad . \tag{2.27}$$

ΔW can be approximated by

$$\begin{aligned} W(f_0+\Delta f) &= 2\pi^2 J(f_0+\Delta f)^2 = \\ W_0+\Delta W &= 2\pi^2 J f_0^2 + 2\pi^2 J 2 f_0 \Delta f + 2\pi^2 J(\Delta f)^2 \\ &= W_0 + \frac{2W_0}{f_0}\Delta f + \frac{W_0}{f_0^2}(\Delta f)^2 \\ \Rightarrow \Delta W &\approx \frac{2W_0}{f_0}\Delta f \\ \Rightarrow \Delta P_M &\approx \frac{2W_0}{f_0}\frac{d\Delta f}{dt} = \frac{2W_0}{f_0}\Delta \dot{f} \end{aligned} \tag{2.28}$$

The frequency dependency of the remaining load can also be written as

$$\frac{\partial P_{load}}{\partial f}\Delta f = K_l \Delta f = \frac{1}{D_l}\Delta f \quad . \tag{2.29}$$

The values of W_0 and D_l are obviously highly dependent on the structure of the load and can be variable over time. Especially W_0 is only a factor in power systems with large industrial consumers running heavy rotating machines. The constant D_l has typical values such that the variation of the load is equal to $0 \ldots 2$ % per % of frequency variation.

The block diagram in Figure 2.5 represents the dynamic load model. Together with the power system dynamics derived before, we obtain a dynamical system with a "proportional/differential control" caused by the loads. However, this effect is too small to be able to keep the frequency within reasonable bounds. As we will see in the next section, the absence of any other control equipment would lead to unacceptable and remaining frequency deviations even for moderate disturbances.

The power system model derived so far is shown in Figure 2.6.

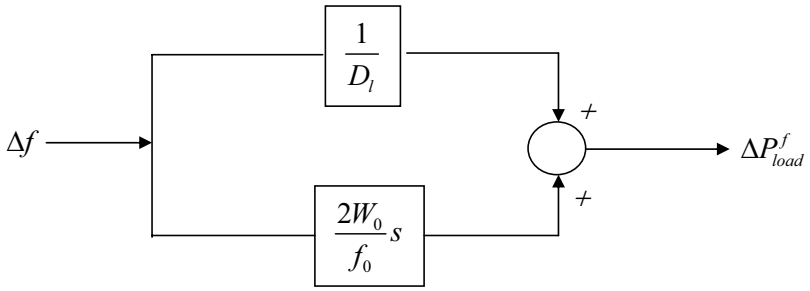

Figure 2.5. Block diagram of the dynamic load model.

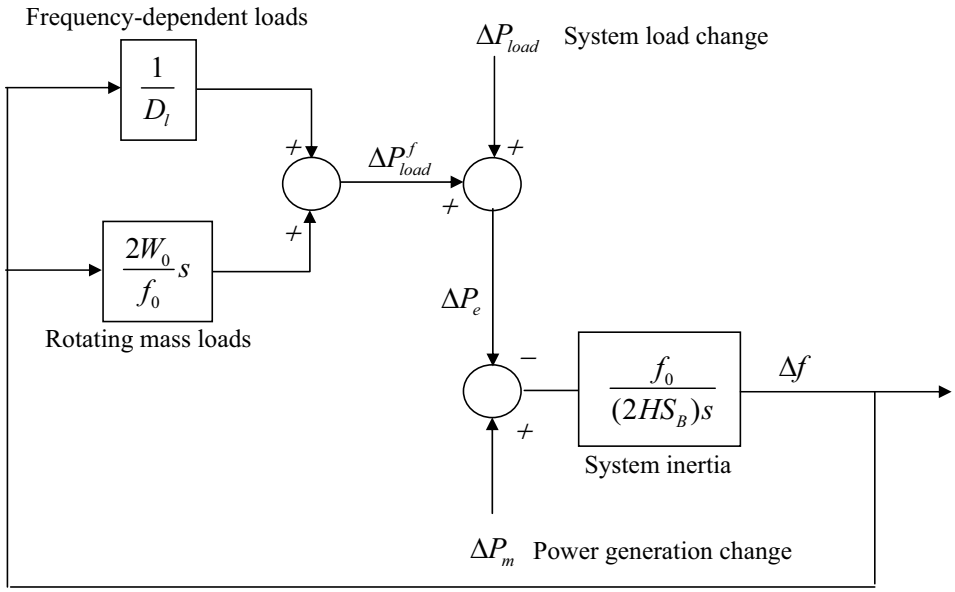

Figure 2.6. Model of power system without control.

2.2 Dynamic Response of Uncontrolled Power System

Now we will conduct a numerical simulation of the uncontrolled frequency dynamics after a disturbance. Both loss of generation and loss of load will be shown, represented by a positive resp. negative step input on the variable ΔP_{load}. Table 2.1 displays the parameters used in the simulation. In Figure 2.7, a time plot of the system frequency is shown corresponding to the different disturbances. Note that this result is purely theoretic as such large frequency deviations could never occur in a real power system because of various protection mechanisms. However, it illustrates well the possible frequency rise or decay and the stabilizing self-control effect caused by the frequency dependency of the load.

Parameter	Value	Unit
H	5	s
S_B	10	GW
f_0	50	Hz
D_L	$\frac{1}{200}$	$\frac{\text{Hz}}{\text{MW}}$
W_0	100	$\frac{\text{MW}}{\text{Hz}}$

Table 2.1. Parameters for time domain simulation of power system.

The plot shows the time evolution of the system frequency for a disturbance of (top to bottom) $\Delta P_{load} = -1000$ MW, $\Delta P_{load} = -500$ MW, $\Delta P_{load} = -100$ MW (sudden loss of load) and $\Delta P_{load} = 100$ MW, $\Delta P_{load} = 500$ MW, $\Delta P_{load} = 1000$ MW (sudden increase of load or loss of generation).

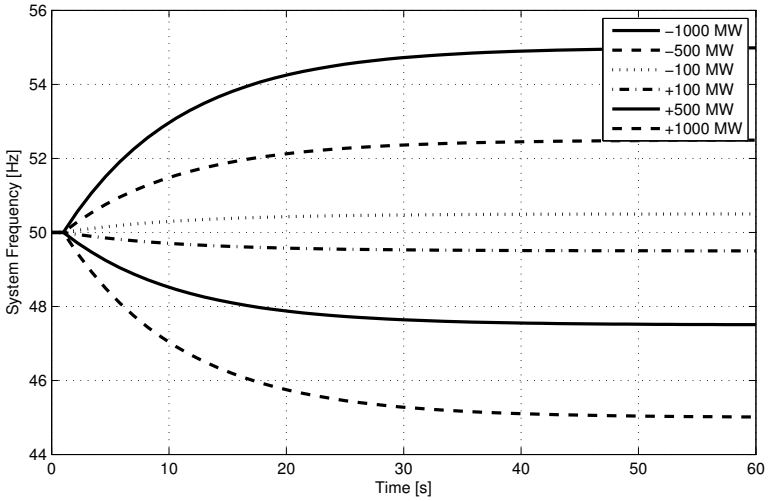

Figure 2.7. Theoretical frequency responses of uncontrolled power system ($D_L = 1/200$ Hz/MW).

2.3 The Importance of a Constant System Frequency

In the most common case $\Delta P_m - \Delta P_{load}$ is negative after a disturbance, like the tripping of a generator. It is also possible that the frequency rises during a disturbance, for example when an area that contains much generation capacity is isolated. Since too large frequency deviations in a system are not acceptable, automatic frequency control, which has the goal of keeping the frequency during disturbances at an acceptable level, is used. Furthermore, the spontaneous load variations in an electric power system result in a minute–to–minute variation of up to 2%. This alone requires that some form of frequency control must be used in most systems.

There are at least two reasons against allowing the frequency to deviate too much from its nominal value. A non–nominal frequency in the system results in a lower quality of the delivered electrical energy. Many of the devices that are connected to the system work best at nominal frequency. Further, too low frequencies (lower than $\approx 47 - 48$ Hz) lead to damaging vibrations in steam turbines, which in the worst case have to be disconnected. This constitutes an even worse stress on the system and can lead to a complete power system collapse. In comparison with thermal units, hydro power plants are more robust and can normally cope with frequencies down to 45 Hz.

2.4 Control Structures for Frequency Control

In the following two chapters, the control structures that ensure a constant system frequency of 50 Hz will be described. The automatic control system consists of two main parts, the primary and secondary control. Tertiary control, which is manually activated in order to release the used primary and secondary control reserves after a disturbance, is not discussed here. This is due to the fact that the utilization of tertiary control reserves is more similar to the electricity production according to generations schedules (dispatch), which are based on economic off-line optimizations.

The primary control refers to control actions that are done locally (on the power plant level) based on the setpoints for frequency and power. The actual values of these can be measured locally, and deviations from the set values results in a signal that will influence the valves, gates, servos, etc. in a primary-controlled power plant, such that the desired active power output is delivered. In primary frequency control, the control task of priority is to bring the frequency back to (short term) acceptable values. However, there remains an unavoidable frequency control error because the control law is purely proportional. The control task is shared by all generators participating in the primary frequency control irrespective of the location of the disturbance. Further explanations follow in chapter 3.

In the secondary frequency control, also called *Load Frequency Control*, the power setpoints of the generators are adjusted in order to compensate for the remaining frequency error after the primary control has acted. Apart from that, another undesired effect has to be compensated by secondary control: active power imbalances and primary control actions cause changes in the load flows on the tie-lines to other areas, i.e. power exchanges not according to the scheduled transfers. The secondary control ensures by a special mechanism that this is remedied after a short period of time. Note that in this control loop the location of the disturbance is considered when the control action is determined: only disturbances within its own control zone (area) are "seen" by the secondary controller. Note that Load Frequency Control can also be performed manually as in the Nordel power system. In the ENTSO-E Continental Europe interconnected system, an automatic scheme is used, which can also be called *Automatic Generation Control*. This is further discussed in chapter 4.

The basic control structures described above are depicted in Figure 2.8. Figure 2.9 shows an illustration of the time spans in which these different control loops are active after a disturbance. Note that primary and secondary control are continuously active also in normal operation of the grid in order to compensate for small fluctuations. Conversely, the deployment of tertiary reserves occurs less often.

Under-frequency load shedding is a form of system protection and acts on timescales well under one second. As the activation of this scheme implies the loss of load in entire regions, it must only be activated if absolutely necessary in order to save the system. In the ENTSO-E Continental Europe system, the first load shedding stage is activated at a frequency of 49 Hz, causing the shedding of about 15 % of the overall load. In many systems, a rotating scheme for how the load should be shed, if that is necessary, is devised. Such a scheme is often called rotating load shedding.

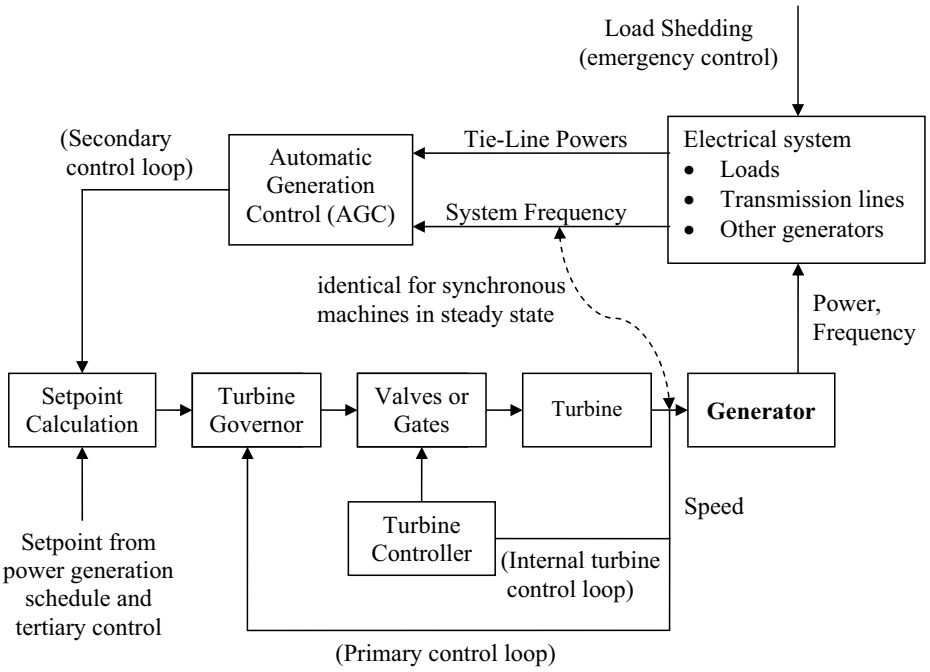

Figure 2.8. Basic structure of frequency control in electric power systems.

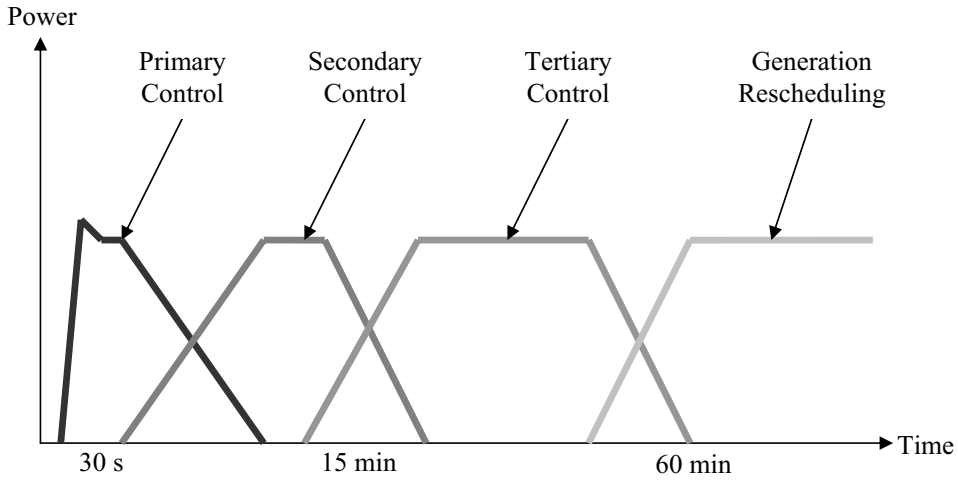

Figure 2.9. Temporal structure of control reserve usage after a disturbance (terminology according to ENTSO-E for region Continental Europe (former UCTE).

3
Primary Frequency Control

In this chapter, the mechanisms for primary frequency control are illustrated. As will be shown, they are implemented entirely on the power plant level. In an interconnected power system, not all generation units need to have primary control equipment. Instead, the total amount of necessary primary control reserves are determined by statistical considerations and the distribution on the power plants can vary. Primary control can also be used in islanded operation of a single generator. These different applications will be discussed along with their principal static and dynamic characteristics.

3.1 Implementation of Primary Control in the Power Plant

For a thermal unit, a schematic drawing of the primary control is shown in Figure 3.1. The turbine governor (depicted here together with the internal turbine controller) acts on a servomotor in order to adjust the valve through which the live steam (coming from the boiler with high pressure and high temperature) flows to the turbines. In the high pressure turbine, part of the energy of the steam is converted into mechanical energy. Often the steam is then reheated before it is injected into a medium pressure or low pressure turbine, where more energy is extracted from the steam. In practice, these turbine-generator systems can be very large. In a big thermal unit of rating 1000 MW, the total length of the turbine-generator shaft may exceed 50 m.

The control law, which is shown as a block diagram in Figure 3.2, is a proportional feedback control. It establishes an affine relation between the measured frequency and the power generation of the plant in steady state.

Note that the turbine dynamics plays in important role in the overall dynamical response of the system. However, we will neglect this for the sake of simplicity in the first three sections of this chapter. In section 3.4.1, different steam and hydro turbines and their modelling are discussed and later their effect on the dynamical response will be shown.

Primary control is implemented on a purely local level; there is no coordination between the different units. This is also why the control law cannot have an integral component: integrators of different power plants could start "competing" each other for power production shares, which can lead to an unpredictable and unreasonable distribution of power generation on the available plants.

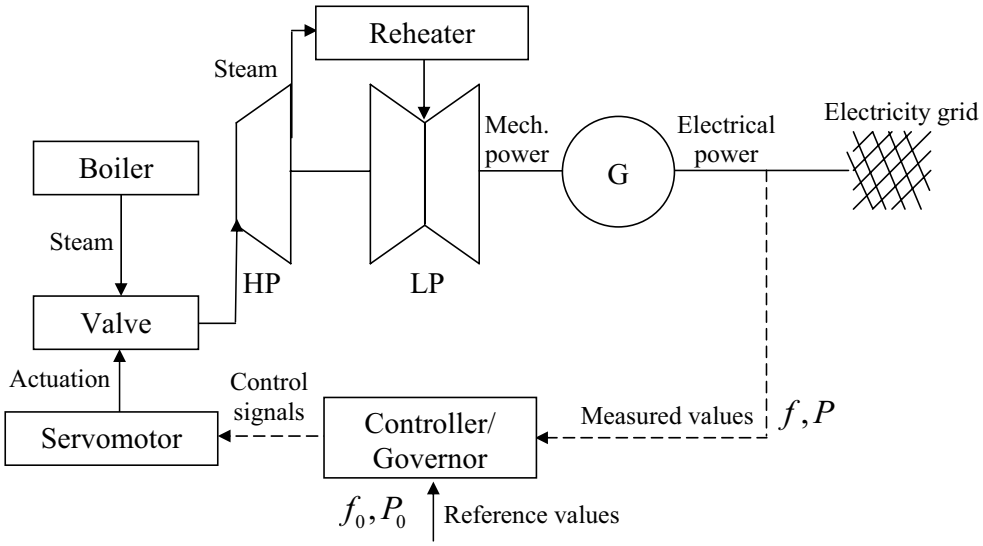

Figure 3.1. Schematic drawing of the primary control installed in a thermal unit. HP = High Pressure Turbine. LP = Low Pressure turbine.

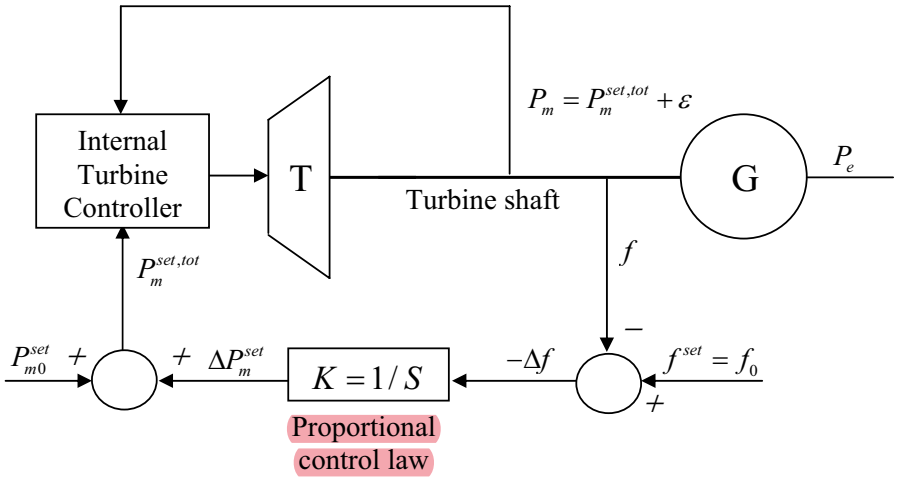

Figure 3.2. Block diagram describing the primary control law. The measured power value corresponds to P_m in our notation, while in practice the measurement can be done on the electrical side.

3.2 Static Characteristics of Primary Control

First, it is of particular interest to study the properties of the primary frequency control in steady state. Referring to the block diagram in Figure 3.2, the equation describing the primary control is given by

$$(f_0 - f) \cdot \frac{1}{S} + (P_{m0}^{set} - P_m^{set,tot}) = 0 \ , \tag{3.1}$$

which can be written as

$$S = -\frac{f_0 - f}{P_{m0}^{set} - P_m^{set,tot}} = -\frac{f - f_0}{P_m^{set,tot} - P_{m0}^{set}} \text{ Hz/MW} > 0 \tag{3.2}$$

or in per unit as

$$S = -\frac{\dfrac{f - f_0}{f_0}}{\dfrac{P_m^{set,tot} - P_{m0}^{set}}{P_{m0}^{set}}} \ . \tag{3.3}$$

Under the assumption that the turbine power controller has an integrating characteristic ($\varepsilon \to 0$ when $t \to \infty$ in Figure 3.2), it follows that in steady state holds $P_m = P_m^{set,tot}$.

The speed droop characteristic, Figure 3.3, yields all possible steady-state operating points ($P_m^{set,tot}$, f) of the turbine. The position and slope of the straight line can be fixed by the parameters P_{m0}^{set}, f_0 and S. We have chosen to label the horizontal axis with the power $P_m^{set,tot}$ which for small deviations of the frequency around the nominal value is identical to the torque T. In the literature the speed droop characteristics is sometimes also described by ω instead of by f.

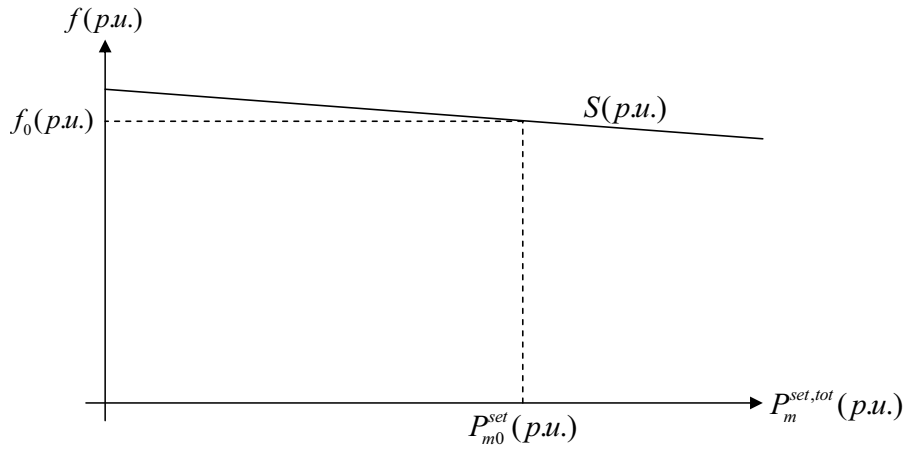

Figure 3.3. Static characteristic of primary control.

3.2.1 Role of speed droop depending on type of power system

We will now study how the frequency control of a generator will act in three different situations. First, when the generator is part of a large interconnected system, and second when the generator is in islanded operation feeding a load. The third system to be studied is a two machine system.

Generator in Large System If a generator is embedded in a large interconnected system, it can be modelled with a very good approximation as connected to an infinite bus. This is shown in Figure 3.4.

In steady state the frequency is given by the grid frequency f_G (represented by the infinite bus). From the speed droop characteristics, Figure 3.5, the power produced by the generator can then be determined. The turbine governor controls thus only the power, not the frequency, see Figure 3.5.

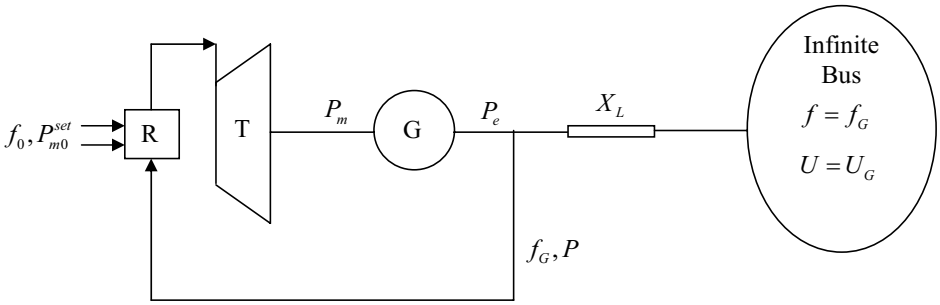

Figure 3.4. Generator operating in a large interconnected system.

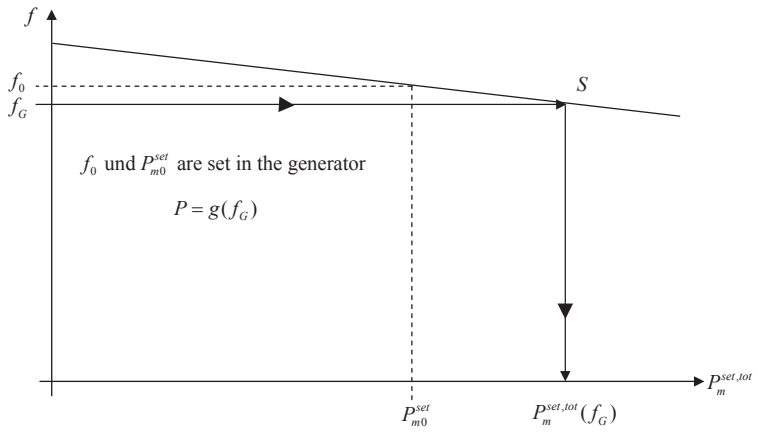

Figure 3.5. Speed droop characteristics for the case when the generator is connected to an infinite bus (large system).

Islanded Operation As depicted in Figure 3.6, the generator feeds a load in islanded operation, which here is assumed to be a purely resistive load. By a voltage controller the voltage U is kept constant and thus also P_e. In this case the primary control loop will control the frequency, not the power. The resulting frequency can be determined from the speed droop characteristics, Figure 3.7.

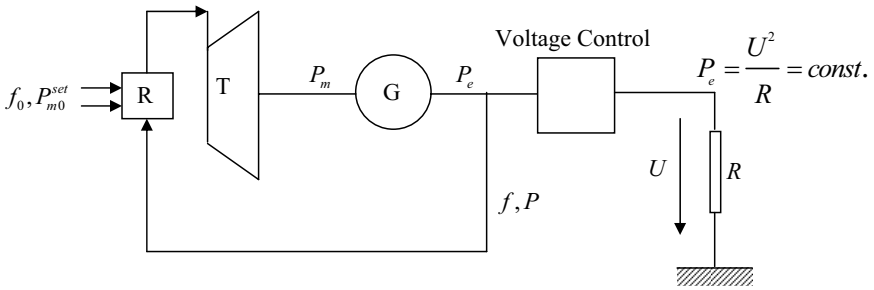

Figure 3.6. Generator in islanded operation.

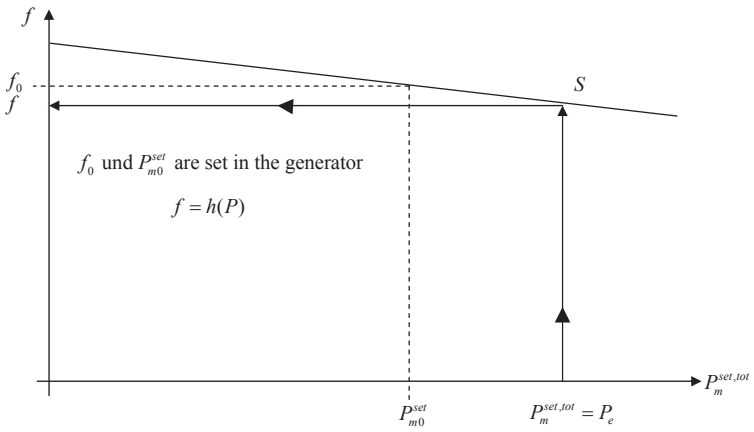

Figure 3.7. Speed droop characteristics for the case when the generator is in islanded operation.

Two Generator System The two generator system, Figure 3.8, provides a simple model that is often used to study the interaction between two areas in a large system. In this model the two generators could represent two subsystems, and the speed droop is then the sum of all the individual speed droops of the generators in the two subsystems, Figure 3.9. With the help of the speed droop characteristics of the two systems, we will determine how a change in load will be compensated by the two systems. Thus, if we have a change ΔP_{load} of the overall load, what will the changes in $P_{m,1}$, $P_{m,2}$, and f be?

This will be solved in the following way:

- The quantities ($P^{set}_{m0,1}$, $f_{0,1}$, S_1) and ($P^{set}_{m0,2}$, $f_{0,2}$, S_2) describe the speed droop characteristics of the two systems g_1 and g_2.
- From these the sum $g_3 = g_1 + g_2$ is formed.
- From the given P_{load} we can determine $P^{set}_{m,1}$, $P^{set}_{m,2}$ and f_N from g_3.
- In a similar way: From $P_{load}+\Delta P_{load}$ can $P^{set}_{m0,1}+\Delta P^{set}_{m,1}$, $P^{set}_{m0,2}+\Delta P^{set}_{m,2}$ and $f_N + \Delta f$ be determined, and thus $\Delta P^{set}_{m,1}$, $\Delta P^{set}_{m,2}$ und Δf.

All these steps are shown in Figure 3.9.

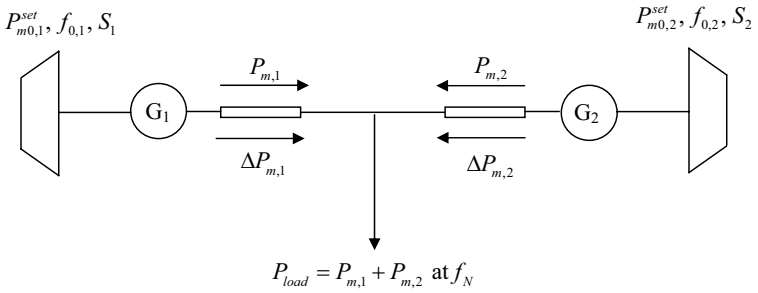

Figure 3.8. Two generator system.

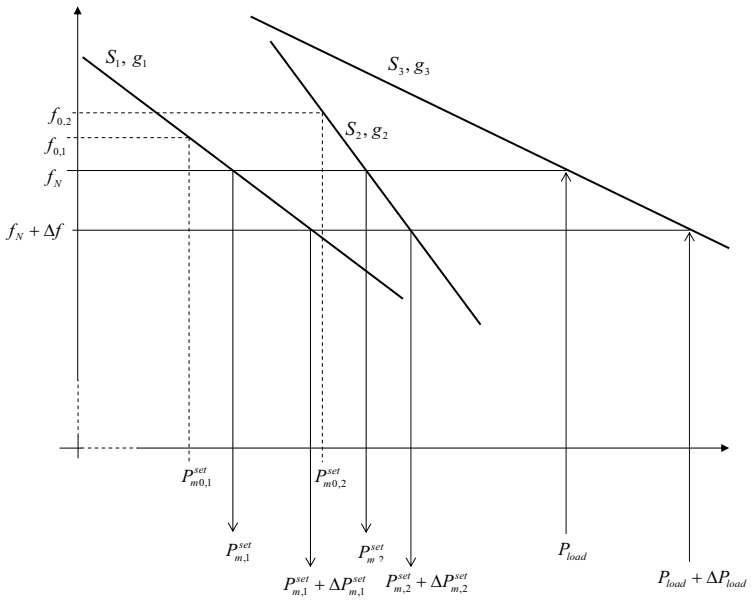

Figure 3.9. Speed droop characteristics for a two machine system.

3.3 Dynamic Characteristics of Primary Control

3.3.1 Dynamic Model of a One-Area System

In this section, we are going to extend the dynamic frequency model introduced in Chapter 2 by the primary control loop in the power plants. For an individual generator, the block diagram has been introduced in the previous section.

Following the nomenclature introduced in Figure 3.2, we start with

$$P_m^{set,tot} = P_{m0}^{set} + \Delta P_m^{set} = P_{m0}^{set} - \frac{1}{S}\Delta f \quad , \tag{3.4}$$

where $P_m^{set,tot}$ describes the power setpoint of the turbine including the scheduled value P_{m0}^{set} and the component imposed by primary control. For the linearized consideration of the power system in Δ quantities, we set

$$P_{m0}^{set} = \Delta P_{m0}^{set} \tag{3.5}$$

as the steady-state component cancels out against the other steady-state quantities. The remaining question is how a change in $\Delta P_m^{set,tot}$ translates into an actual mechanical power output change ΔP_m. Thus, we regard now the internal turbine control loop as depicted in Figure 3.10.

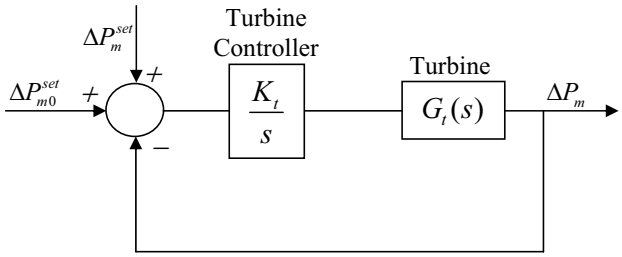

Figure 3.10. Block diagram of the turbine and turbine control dynamics.

From this figure it follows that

$$\Delta P_m(s) = \frac{G_t(s)}{G_t(s) + \frac{1}{K_t}s}\left[\Delta P_{m0}^{set}(s) + \Delta P_m^{set}(s)\right] \quad . \tag{3.6}$$

If the dynamics of the turbine is neglected ($G_t(s) = 1$), one obtains

$$\Delta P_m(s) = \frac{1}{1 + T_t s}\left[\Delta P_{m0}^{set}(s) + \Delta P_m^{set}(s)\right] \quad . \tag{3.7}$$

Note that the time constant $T_t = 1/K_t$ is fairly small compared with the frequency dynamics of the system. Regarding now only the frequency control component ($\Delta P_{m0}^{set} = 0$), we obtain in steady state as before

$$\Delta P_m = -\frac{1}{S}\Delta f \quad . \tag{3.8}$$

For the case of n controllers for n generators we obtain analogously for controller i

$$\Delta P_{mi} = -\frac{1}{S_i}\Delta f \qquad i = 1, \ldots, n \tag{3.9}$$

$$\sum_i \Delta P_{mi} = -\sum_i \frac{1}{S_i}\Delta f \tag{3.10}$$

where

$$\Delta P_m = \sum_i \Delta P_{mi} \tag{3.11}$$

is the total change in turbine power. By defining

$$\frac{1}{S} = \sum_i \frac{1}{S_i} \tag{3.12}$$

we thus have

$$\Delta P_m = -\frac{1}{S}\Delta f \ . \tag{3.13}$$

This can be inserted into the dynamic system frequency model derived in Chapter 2 as depicted in Figure 3.11.

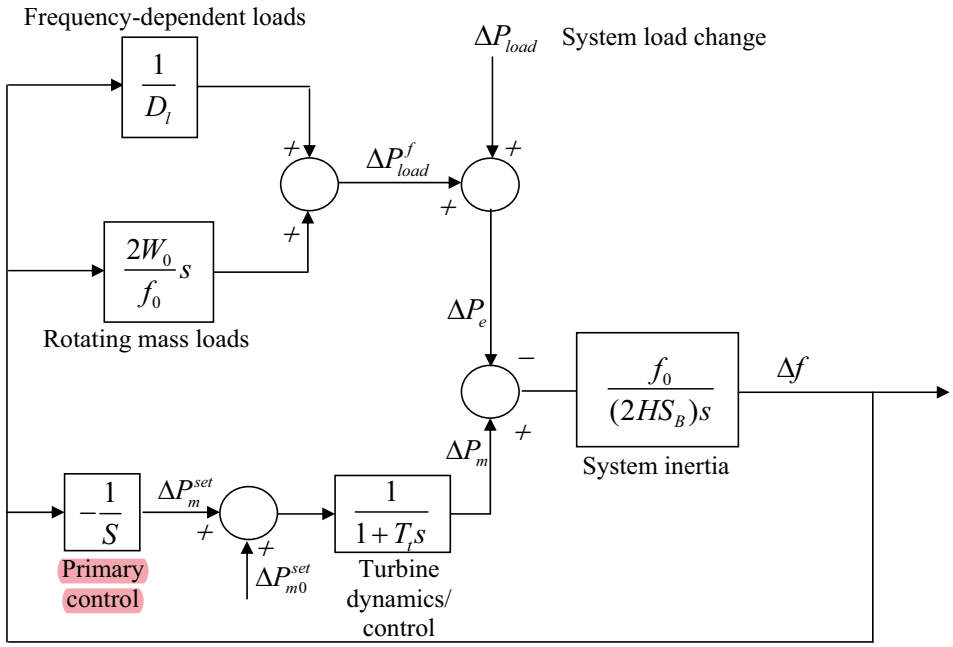

Figure 3.11. Dynamic frequency model of the power system with primary-controlled power plants.

3.3.2 Dynamic Response of the One-Area System

Now we are going to study the effect of a disturbance in the system derived above. Both loss of generation and loss of load can be simulated by imposing a positive or negative step input on the variable ΔP_{load}. A change of the set value of the system frequency f_0 is not considered as this is not meaningful in real power systems.

From the block diagram in Figure 3.11 it is straightforward to derive the transfer function between ΔP_{load} and Δf ($\Delta P_{m0}^{set} = 0$):

$$\Delta f(s) = -\frac{1 + sT_t}{\frac{1}{S} + \frac{1}{D_l}(1 + sT_t) + (\frac{2W_0}{f_0} + \frac{2HS_B}{f_0})s(1 + sT_t)} \Delta P_{load}(s) \quad (3.14)$$

The step response for

$$\Delta P_{load}(s) = \frac{\Delta P_{load}}{s} \quad (3.15)$$

is given in Figure 3.12. The frequency deviation in steady state is

$$\Delta f_\infty = \lim_{s \to 0}(s \cdot \Delta f(s)) = \frac{-\Delta P_{load}}{\frac{1}{S} + \frac{1}{D_l}} = \frac{-\Delta P_{load}}{\frac{1}{D_R}} = -\Delta P_{load} \cdot D_R \quad (3.16)$$

with

$$\frac{1}{D_R} = \frac{1}{S} + \frac{1}{D_l} \quad (3.17)$$

In order to calculate an equivalent time constant T_{eq}, T_t is put to 0. This can be done since for realistic systems the turbine controller time constant T_t is much smaller than the time constant of the frequency dynamics T_M:

$$T_t \ll T_M = \frac{f_0}{S_B}(\frac{2W_0}{f_0} + \frac{2HS_B}{f_0}) \ . \quad (3.18)$$

This means that the transfer function in eq. (3.14) can be approximated by a first order function

$$\Delta f(s) = \frac{-\Delta P_{load}(s)}{\frac{1}{D_R} + T_M \frac{S_B}{f_0} s} = \frac{-1}{1 + T_M D_R \frac{S_B}{f_0} s} \frac{D_R \Delta P_{load}}{s} \quad (3.19)$$

or

$$\Delta f(s) = \frac{1}{1 + T_M D_R \frac{S_B}{f_0} s} \frac{\Delta f_\infty}{s} \quad (3.20)$$

with

$$T_{eq} = T_M D_R \frac{S_B}{f_0} \quad (3.21)$$

as the equivalent time constant.

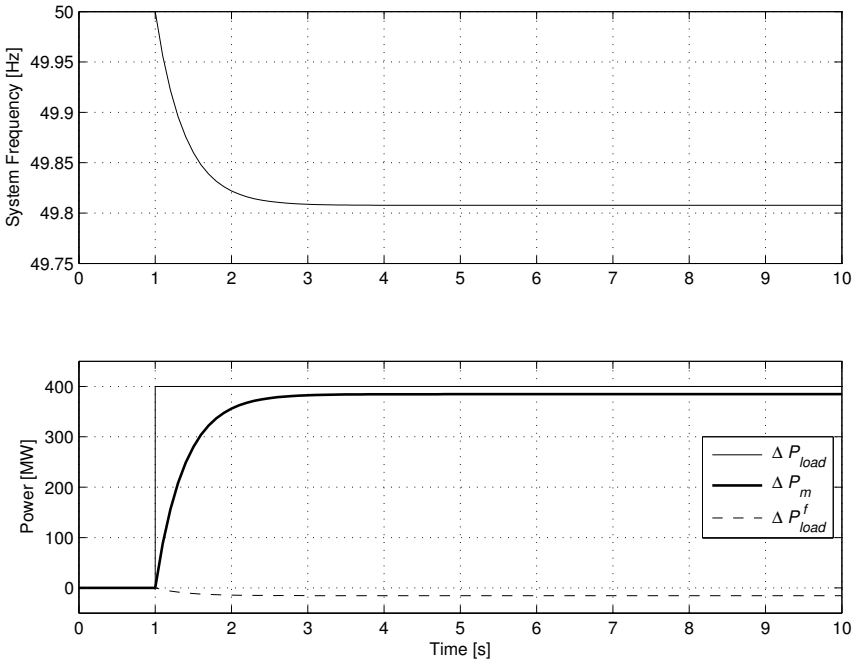

Figure 3.12. Behaviour of the one-area system (no turbine dynamics, parameterized as described in the example below) after a step increase in load. The upper plot shows the system frequency f. The lower plot shows the step function in ΔP_{load}, the increase in turbine power ΔP_m, and the frequency-dependent load variation ΔP^f_{load}.

Example

- $S_B = 4000$ MW
- $f_0 = 50$ Hz
- $S = 4\% = 0.04\frac{f_0}{S_B} = \frac{0.04 \cdot 50}{4000}$ Hz/MW $= \frac{1}{2000}$ Hz/MW
- $D_l = 1\,\%/1\,\% \Rightarrow D_l = \frac{f_0}{S_B} = \frac{50}{4000}$ Hz/MW $= \frac{1}{80}$ Hz/MW
- $\Delta P_{load} = 400$ MW
- $T_M = 10$ s

Then follows

$$\Delta f_\infty = -D_R \cdot \Delta P_{load} = -\frac{1}{2000\frac{\text{MW}}{\text{Hz}} + 80\frac{\text{MW}}{\text{Hz}}} \cdot 400MW = -0.19 \text{ Hz} \quad (3.22)$$

and

$$T_{eq} = 10 \text{ s} \cdot \frac{1}{2000\frac{\text{MW}}{\text{Hz}} + 80\frac{\text{MW}}{\text{Hz}}} \frac{4000 \text{ MW}}{50 \text{ Hz}} = 0.39 \text{ s} \ . \quad (3.23)$$

3.3.3 Extension to a Two-Area System

Up to now we have mostly studied the behaviour of a power system consisting of a single area. If the power system is highly meshed in this case, it can be represented by a single bus where all units are connected. In practice, however, a large interconnected power system is always divided into various "control zones" or "areas", corresponding e.g. to countries. Understanding the interactions between these areas is therefore highly important for the flawless operation of the entire system. For simplified simulation studies, a system with two areas can be represented by two single bus systems with a tie-line in between them. This is depicted in Figure 3.13.

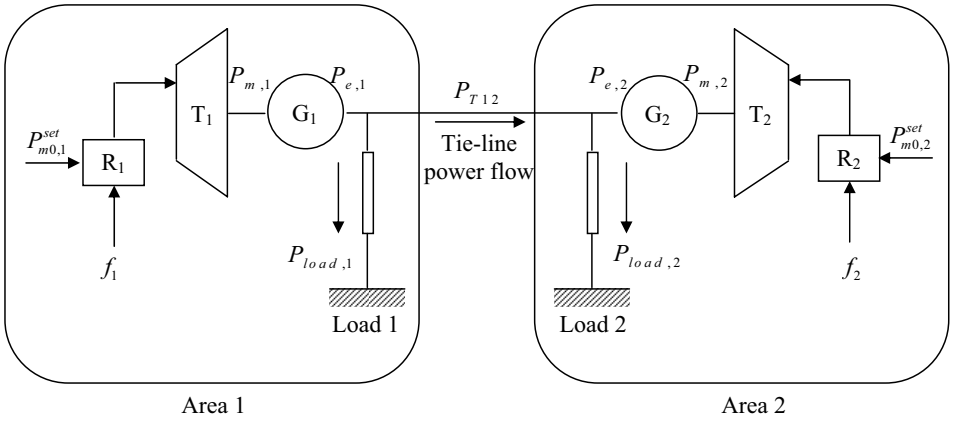

Figure 3.13. Simplified representation of a power system with two areas.

In order to adapt our dynamic frequency model accordingly, the power exchange P_{T12} over the tie line between the areas 1 and 2 has to be modelled. This is given by

$$P_{T12} = \frac{U_1 U_2}{X} \sin(\varphi_1 - \varphi_2) \tag{3.24}$$

where X is the (equivalent) reactance of the tie line. For small deviations (U_1 and U_2 are constant) one gets

$$\Delta P_{T12} = \frac{\partial P_{T12}}{\partial \varphi_1} \Delta\varphi_1 + \frac{\partial P_{T12}}{\partial \varphi_2} \Delta\varphi_2 = \frac{U_1 U_2}{X} \cos(\varphi_{0,1} - \varphi_{0,2})(\Delta\varphi_1 - \Delta\varphi_2) \tag{3.25}$$

or

$$\Delta P_{T12} = \hat{P}_T (\Delta\varphi_1 - \Delta\varphi_2) \tag{3.26}$$

with

$$\hat{P}_T = \frac{U_1 U_2}{X} \cos(\varphi_{0,1} - \varphi_{0,2}) \quad . \tag{3.27}$$

By using this model, the block diagram of the power system can be extended as shown in Figure 3.14.

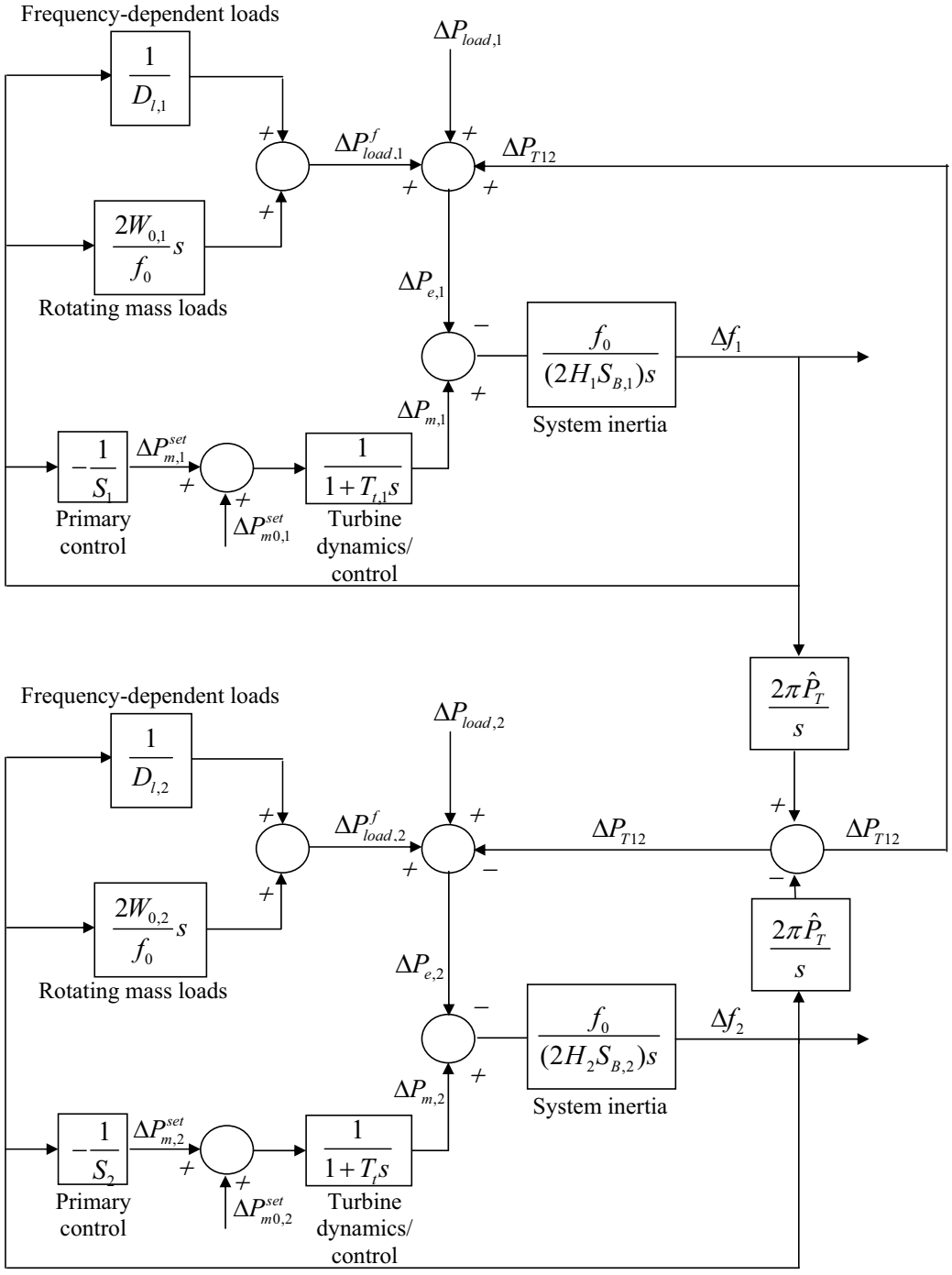

Figure 3.14. Two-area dynamic model including tie-line flows.

3.3.4 Dynamic Response of the Two-Area System

For the case regarded here, it is assumed that one of the areas is much smaller than the other. The bigger one of the two areas can then be regarded as an infinite bus in our analysis. We will now study the behaviour after a load change in the smaller area, Area 1. The system to be studied is depicted in Figure 3.15.

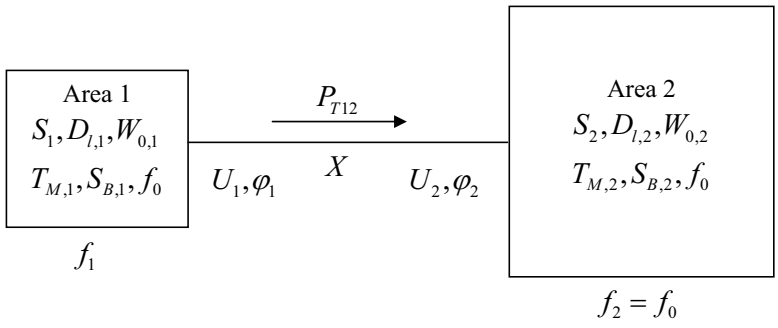

Figure 3.15. Model of a two area system. Area 1 is much smaller than Area 2.

As Area 2 is very big (infinite bus) it follows that

$$\frac{T_{M,2}S_{B2}}{f_0} \gg \frac{T_{M,1}S_{B1}}{f_0} \Rightarrow f_2 = \text{constant} \Rightarrow \Delta\varphi_2 = 0 \tag{3.28}$$

and consequently

$$\Delta P_{T12} = -\Delta P_{T21} = \hat{P}_T \Delta\varphi_1 = 2\pi\hat{P}_T \int \Delta f_1 dt \tag{3.29}$$

Without any scheduled generator setpoint changes, i.e. $\Delta P^{set}_{m0,i} = 0$, the following transfer functions apply for a change in the Area 1 system load $\Delta P_{load,1}(s)$:

$$\Delta f_1(s) = \frac{-s}{2\pi\hat{P}_T + (\frac{1}{D_{l,1}} + \frac{1}{S_{B,1}(1+sT_t)})s + \frac{T_{M,1}S_{B,1}}{f_0}s^2}\Delta P_{load,1}(s) \tag{3.30}$$

$$\Delta P_{T12}(s) = \frac{2\pi\hat{P}_T}{s}\Delta f_1(s) \tag{3.31}$$

$$\Delta P_{T12}(s) = \frac{-2\pi\hat{P}_T}{2\pi\hat{P}_T + (\frac{1}{D_{l,1}} + \frac{1}{S_{B,1}(1+sT_t)})s + \frac{T_{M,1}S_{B,1}}{f_0 s^2}}\Delta P_{load,1}(s) \tag{3.32}$$

The response for

$$\Delta P_{load,1}(s) = \frac{\Delta P_{load,1}}{s} \tag{3.33}$$

is shown if Figure 3.16. The steady state frequency deviation is

$$\Delta f_{1,\infty} = \lim_{s \to 0}(s \cdot \Delta f_1(s)) = 0 \tag{3.34}$$

and the steady state deviation of the tie line power is

$$\Delta P_{T12,\infty} = \lim_{s \to 0}(s \cdot \Delta P_{T12}(s)) = -\Delta P_{load,1} \tag{3.35}$$

The infinite bus brings the frequency deviation Δf_1 back to zero. This is achieved by increasing the tie-line power so the load increase is fully compensated. While this is beneficial for the system frequency in Area 1, a new, unscheduled and persisting energy exchange has arisen between the two areas.

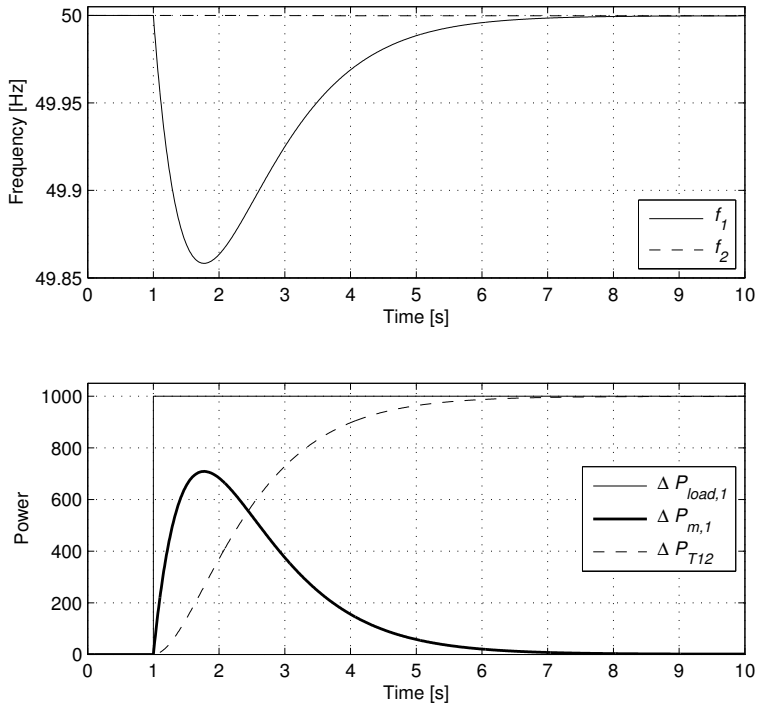

Figure 3.16. Step response for the system in Figure 3.14 resp. Figure 3.15. Only primary control is used and the system is parameterized according to Table 3.1. The upper diagram shows the frequencies f_1 in Area 1 and f_2 in Area 2. The lower diagram shows the step in the system load $\Delta P_{load,1}$, the turbine power $\Delta P_{m,1}$ and the tie-line power $\Delta P_{T21} = -\Delta P_{T12}$.

Parameter	Value	Unit
H_1	5	s
H_2	5	s
$S_{B,1}$	10	GW
$S_{B,2}$	10	TW
f_0	50	Hz
$D_{l,1}$	$\frac{1}{200}$	$\frac{\text{Hz}}{\text{MW}}$
$D_{l,2}$	$\frac{1}{200}$	$\frac{\text{Hz}}{\text{TW}}$
$W_{0,1}$	0	$\frac{\text{MW}}{\text{Hz}}$
$W_{0,2}$	0	$\frac{\text{MW}}{\text{Hz}}$
S_1	$\frac{1}{5000}$	$\frac{\text{Hz}}{\text{MW}}$
S_2	$\frac{1}{5000}$	$\frac{\text{Hz}}{\text{MW}}$
$\hat{P}_T$	533.33	MW
$\Delta P_{load,1}$	1000	MW

Table 3.1. Parameters for time domain simulation of the two-area power system corresponding to Figure 3.16.

3.4 Turbine Modelling and Control

This section gives an overview of the modelling of both steam and hydro turbines, control valves and governors. Their characteristics and behaviour are also briefly discussed. The aim here is to give an understanding of the basic physical mechanisms behind these models that are very commonly used in simulation packages for the study of power systems dynamics. In the dynamic frequency model of the power system derived so far (as depicted in Figure 3.11), the linearized dynamic models of the turbines will enter in the block "Turbine dynamics/control".

3.4.1 Turbine Models

Steam Turbines

Figures 3.17, 3.18, and 3.19 show the most common steam turbines and their models. It is outside the scope of these lecture notes to give a detailed derivation and motivation of these models, only a brief qualitative discussion will be provided. In a steam turbine the stored energy of high temperature and high pressure steam is converted into mechanical (rotating) energy, which then is converted into electrical energy in the generator. The original source of heat can be a furnace fired by fossil fuel (coal, gas, or oil) or biomass, or it can be a nuclear reactor.

The turbine can be either *tandem compound* or *cross compound*. In a tandem compound unit all sections are on the same shaft with a single generator, while a cross compound unit consists of two shafts each connected to a generator. The cross compound unit is operated as one unit with one set of controls. Most modern units are of tandem compound type, even if the crossover compound units are more efficient and have higher capacity. However, the costs are higher and could seldom be motivated.

The power output from the turbine is controlled through the position of the *control valves*, which control the flow of steam to the turbines. The valve position is influenced by the output signal of the turbine controller. Following the nomenclature introduced in Figure 3.10, this signal is defined as

$$\Delta P_m^{ctrl} = \frac{1}{T_t s}(\Delta P_{m0}^{set} + \Delta P_m^{set} - \Delta P_m)\,. \tag{3.36}$$

The delay between the different parts of the steam path is usually modelled by a first order filter as seen in Figures 3.17, 3.18, and 3.19. Certain fractions of the total power are extracted in the different turbines, and this is modelled by the factors F_{VHP}, F_{HP}, F_{IP}, F_{LP} in the models. Typical values of the time constant of the delay between the control valves and the high-pressure turbine, T_{CH}, is $0.1 - 0.4$ s. If a re-heater is installed, the time delay is larger, typically $T_{RH} = 4 - 11$ s. The time constant of the delay between the intermediate and low pressure turbines, T_{CO}, is in the order of $0.3-0.6$ s.

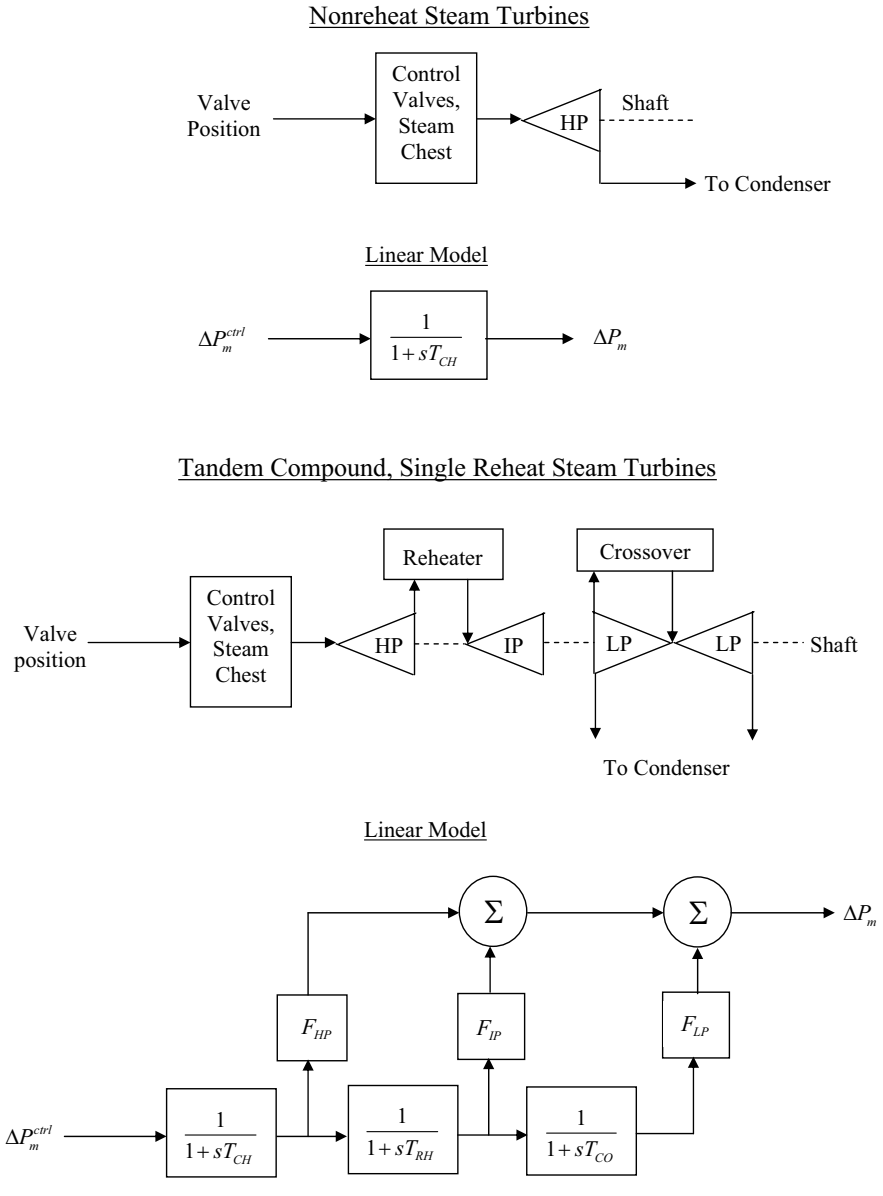

Figure 3.17. Steam turbine configurations and approximate linear models. Nonreheat and tandem compound, single reheat configurations.

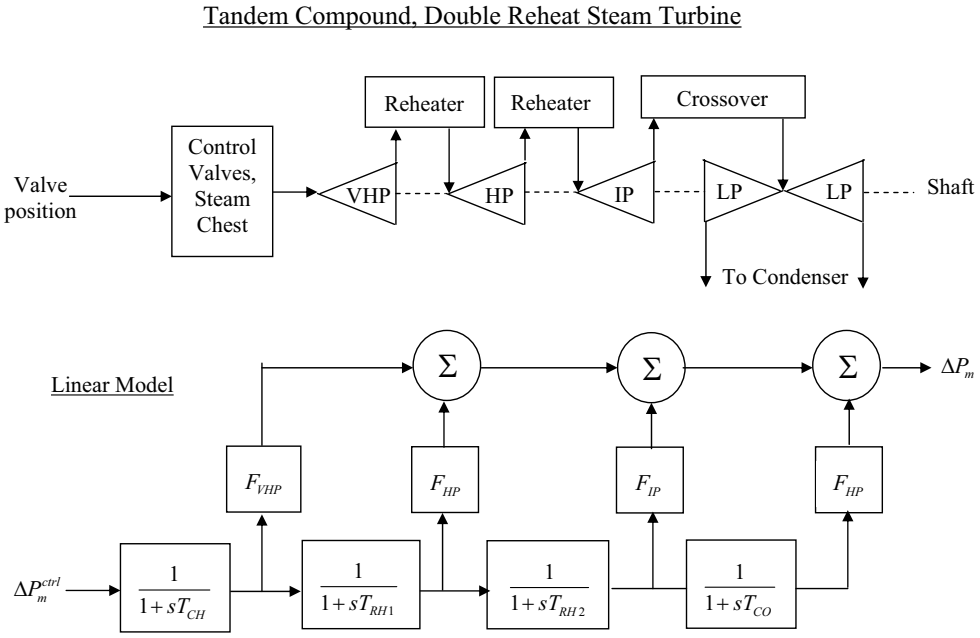

Figure 3.18. Steam turbine configurations and approximate linear models. Tandem compound, double reheat configuration.

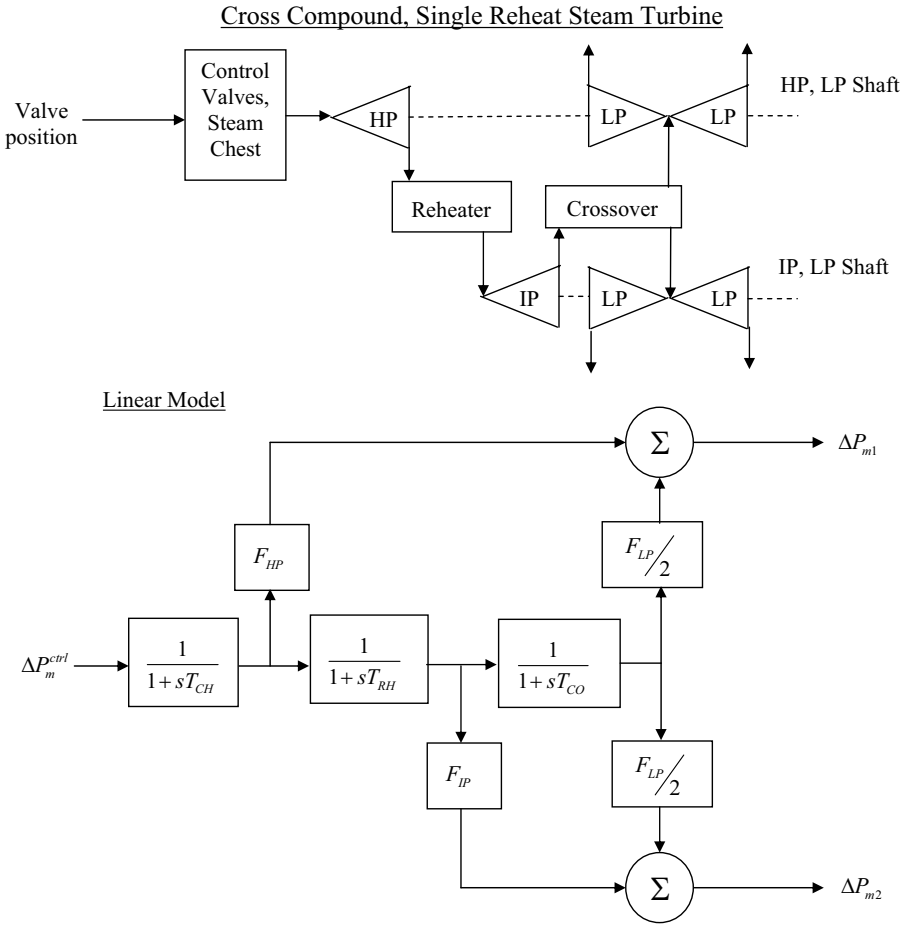

Figure 3.19. Steam turbine configurations and approximate linear models. Cross compound, single reheat configuration.

Step Response To illustrate the dynamics of a steam turbine, the configuration with tandem compound, single reheat, Figure 3.17, with the following data will be studied:

$T_{CH} = 0.1$ s, $T_{RH} = 10$ s, $T_{CO} = 0.3$ s

$F_{HP} = 0.3$, $F_{IP} = 0.4$, $F_{LP} = 0.3$

As $T_{CH} \ll T_{RH}$ und $T_{CO} \ll T_{RH}$, we can assume $T_{CH} = T_{CO} = 0$ for an approximate analysis. Then a simplified block diagram according to Figure 3.20 can be used. For this system the step response is easy to calculate. It is depicted in Figure 3.21.

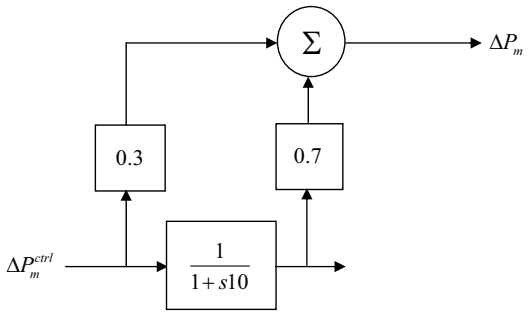

Figure 3.20. Simplified model of tandem compound, single reheat system in Figure 3.17.

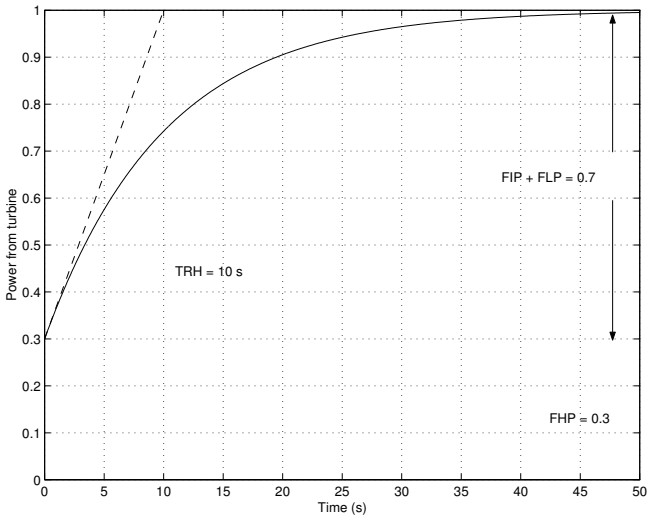

Figure 3.21. Step response of system in Figure 3.20.

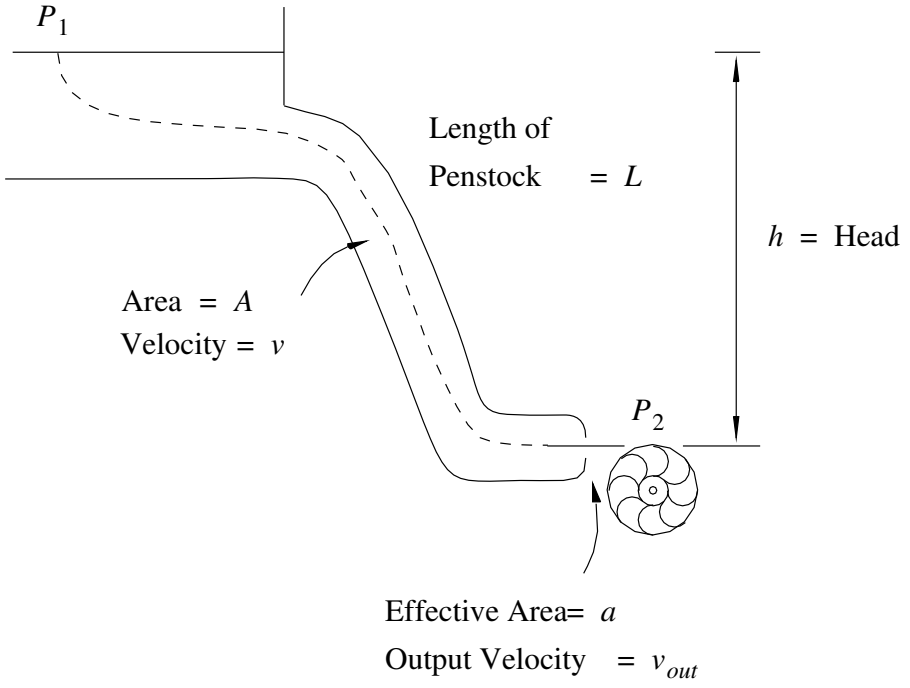

Figure 3.22. Schematic drawing of hydro turbine with water paths.

Hydro Turbines

Compared with steam turbines, hydro turbines are easier and cheaper to control. Thus, frequency control is primarily done in the hydro power plants if available. If the amount of hydro–generated power in a system is not sufficient, the steam turbines have to be included in the frequency control.

The power produced by a generator is determined by the turbine governor and the dynamic properties of the turbine. Thus, to be able to determine the frequency's dynamic behaviour, models for the turbine as well as for the turbine control are necessary.

Figure 3.22 depicts a hydro turbine with penstock and hydro reservoir and defines the notation that will be used from now on. Bernoulli's equation for a trajectory between the points P_1 and P_2 can be written as

$$\int_{P_1}^{P_2} \frac{\partial \overline{v}}{\partial t} \cdot d\overline{r} + \frac{1}{2}(v_2^2 - v_1^2) + \Omega_2 - \Omega_1 + \int_{P_1}^{P_2} \frac{1}{\rho} dp = 0 \ . \tag{3.37}$$

The following assumptions are usually made:

- $v_1 = 0$, since the reservoir is large and the water level does not change during the time scale that is of interest here.

- The water velocity is non–zero only in the penstock.
- The water is incompressible, i.e. ρ does not change with water pressure.
- The water pressure is the same at P_1 and P_2, i.e. $p_1 = p_2$.

Further,

$$\Omega_2 - \Omega_1 = -gh \ . \tag{3.38}$$

The above assumptions together with eq. (3.38) make it possible to write (3.37), with $v_{out} = v_2$ and the length of the penstock L, as

$$L\frac{dv}{dt} + \frac{1}{2}v_{out}^2 - gh = 0 \ . \tag{3.39}$$

The velocity of the water in the penstock is v. The effective opening of the penstock, determined by the opening of the turbine's control valve (guide vanes), is denoted a. If the penstock's area is A,

$$v_{out} = \frac{A}{a}v \tag{3.40}$$

is valid and eq. (3.39) can be written as

$$\frac{dv}{dt} = \frac{1}{L}gh - \frac{1}{2L}\left(\frac{A}{a}v\right)^2 \ . \tag{3.41}$$

The maximum available power at the turbine is

$$P = \frac{1}{2}\rho a v_{out}^3 = \frac{1}{2}\rho\frac{A^3v^3}{a^2} \ . \tag{3.42}$$

To get the system into standard form,

$$\begin{cases} x &= v \ , \\ u &= \dfrac{a}{A} \ , \\ y &= P \ , \end{cases} \tag{3.43}$$

are introduced. (Here, we have used the standard notation, i.e. x for state, u for control signal, and y for output signal.) The system now can be written as

$$\begin{cases} \dot{x} &= \dfrac{gh}{L} - x^2\dfrac{1}{2Lu^2} \ , \\ y &= \rho A\dfrac{x^3}{2u^2} \ . \end{cases} \tag{3.44}$$

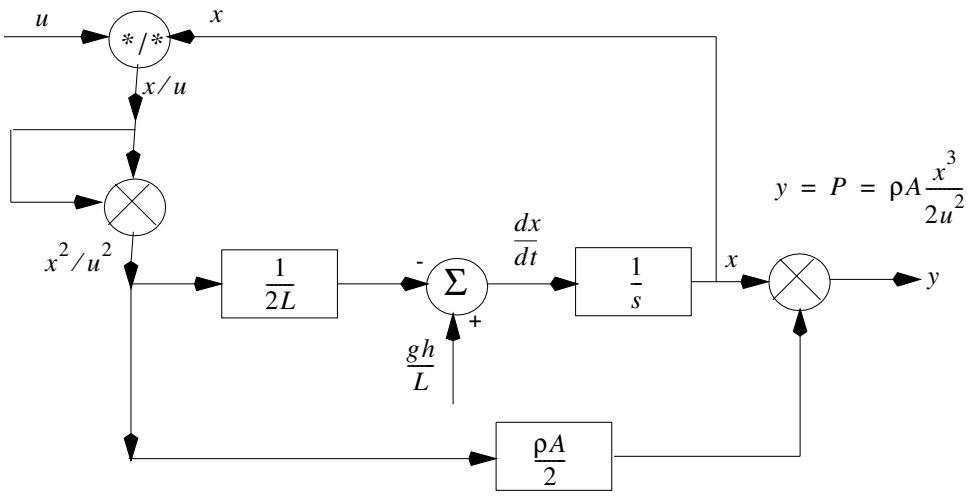

Figure 3.23. Block diagram showing model of hydro turbine.

The system corresponding to eq. (3.44) can be described with the block diagram in Figure 3.23.

Eq. (3.44) is nonlinear and a detailed analysis is beyond the scope of these lecture notes. To get an idea of the system's properties, the equations are linearised, and small variations around an operating point are studied. In steady state, $\dot{x} = 0$, and the state is determined by x_0, u_0, and y_0, which fulfils

$$\begin{cases} x_0 &= u_0\sqrt{2gh} \ , \\ \\ y_0 &= \dfrac{\rho A x_0^3}{2u_0^2} \ . \end{cases} \tag{3.45}$$

Small deviations Δx, Δu, and Δy around the operating point satisfy

$$\begin{cases} \Delta\dot{x} &= -2x_0\dfrac{1}{2Lu_0^2}\Delta x + \dfrac{2x_0^2}{2Lu_0^3}\Delta u \ , \\ \\ \Delta y &= 3\rho\dfrac{Ax_0^2}{2u_0^2}\Delta x - 2\rho\dfrac{Ax_0^3}{2u_0^3}\Delta u \ , \end{cases} \tag{3.46}$$

which, using eqs. (3.45), can be written as

$$\begin{cases} \Delta\dot{x} &= -\dfrac{\sqrt{2gh}}{u_0 L}\Delta x + \dfrac{2gh}{u_0 L}\Delta u \ , \\ \\ \Delta y &= \dfrac{3y_0}{u_0\sqrt{2gh}}\Delta x - \dfrac{2y_0}{u_0}\Delta u \ . \end{cases} \tag{3.47}$$

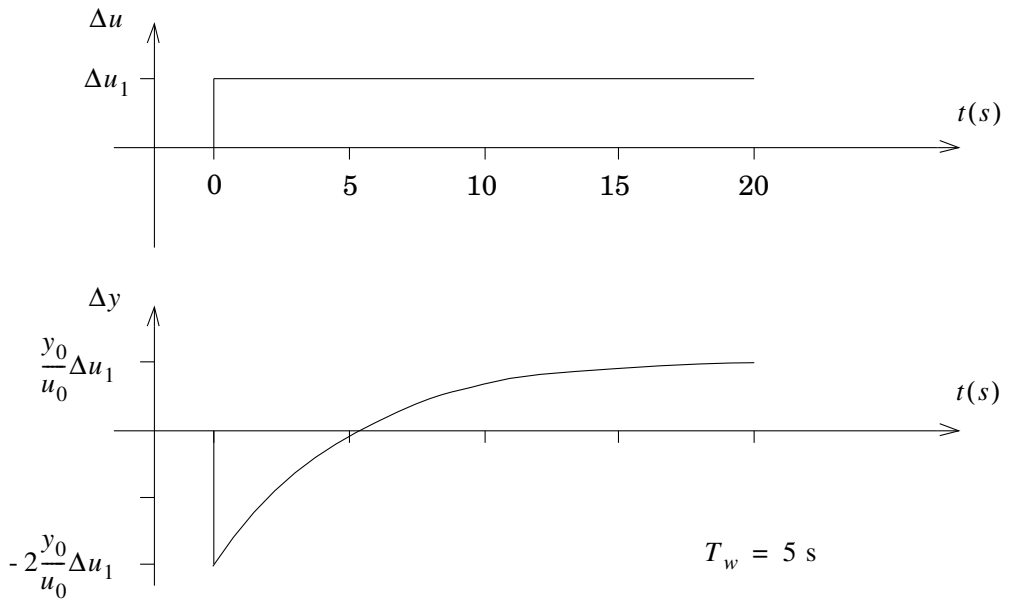

Figure 3.24. The variation of the produced power, Δy, after a step change in the control valve.

The quantity $L/\sqrt{2gh}$ has dimension of time, and from the above equations it is apparent that this is the time it takes the water to flow through the penstock if $a = A$. That time is denoted T:

$$T = L/\sqrt{2gh} \ . \tag{3.48}$$

If eqs. (3.47) are Laplace–transformed, Δx can be solved from the first of the equations, leading to

$$\Delta x = \frac{L/T}{1 + su_0T}\Delta u \ , \tag{3.49}$$

which, when inserted in the lower of eqs. (3.47) gives

$$\Delta y = \frac{y_0}{u_0} \cdot \frac{1 - 2u_0Ts}{1 + u_0Ts}\Delta u \ . \tag{3.50}$$

The quantity $u_0T = a_0T/A$ also has dimension of time and is denoted T_w. The time constant T_w is the time it takes for the water to flow through the penstock when $a = a_0$ or $u = u_0$, i.e. for the operation point where the linearization is done. Eq. (3.50) can thus be written as

$$\Delta y = \frac{y_0}{u_0} \cdot \frac{1 - 2T_ws}{1 + T_ws}\Delta u \ . \tag{3.51}$$

It is evident that the transfer function in eq. (3.51) is of non–minimum phase, i.e. not all poles and zeros are in the left half plane. In this case, one zero is in the right half plane. That is evident from the step response to eq. (3.51), depicted in Figure 3.24.

The system has the peculiar property to give a lower power just after the opening of the control valve is increased before the desired increased power generation is reached. The physical explanation is the lower pressure appearing after the control valve is opened, so that the water in the penstock can be accelerated. When the water has been accelerated, the generated power is increased as a consequence of the increased flow. That property of water turbines places certain demands on the design of the control system for the turbines.

3.4.2 Steam Turbine Control Valves

As stated earlier, the control input of the steam turbine acts on a valve which influences the inflow of live steam into the turbine. As the valve cannot be moved at infinite speed, a further dynamics is introduced into the system. This is usually modelled by a first-order element. Furthermore, constraints exist on the ramp rate (speed of the valve motion) and the absolute valve position. Note that, if the block diagram is expressed in Δ quantities, the latter has to be formulated in Δ quantities as well, taking into account the steady-state valve position. Figure 3.25 depicts the corresponding block diagram.

Note that this block must be inserted between the turbine controller output ΔP_m^{ctrl} and the turbine input when the valve dynamics shall be considered. The output of the valve can be named then ΔP_m^{ctrl} and its input could be renamed to e.g. $\Delta P_m^{ctrl^*}$.

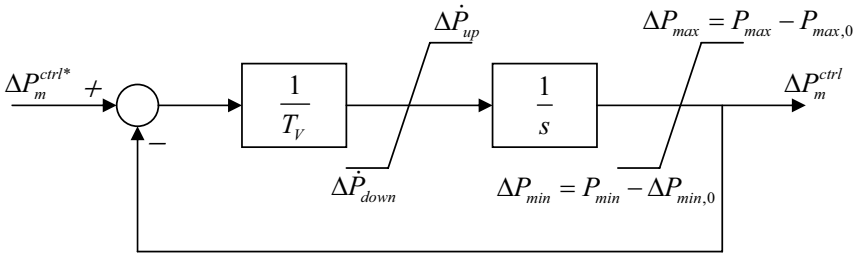

Figure 3.25. Model of a control valve.

3.4.3 Hydro Turbine Governors

The task of a turbine governor is to control the turbine power output such that it is equal to a set value which consists of a constant and a frequency-dependent part, the latter of which is of interest here. For steam turbines, this has been discussed in Section 3.1. Because of the particularities of hydro turbines, which have been shown in Section 3.4.1, another type of governor is needed.

A model of a hydro turbine governor is given in Figure 3.26. The control servo is here represented simply by a time constant T_p. The main servo, i.e. the guide vane, is represented by an integrator with the time constant T_G. Typical values for these parameters are given in Table 3.2. Limits for opening and closing speed as well as for the largest and smallest opening of the control valve are given.

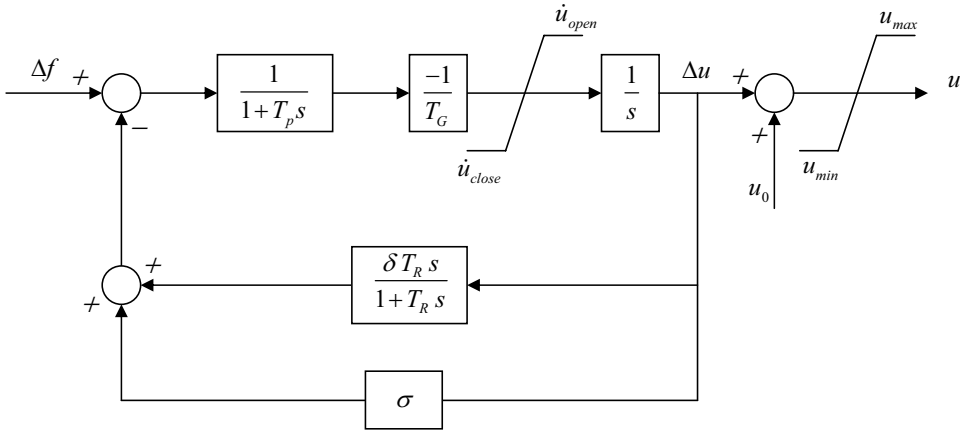

Figure 3.26. Model of turbine governor for hydro turbine.

Parameter	Typical Values
T_R	2.5 – 7.5 s
T_G	0.2 – 0.4 s
T_p	0.03 – 0.06 s
δ	0.2 – 1
σ	0.03 – 0.06

Table 3.2. Typical values for some parameters of the turbine governor for hydro power.

The controller has two feedback loops, a transient feedback loop and a static feedback loop. The transient feedback loop has the amplification δ for high frequencies. Thus, the total feedback after a frequency change is $-(\delta + \sigma)$. In steady state, the transient feedback is zero, and the ratio between the frequency deviation and the change in the control valve is given by

$$\Delta u = -\frac{1}{\sigma}\Delta f \quad . \tag{3.52}$$

Using eq. (3.51), the stationary change of power is obtained as

$$\Delta P = -\frac{1}{\sigma}\frac{P_0}{u_0}\Delta f \quad . \tag{3.53}$$

Thus, the speed droop for generator i, S_i, is

$$S_i = \sigma_i \frac{u_{0i}}{P_{0i}} \quad , \tag{3.54}$$

and the total speed droop, S, in the system is given by

$$S^{-1} = \sum_i S_i^{-1} \quad . \tag{3.55}$$

The transient feedback is needed since the water turbine is a non–minimum phase system as discussed above. With static feedback only, the control performance will be unsatisfactory when closed-loop stability shall be guaranteed. Increasing the static feedback to a range where a reasonable control performance could be attained will make the system unstable.

The transient feedback loop provides an additional feedback component during non-stationary operating conditions. This feedback decays as steady state is attained. The initial total feedback can be about ten times larger than the static feedback, i.e. the speed droop is initially lower than its stationary value.

3.5 Dynamic Responses including Turbine Dynamics

In this section, we will simulate the dynamic responses of a power system consisting of different generation unit types with primary control equipment. The goal is to improve the understanding of the impact of the turbine dynamics on the overall control behaviour of the system.

We consider again the one-area power system as presented in Figure 3.11 with the main parameters given according to Table 3.3. As stated before, the turbine dynamics is inserted in the block "Turbine dynamics/control". The effect of three different turbine dynamics will be studied: a steam turbine without reheater, a steam turbine with reheater and a hydro turbine.

In Figure 3.27, the power system response to a load increase disturbance of $\Delta P_{load} = +1000$ MW is compared. Note that this is equivalent to the loss of a major generation unit, e.g. a nuclear power plant.

Parameter	Value	Unit
H	5	s
S_B	10	GW
f_0	50	Hz
D_L	$\frac{1}{200}$	$\frac{\text{Hz}}{\text{MW}}$
W_0	0	$\frac{\text{MW}}{\text{Hz}}$
T_{CH}	0.3	s
T_{RH}	8	s
T_{CO}	0.5	s
S	0.04	p.u.
T_W	1.4	s
T_G	0.2	s
T_R	6.5	s
σ	0.04	p.u.
δ	0.3	p.u.

Table 3.3. Parameters for time domain simulation of the power system.

The upper plot shows the frequency response of the uncontrolled power system just as a comparison. It can be seen in the following plots that the frequency control performance is highly dependent on the turbine type. While steam turbines without reheating equipment do not allow the frequency to decay substantially more than their steady-state deviation, the time delays caused by the reheater make the response a lot slower. The hydro turbine allows the most significant frequency decay before the system is brought back to the steady-state frequency.

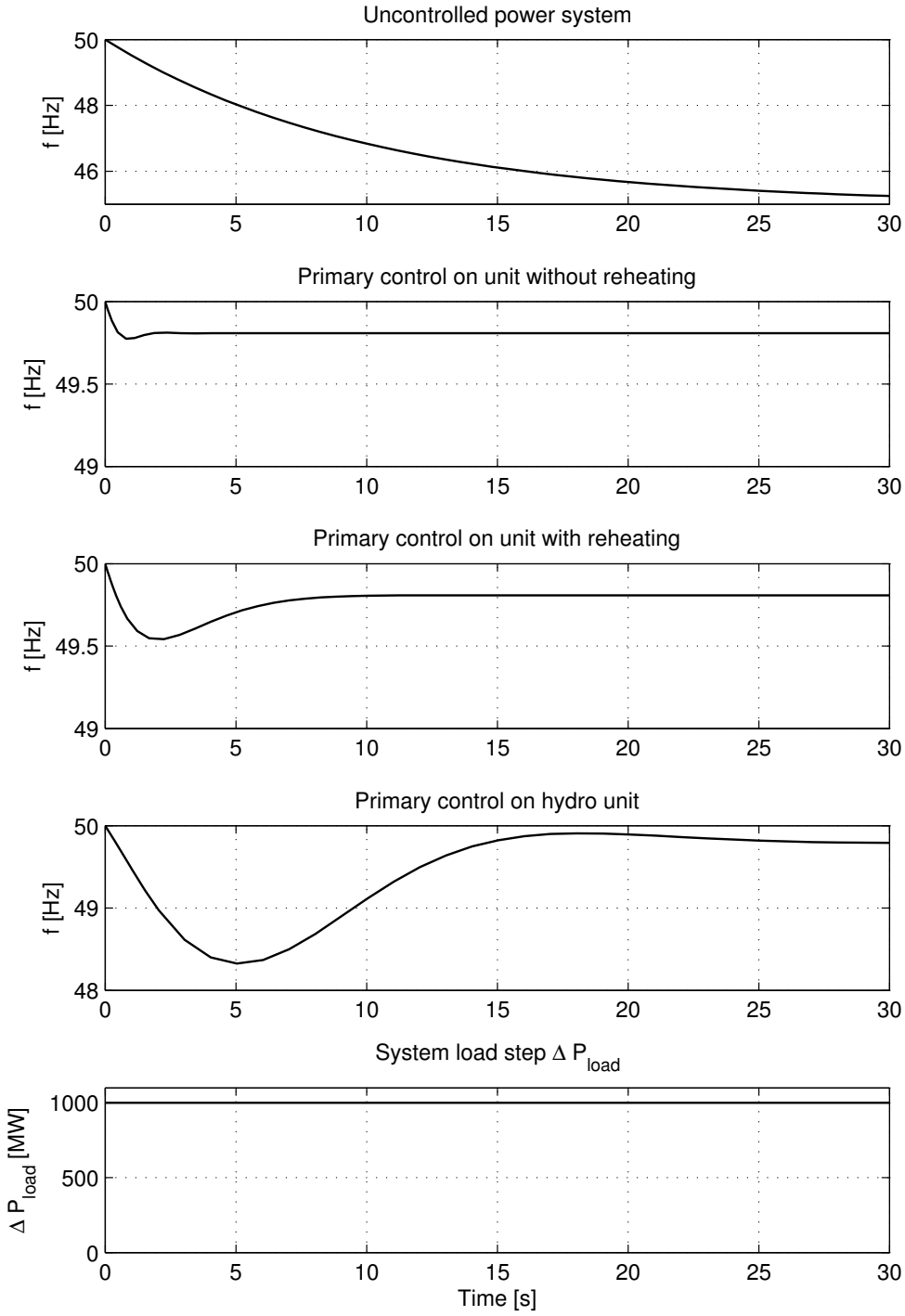

Figure 3.27. Dynamic response of the power system without primary control, with primary control on steam turbines without reheater, steam turbines with reheater, and hydro turbines.

Finally, one more illustration of the effect of the turbine dynamics shall be given. For a direct comparison of a primary-controlled one-area system without and with turbine dynamics, the exemplary system simulated in Figure 3.12 is now simulated again with a steam turbine model without reheater ($T_{CH} = 0.3$ s). The result is shown in Figure 3.28.

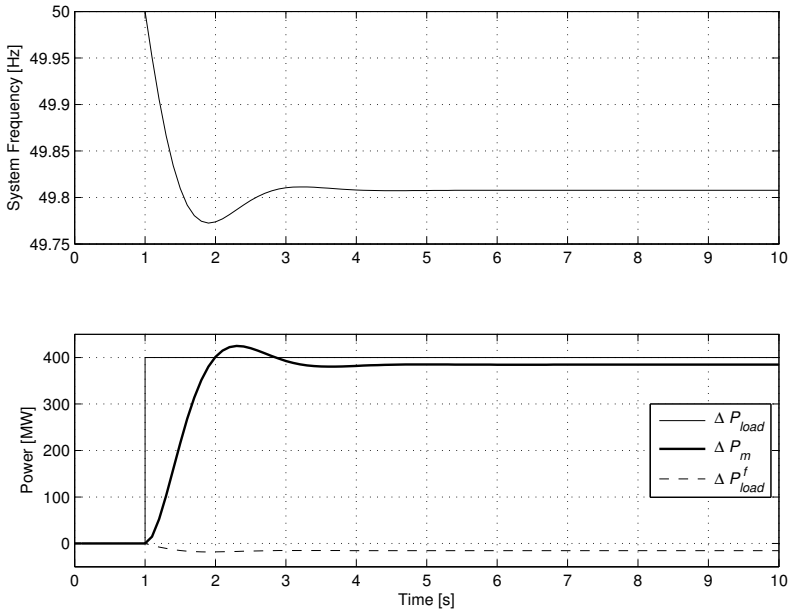

Figure 3.28. Behaviour of the one-area system (including dynamics of steam turbine without reheater, otherwise same parameterization as in Figure 3.12) after a step increase in load. The upper plot shows the system frequency f. The lower plot shows the step function in ΔP_{load}, the increase in turbine power ΔP_m, and the frequency-dependent load variation ΔP^f_{load}.

4
Load Frequency Control

In this chapter the secondary, or load-frequency, control of power systems will be discussed. Simple models that enable the simulation of the dynamic behaviour during the action of frequency controllers will also be derived and studied.

In the previous chapter, the role of the primary frequency control was dealt with. It was shown that after a disturbance a static frequency error will persist unless additional control actions are taken. Furthermore, the primary frequency control might also change the scheduled interchanges between different areas in an interconnected system. To restore the frequency and the scheduled power interchanges, additional control actions must be taken. This is done through the *Load-Frequency Control* (LFC). The LFC can be done either manually through operator interaction or automatically. In the latter case it is often called *Automatic Generation Control* (AGC). The characteristics of AGC will be studied in the subsequent sections, both during steady state and dynamic conditions.

4.1 Static Characteristics of AGC

The overall purpose of the Automatic Generation Control comprises two main aspects:

- Keep the frequency in the interconnected power system close to the nominal value.[1]
- Restore the scheduled interchanges between different areas, e.g. countries, in an interconnected system.

The mechanisms of AGC that enable it to fulfill these requirements will be outlined in the sequel.

[1] In many systems, deviations of up to ± 0.1 Hz from the nominal value (50 or 60 Hz) is deemed as acceptable in steady state. In some systems, North America, even tighter tolerance bands are applied, while recently in UK the tolerance band has been relaxed somewhat.

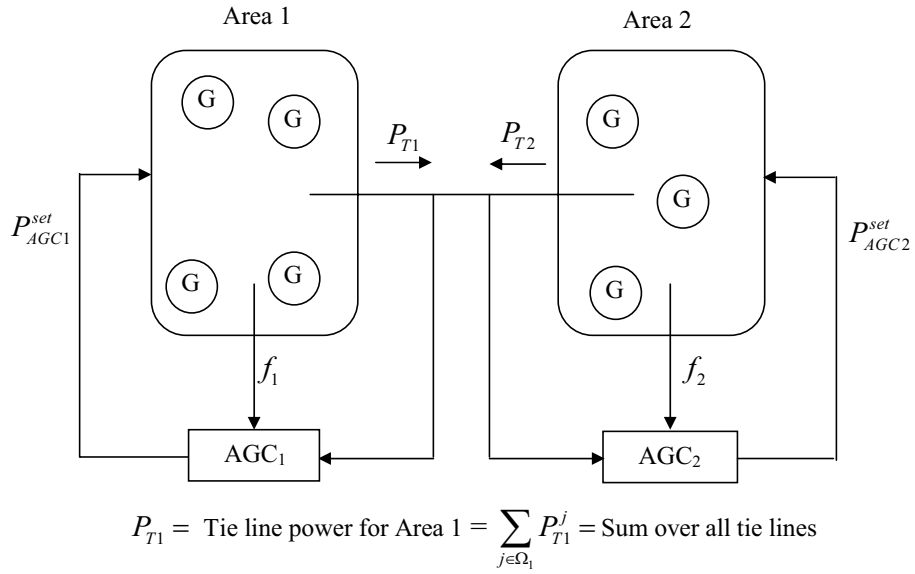

Figure 4.1. Two area system with AGC.

Consider a two area system as depicted in Figure 4.1. The two secondary frequency controllers, AGC_1 and AGC_2, will adjust the power reference values of the generators participating in the AGC. In an N-area system, there are N controllers AGC_i, one for each area i. A block diagram of such a controller is given in Figure 4.2. A common way is to implement this as a proportional-integral (PI) controller:

$$\Delta P_{AGCi} = -(C_{pi} + \frac{1}{sT_{Ni}})\Delta e_i \tag{4.1}$$

where $C_{pi} = 0.1 \ldots 1.0$ and $T_{Ni} = 30 \ldots 200$ s. The error Δe_i is called *Area Control Error, ACE_i* for area i.

We will now consider a system with N areas. The ACEs are in this case:

$$ACE_i = \sum_{j\in\Omega_i} (P^j_{Ti} - P^j_{T0i}) + B_i(f - f_0) \quad i = 1, 2, \ldots, N \ . \tag{4.2}$$

Defining now

$$\Delta P_{Ti} = \sum_{j\in\Omega_i} (P^j_{Ti} - P^j_{T0i}) \ , \tag{4.3}$$

the ACE can be written as

$$ACE_i = \Delta P_{Ti} + B_i\Delta f \quad i = 1, 2, \ldots, N \ . \tag{4.4}$$

The set Ω_i consist of all areas connected to area i for which the tie line powers should be controlled to the set value P^j_{T0i}. The constants B_i are

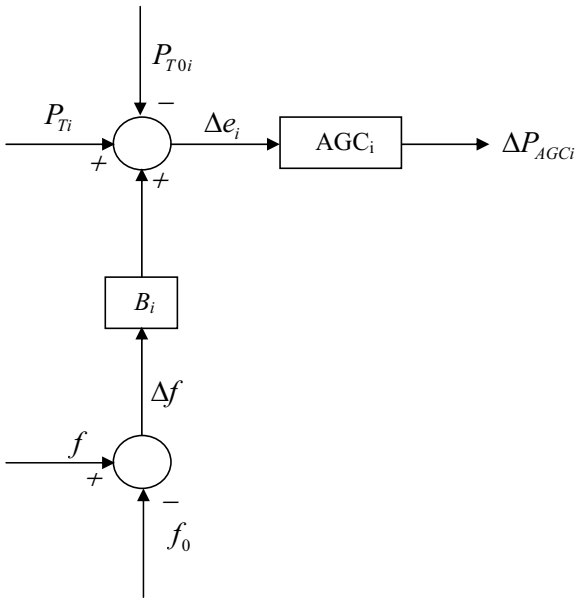

Figure 4.2. Control structure for AGC (Δe_i = Error = ACE_i = Area Control Error for area i)

called *frequency bias factors* [MW/Hz]. It is assumed that the frequency references are the same in all areas, i.e. $f_{0i} = f_0$ for all i, and f is also the same in steady state for all areas. The goal is to bring all $ACE_i \to 0$.

The variables are thus ΔP_{Ti} (N variables) and f, i.e. in total $N + 1$ variables. Since we have N equations ($ACE_i = 0$), we need one more equation. As a fifth equation we have the power balance:

$$\sum_i \Delta P_{Ti} = 0 \ , \tag{4.5}$$

and consequently a solution can be achieved.

In steady state, f is identical for all areas, and we assume that the frequency is controlled back to the reference value, i.e. $f_0 = f$. If the sum of the reference values of the tie line powers P^j_{T0i} is 0, then the system will settle down to an operating point where $P^j_{T0i} = P^j_{Ti}$ for all tie line powers. The time constants of the AGC is chosen such that it reacts much slower than the primary frequency control.

Selection of Frequency Bias Factors

Consider the two area system in Figure 4.1. The load is now increased with ΔP_{load} in area 2. If the tie line power should be kept the same, the generation must be increased in area 2 with ΔP_{load} after the AGC has reacted. Before the AGC has reacted we have a frequency deviation of Δf in both areas,

which means that for area 1

$$\Delta f = -S_1 \Delta P_{T1} \tag{4.6}$$

and for area 2

$$\Delta f = -S_2(\Delta P_{load} - \Delta P_{T1}) \tag{4.7}$$

and $\Delta P_{T1} = -\Delta P_{T2}$. The two ACEs can now be written as

$$ACE_1 = \Delta P_{T1} + B_1 \Delta f = \Delta P_{T1} + B_1(-S_1 \Delta P_{T1}) = \Delta P_{T1}(1 - B_1 S_1) \tag{4.8}$$

and

$$ACE_2 = \Delta P_{T2} + B_2 \Delta f = \Delta P_{T2} + B_2(-S_2(\Delta P_{load} - \Delta P_{T1})) = \Delta P_{T2}(1 - B_2 S_2) - B_2 S_2 \Delta P_{load} \tag{4.9}$$

In this case it is desirable that the AGC controller in area 1 does not react. If we set $B_1 = 1/S_1$ we see from eq. (4.8) that $ACE_1 = 0$. This is called *Non Interactive Control*. If $B_2 = 1/S_2$ is chosen the ACE in area 2 becomes

$$ACE_2 = -\Delta P_{load} \tag{4.10}$$

This means that only controller 2 reacts and the load increase ΔP_{load} is compensated for in area 2 by the PI control law as stated in eq. (4.1).

However, as long as the controller in eq. (4.1) has an integrating part, all positive values of B_i will guarantee that all $ACE_i \to 0$. The choice according to *Non Interactive Control* has been found to give the best dynamic performance through a number of investigations. In a multi-area case this corresponds to selecting $B_i = 1/S_i$ for all areas.

4.2 Dynamic Characteristics of AGC

As in the previous chapter on primary frequency control, we will now develop a dynamic model of the power system where the newly introduced AGC is included. As the way of extracting input-output transfer functions from block diagrams has already been presented in the last chapter, we omit the analytical derivation here for shortness. The interested reader is welcome to calculate the transfer function between the load disturbance and the frequency as an exercise.

4.2.1 One-area system

In a single-area power system, there is obviously no tie-line power to be controlled. In this case, the AGC only fulfills the purpose of restoring the nominal system frequency. Figure 4.3 shows the known block diagram which has been extended by the proportional-integral control law of the AGC. Figure 4.4 shows a plot of the system frequency which is brought back to the nominal value. The parameters of the system are as presented in Table 3.3 (turbine dynamics neglected), and $B = 1/S$, $C_p = 0.17$, $T_N = 120$ s.

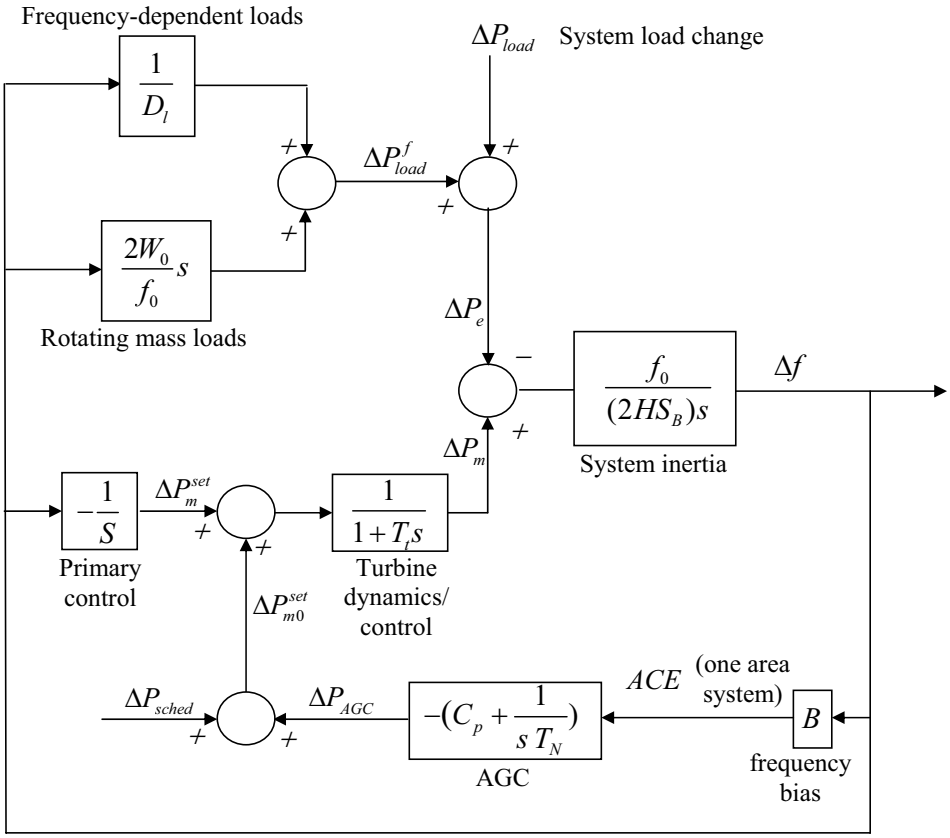

Figure 4.3. Dynamic model of one-area system with AGC.

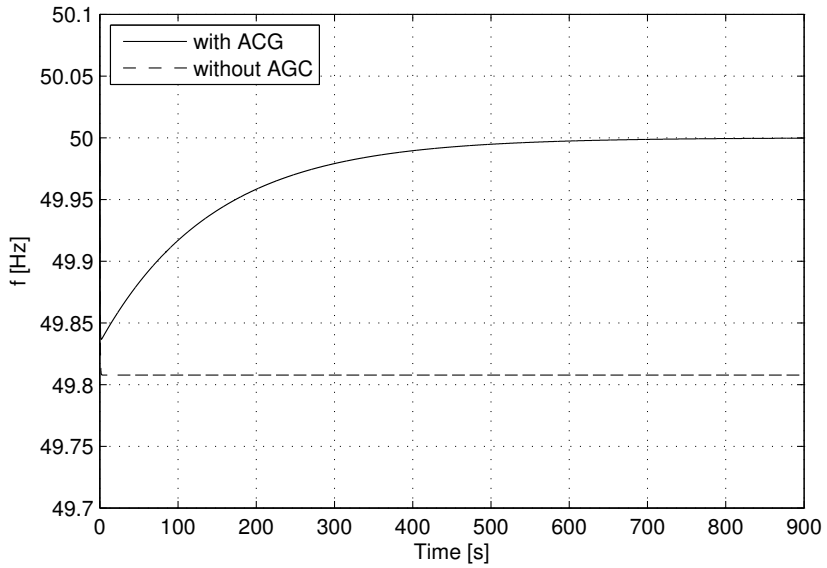

Figure 4.4. Dynamic response of the one-area system equipped with primary control and AGC compared with the same system without AGC.

4.2.2 Two-area system – unequal sizes – disturbance response

Here we consider the same two-area power system as in section 3.3.4 where Area 1 is assumed to be much smaller than Area 2. The corresponding block diagram including the AGC is shown in Figure 4.6. Because of the secondary control (AGC) one obtains the step response in Figure 4.5. The load increase of $\Delta P_{load,1} = 1000$ MW in Area 1 is in this case fully compensated by the generators in Area 1.

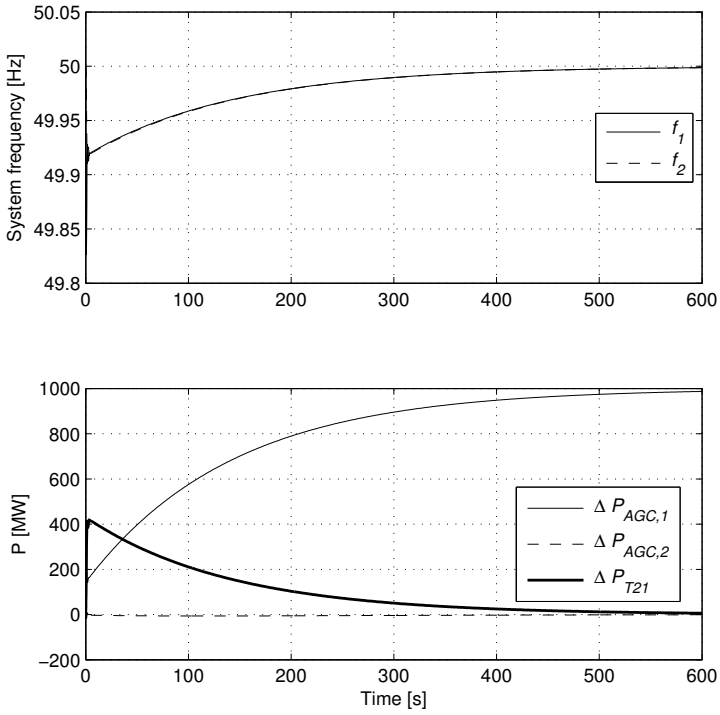

Figure 4.5. Step response for the system in Figure 4.6 with AGC. The upper diagram shows the system frequencies of Area 1 and Area 2. The lower diagram shows the control action of the AGCs in Area 1 $\Delta P_{AGC,1}$ which compensates the power deficit and in Area 2 $\Delta P_{AGC,2}$ which is largely uninfluenced by the disturbance. Furthermore, the tie line power ΔP_{T21} is shown, which initially compensates the disturbance and then slowly decays to 0.

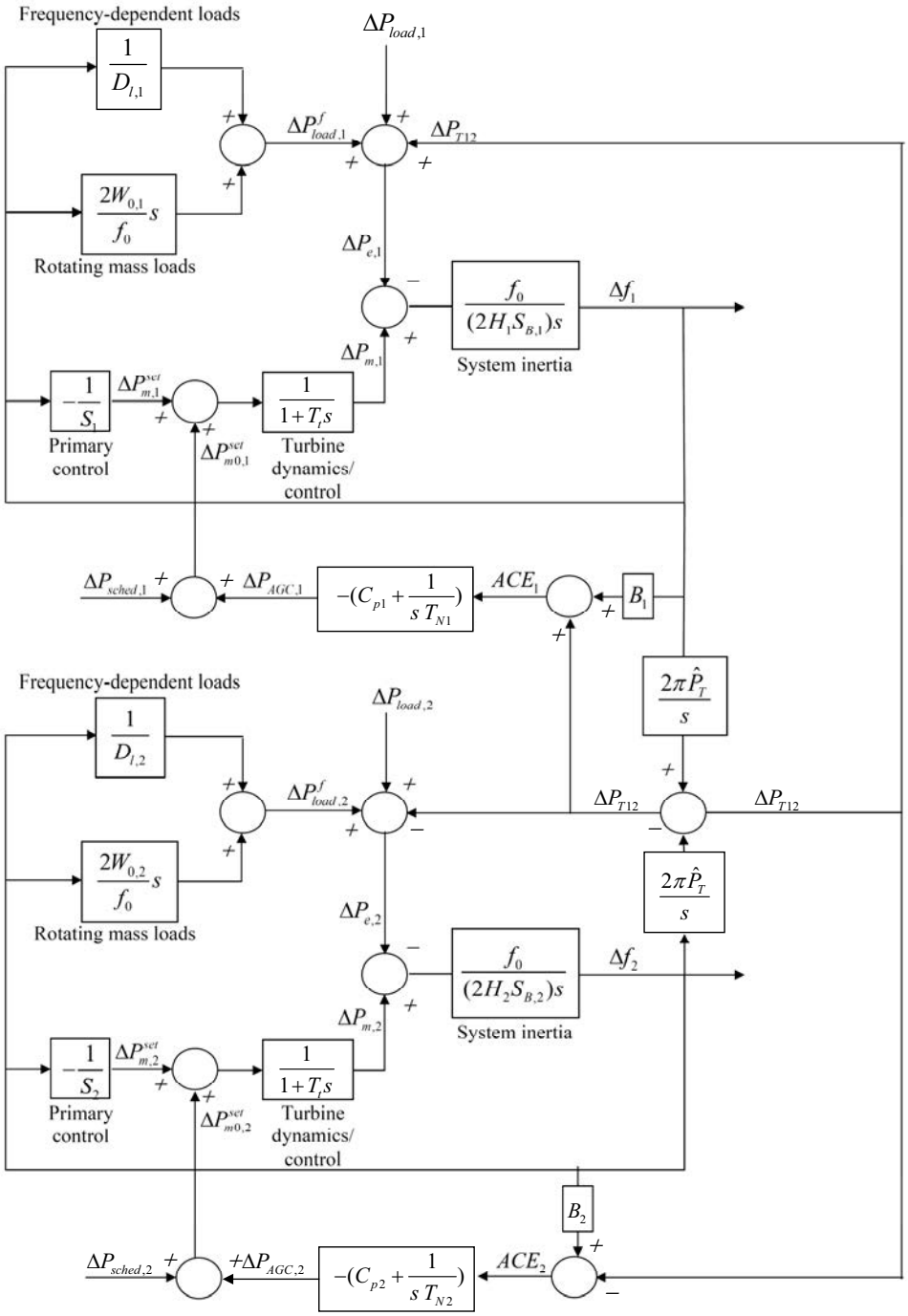

Figure 4.6. Dynamic model of two-area system with AGC.

4.2.3 Two-area system, unequal sizes – normal control operation

So far, we only simulated the dynamic response of the power system to step-wise disturbances in the load. During the everyday normal operation of a power system, however, the automatic control loops of primary and secondary control are always active to compensate for the continuously arising small imbalances between generation and load. These normal-operation imbalances are due to load fluctuations, load prediction errors, and, in the presence of intermittent infeeds (from wind power etc.) in the control area, infeed fluctuations and infeed prediction errors. In this context, the difference between fluctuation and prediction errors is constituted by the time scales on which they occur: while the term "fluctuation" is usually defined as largely uncorrelated stochastic noise on a second or minute time scale, "prediction error" usually refers to a mismatch of predicted and actual consumption/infeed on a 15-minute time scale. The latter usually shows a certain autocorrelation, which means that the probability of the signal to assume a certain value is dependent on the previously assumed signal values.

Another important impact on the AGC arises from schedule changes that occur at the full hour. The reason for this timing is the trading on electricity markets which is usually done in an hourly framework. Because of ramping actions of power plants which often deviate from the ramping profiles they are supposed to follow, imbalances just before the full hour (either positive or negative), as well as just after the full hour (then in the opposite direction) arise. This effect, however, is disregarded in the present setup.

Figure 4.7 demonstrates the response of the two-area system to a stochastically varying load. The system is parameterized again according to Table 3.1. To increase the degree of realism, the dynamic model of a steam turbine without reheater is included. As often found in practice, the primary controls are equipped with a dead band of ± 10 mHz. Saturation of the control variables (due to limited amounts of contracted control reserves) is not modelled. A detailed discussion of the synthesis of the load fluctuation and prediction error signals is beyond the scope of this lecture. Thus, only the input time series $\Delta P_{load,1}$ and $\Delta P_{load,2}$ are shown in the plot.

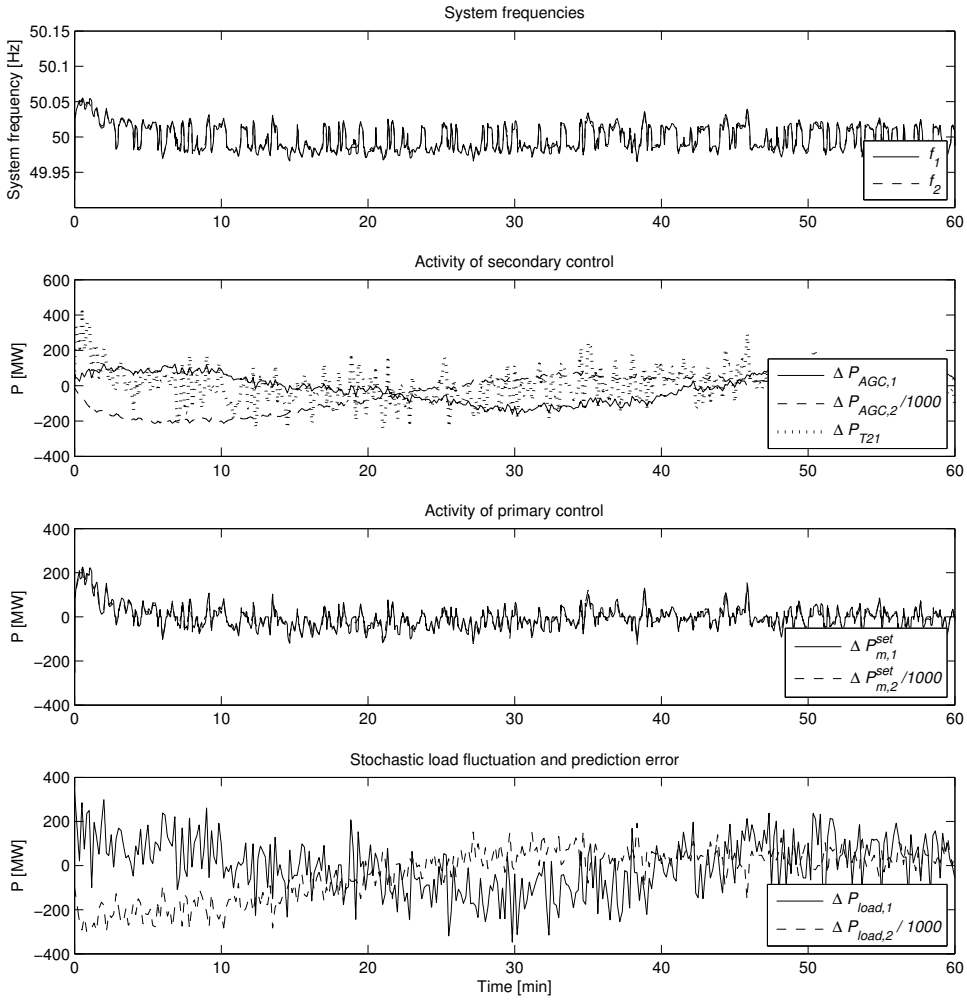

Figure 4.7. Normal operation of the two area system. The usual small mismatches between generation and demand are modelled by a stochastic disturbance in the load.

4.2.4 Two-area system – equal sizes, including saturations – disturbance response

Finally we briefly investigate the dynamic behaviour of a two-area system where both areas are of the same size. Turbine dynamics are again neglected in this scenario. Here, saturations of the control inputs which represent the limited amount of contracted primary and secondary control reserves are modelled (primary control: ±75 MW, secondary control: ±350 MW). A graphical representation of the saturations in a block diagram is omitted here for shortness. Referring again to Figure 4.6, the saturation blocks would have to be inserted in the signal path of ΔP_m^{set} (primary control) and ΔP_{AGC} (secondary control). Furthermore, countermeasures against integrator wind-up have to be taken, which shall not be discussed here.

Figure 4.8 shows the step response ($\Delta P_{load,1} = 400$ MW) for the system with two equally sized areas. It is clearly visible that the AGC of Area 1 cannot compensate for the deviation and remains at its saturation of +350 MW. The system frequency is not brought back to 50 Hz. In real power system operation, the ancillary service dispatcher in the control center would now manually activate tertiary control reserves in order to relieve the saturated secondary reserves.

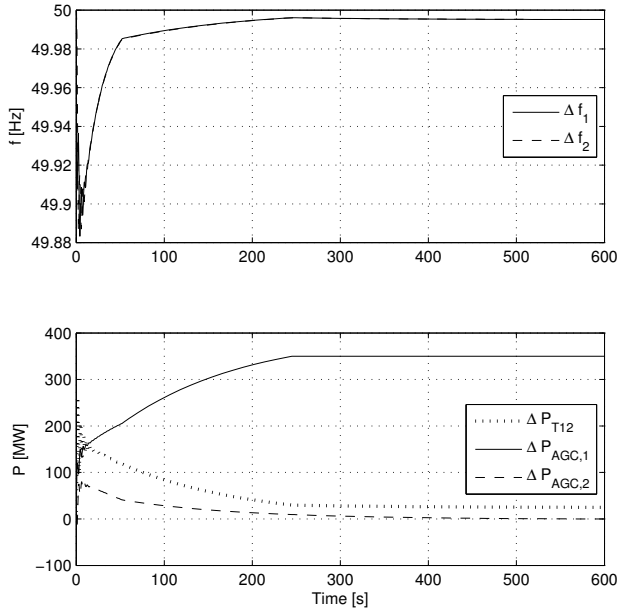

Figure 4.8. Step response for the system in Figure 4.6 with AGC, equal areas with a rated power of 10 GW each. Because of the saturated secondary control, the power system frequency cannot be brought back to the nominal value of 50 Hz.

5
Synchronous Machine Model

Almost all energy consumed by various loads in an electric power system is produced by synchronous machines, or, more correctly, the conversion from the primary energy sources, like water energy, nuclear energy, or chemical energy, to electrical energy is done in synchronous machines with a mechanical intermediate link, the turbine. This is true in larger power systems, but not always in smaller systems like isolated islands, power supply of equipment in deserts, or other smaller systems. In these systems, the energy can come from asynchronous generators, for example in wind generation units, batteries, or some other source of electrical energy. In systems with synchronous generators, these have an extremely important part in many dynamic phenomena. Thus, it is very important to develop usable and realistic models of the synchronous machines. In the previous chapters, mainly the mechanical properties of the synchronous machines have been modelled using the swing equation, while a very simplistic model of the electrical properties of the synchronous machine has been used. In this chapter, a more general, detailed model of the electric parts of the synchronous machine will be derived. The simple models used earlier will be justified. It should be emphasized that the description here aims towards the development of models usable for studying dynamic phenomena in the power system. It is not the purpose of these models to give a detailed and deep understanding of the physical functions of the synchronous machine. Of course, it is desirable to have a good insight into the physics of the synchronous machine to be able to derive appropriate models. For a detailed discussion of these aspects, books and courses dealing with the theory of electrical machines should be studied.

5.1 Park's Transformation

Park's transformation is a phase transformation (coordinate transformation) between the three physical phases in a three phase system and three new phases, or coordinates, that are convenient for the analysis of synchronous machines. This transformation is also known as the dq–transformation or Blondel's transformation. A reason why the transformation is suitable can be derived from Figure 5.1.

It is obvious that the phase quantities in the a–, b–, and c–phases will vary periodically in steady state. Further, the self and mutual inductances between stator circuits and rotor circuits will vary with the rotor position. Instead of performing all computations in the fixed stator system, the stator

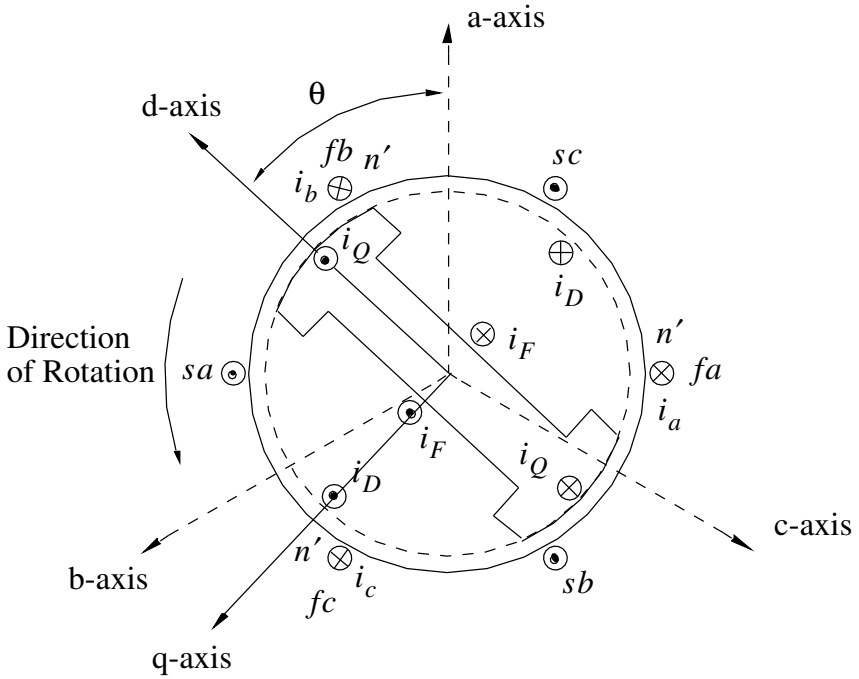

Figure 5.1. Definition of quantities in Park's transformation.

quantities voltages, currents, and fluxes can be transformed to a system that rotates with the rotor. Thus, two orthogonal axes are defined as shown in Figure 5.1: One along the axis in which the current in the rotor windings generates a flux, and one in an axis perpendicular to this. The first is the direct axis (d–axis), and the other is the quadrature axis (q–axis). From now on, the denominations d–axis and q–axis will be used. To make the system complete, a third component corresponding to the zero sequence must be defined.

Figure 5.1 is a simplified picture of a synchronous machine and should only be viewed as an intuitive basis for the transformation given below. The machine in Figure 5.1 has one pole pair, but Park's transformation can, of course, be applied to machines with an arbitrary number of pole pairs.

Park's transformation is, as a consequence of the reasoning above, time dependent, and the connection between the phase currents and the trans-

formed currents is given by

$$\begin{cases} i_0 &= \sqrt{\frac{1}{3}}(i_a + i_b + i_c) \ , \\ i_d &= \sqrt{\frac{2}{3}}\left[i_a \cos\theta + i_b \cos\left(\theta - \frac{2\pi}{3}\right) + i_c \cos\left(\theta + \frac{2\pi}{3}\right)\right] \ , \\ i_q &= \sqrt{\frac{2}{3}}\left[-i_a \sin\theta - i_b \sin\left(\theta - \frac{2\pi}{3}\right) - i_c \sin\left(\theta + \frac{2\pi}{3}\right)\right] \ . \end{cases} \tag{5.1}$$

If the a–axis is chosen as reference,

$$\theta = \omega t + \theta_0 \tag{5.2}$$

is obtained and the time dependence in the transformation is obvious. It should be pointed out that i_a, i_b, and i_c are the real physical phase currents as functions of time and not a phasor representation of those. Now,

$$\begin{aligned} x_{abc} &= (x_a, x_b, x_c)^T \\ x_{0dq} &= (x_0, x_d, x_q)^T \end{aligned} \tag{5.3}$$

can be defined. x can here be an arbitrary quantity, like voltage, current, or flux. With this notation, Park's transformation can be written as

$$x_{0dq} = P x_{abc} \tag{5.4}$$

with

$$P = \sqrt{\frac{2}{3}} \begin{pmatrix} 1/\sqrt{2} & 1/\sqrt{2} & 1/\sqrt{2} \\ \cos\theta & \cos(\theta - \frac{2\pi}{3}) & \cos(\theta + \frac{2\pi}{3}) \\ -\sin\theta & -\sin(\theta - \frac{2\pi}{3}) & -\sin(\theta + \frac{2\pi}{3}) \end{pmatrix} \ . \tag{5.5}$$

The inverse transformation is then given by

$$x_{abc} = P^{-1} x_{0dq} \ , \tag{5.6}$$

and it can easily be shown that

$$P^{-1} = P^T \ . \tag{5.7}$$

A mnemonic for Park's transformation can be obtained from Figure 5.1 by projecting the a–, b–, and c–axes onto the d– and q–axes in the figure.

Equation (5.7) implies that Park's transformation is an orthonormal transformation. This is reflected in the expression for the momentary power that is produced in the stator windings

$$\begin{aligned} &p = u_a i_a + u_b i_b + u_c i_c = u_{abc}^T i_{abc} = \\ &(P^{-1} u_{0dq})^T P^{-1} i_{0dq} = (P^T u_{0dq})^T P^{-1} i_{0dq} = \\ &u_{0dq}^T P P^{-1} i_{0dq} = u_{0dq}^T i_{0dq} = \\ &u_0 i_0 + u_d i_d + u_q i_q \ . \end{aligned} \tag{5.8}$$

Here, Equations (5.6) and (5.7) have been used. Equation (5.8) can therefore be written as

$$p = u_a i_a + u_b i_b + u_c i_c = u_0 i_0 + u_d i_d + u_q i_q \ . \tag{5.9}$$

Equation (5.9) shows that the introduced transformation is power invariant, which is a consequence of Equation (5.7).

It should be pointed out that there are several different variants of Park's transformation appearing in literature. They can differ from the form presented here by the direction of the q–axis and by constants in the transformation matrix. When using equations from some book or paper, it is thus important to make sure that the definition of Park's transformation used is the same as one's own. Otherwise, wrong results might be obtained.

The rotor windings produce a flux linkage that mainly lies in the direction of the d–axis. That flux induces an electro-magnetic field, E, which is lagging by 90°, hence in the direction of the negative q–axis. For generator operation, the phasor for E leads by an angle δ before the phasor for the terminal voltage U. At $t = 0$, the negative q–axis thus leads by an angle δ before the phasor for the voltage along the a–axis, cf. Figure 5.1. For $t > 0$, the d– and q–axes have moved by an angle ωt with the angular speed of the rotor ω. The rotor's d–axis will hence be in position

$$\theta = \omega t + \delta + \frac{\pi}{2} \ . \tag{5.10}$$

It is particularly of interest to study how zero sequence, negative sequence, and positive sequence quantities are transformed by Park's transformation. It is comparatively easy to show that a pure zero sequence quantity only leads to a contribution in x_0 with $x_d = x_q = 0$. A pure positive sequence quantity

$$x_{abc}(+) = \sqrt{2}x \begin{pmatrix} \sin(\theta + \alpha) \\ \sin(\theta + \alpha - \frac{2\pi}{3}) \\ \sin(\theta + \alpha + \frac{2\pi}{3}) \end{pmatrix} \tag{5.11}$$

is transformed to

$$x_{0dq}(+) = \sqrt{3}x \begin{pmatrix} 0 \\ \sin(\alpha) \\ -\cos(\alpha) \end{pmatrix} \ , \tag{5.12}$$

i.e. pure DC-quantities (time independent) in the dq–system with the zero sequence component equal zero. A pure negative sequence quantity gives rise to quantities in d– and q–directions that vary with the angular frequency 2ω. The zero sequence component vanishes also in this case. (Show this!)

5.2 The Inductance Matrices of the Synchronous Machine

In the following, a synchronous machine with one damper winding in d– and one in q–axis and, of course, a field winding is considered. Quantities related to these windings are denoted with the indices D, Q, and F, respectively. The flux linkages in the stator windings (Ψ_{abc}) and in the windings F, D, and Q (Ψ_{FDQ}) depend on the currents in these windings according to

$$\begin{pmatrix} \Psi_{abc} \\ \Psi_{FDQ} \end{pmatrix} = \begin{pmatrix} L_{abc,abc} & L_{abc,FDQ} \\ L_{FDQ,abc} & L_{FDQ,FDQ} \end{pmatrix} \begin{pmatrix} i_{abc} \\ i_{FDQ} \end{pmatrix} \quad . \tag{5.13}$$

$L_{abc,abc}$, ..., $L_{FDQ,FDQ}$ are 3×3 matrices with self and mutual inductances as matrix elements. These will depend on the rotor position, hence they are time dependent. The following approximation for inductances $L(\theta)$ proves to be useful: $L(\theta) = L_s + L_m \cos 2\theta$ with $L_s > L_m > 0$, where L_s and L_m are machine constants that can be identified from measurements. The same holds for the machine constant M_s that will be used in the case of mutual inductances. Keeping that in mind, the matrix elements are calculated.

- $L_{abc,abc}$:

$$\begin{cases} L_{aa} = L_s + L_m \cos 2\theta \ , \\ L_{bb} = L_s + L_m \cos(2\theta - \frac{4\pi}{3}) \ , \\ L_{cc} = L_s + L_m \cos(2\theta + \frac{4\pi}{3}) \ , \\ L_{ab} = L_{ba} = -M_s - L_m \cos(2\theta + \frac{\pi}{3}) \ , \\ L_{bc} = L_{cb} = -M_s - L_m \cos(2\theta + \pi) \ , \\ L_{ac} = L_{ca} = -M_s - L_m \cos(2\theta + \frac{5\pi}{3}) \ . \end{cases} \tag{5.14}$$

- $L_{abc,FDQ}$ and $L_{FDQ,abc}$:

$$\begin{cases} L_{aF} = L_{Fa} = M_F \cos\theta \ , \\ L_{bF} = L_{Fb} = M_F \cos(\theta - \frac{2\pi}{3}) \ , \\ L_{cF} = L_{Fc} = M_F \cos(\theta + \frac{2\pi}{3}) \ , \\ \\ L_{aD} = L_{Da} = M_D \cos\theta \ , \\ L_{bD} = L_{Db} = M_D \cos(\theta - \frac{2\pi}{3}) \ , \\ L_{cD} = L_{Dc} = M_D \cos(\theta + \frac{2\pi}{3}) \ , \\ \\ L_{aQ} = L_{Qa} = -M_Q \sin\theta \ , \\ L_{bQ} = L_{Qb} = -M_Q \sin(\theta - \frac{2\pi}{3}) \ , \\ L_{cQ} = L_{Qc} = -M_Q \sin(\theta + \frac{2\pi}{3}) \ . \end{cases} \tag{5.15}$$

- $L_{FDQ,FDQ}$:

$$\begin{cases} L_{FF} = L_F \ , \\ L_{DD} = L_D \ , \\ L_{QQ} = L_Q \ , \\ \\ L_{FD} = L_{DF} = M_R \ , \\ L_{FQ} = L_{QF} = 0 \ , \\ L_{DQ} = L_{QD} = 0 \ . \end{cases} \tag{5.16}$$

All inductances with only one index in Equations (5.14) – (5.16) are constants and depend on the design of the synchronous machine. The resulting inductances are of course, as mentioned before, not quite exact. They can be called exact in an ideal machine, where spatial harmonics and other unsymmetries are neglected. For a real synchronous machine, the approximations are usually very good and lead to fully acceptable results for the computations and analyses treated here. It should be emphasized that the model developed here is for use in computations where the synchronous machines are part of a larger system. The model is not primarily aimed at studies of the internal quantities in the generator.

It is now natural to transform the abc–components in Equation (5.13) to 0dq–components. For this, an extended transformation given by

$$P_{ex} = \begin{pmatrix} P & 0 \\ 0 & I \end{pmatrix} \ , \tag{5.17}$$

with P according to (5.5) and a 3×3 unit matrix I is used. The result is

$$\begin{pmatrix} \Psi_{0dq} \\ \Psi_{FDQ} \end{pmatrix} = \begin{pmatrix} L_{0dq,0dq} & L_{0dq,FDQ} \\ L_{FDQ,0dq} & L_{FDQ,FDQ} \end{pmatrix} \begin{pmatrix} i_{0dq} \\ i_{FDQ} \end{pmatrix} \ , \tag{5.18}$$

with the inductance matrix given by

$$\begin{pmatrix} L_{0dq,0dq} & L_{0dq,FDQ} \\ L_{FDQ,0dq} & L_{FDQ,FDQ} \end{pmatrix} = \begin{pmatrix} P & 0 \\ 0 & I \end{pmatrix} \begin{pmatrix} L_{abc,abc} & L_{abc,FDQ} \\ L_{FDQ,abc} & L_{FDQ,FDQ} \end{pmatrix} \begin{pmatrix} P^{-1} & 0 \\ 0 & I \end{pmatrix} . \tag{5.19}$$

The virtue of the Park's transformation is apparent in the following equation, where the inductance matrix in (5.18) is computed

$$L_{0dq,0dq} = \begin{pmatrix} L_0 & 0 & 0 \\ 0 & L_d & 0 \\ 0 & 0 & L_q \end{pmatrix} \ , \tag{5.20}$$

with

$$\begin{cases} L_0 = L_s - 2M_s \ , \\ L_d = L_s + M_s + \frac{3}{2}L_m \ , \\ L_q = L_s + M_s - \frac{3}{2}L_m \ , \end{cases} \tag{5.21}$$

and

$$L_{0dq,FDQ} = \begin{pmatrix} 0 & 0 & 0 \\ kM_F & kM_D & 0 \\ 0 & 0 & kM_Q \end{pmatrix} \ , \tag{5.22}$$

where

$$k = \sqrt{\frac{3}{2}} \tag{5.23}$$

and, of course,

$$L_{FDQ,0dq} = L^T_{0dq,FDQ} \ . \tag{5.24}$$

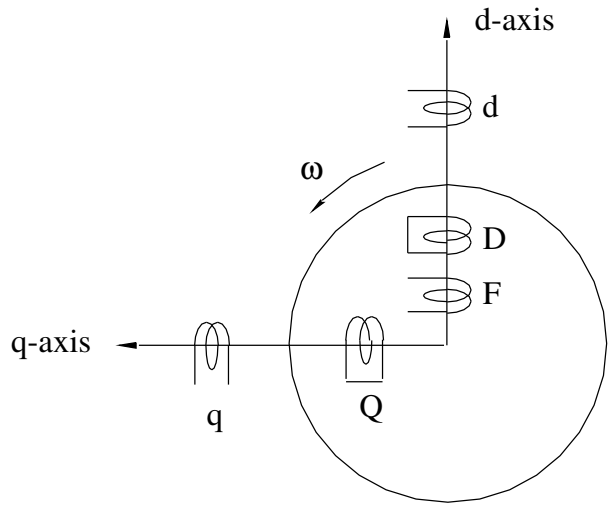

Figure 5.2. Schematic picture of the transformed system. (One damper winding in the d–axis and one in the q–axis.)

$L_{FDQ,FDQ}$ has, of course, not changed, but for completeness it is repeated here.

$$L_{FDQ,FDQ} = \begin{pmatrix} L_F & M_R & 0 \\ M_R & L_D & 0 \\ 0 & 0 & L_Q \end{pmatrix} \quad . \tag{5.25}$$

Two important observations can be made from Equations (5.20)–(5.25):

- The inductances in the inductance matrix in Equation (3.18) are not dependent on time.
- The quantities in d- and q-directions are decoupled. (The induction matrix is block diagonal: one 2×2 matrix and one 1×1 matrix.)

The second observation above leads to a picture of the transformed system according to Figure 5.2.

5.3 Voltage Equations for the Synchronous Machine

For the three stator circuits and the three rotor circuits the following relations can be written:

$$\begin{cases} u_a = -r_a i_a - \dot{\Psi}_a \ , \\ u_b = -r_b i_b - \dot{\Psi}_b \ , \\ u_c = -r_c i_c - \dot{\Psi}_c \ , \end{cases} \tag{5.26}$$

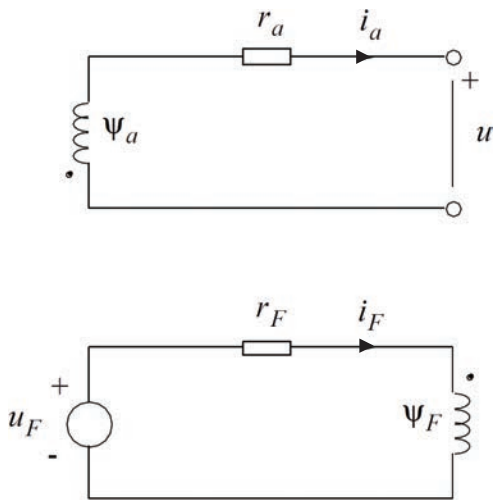

Figure 5.3. Sign convention for stator and rotor circuits.

and

$$\begin{cases} u_F = r_F i_F + \dot{\Psi}_F \ , \\ 0 = r_D i_D + \dot{\Psi}_D \ , \\ 0 = r_Q i_Q + \dot{\Psi}_Q \ . \end{cases} \tag{5.27}$$

Equations (5.26) and (5.27) can be written more compactly in vector form,

$$\begin{pmatrix} u_{abc} \\ u_{FDQ} \end{pmatrix} = - \begin{pmatrix} R_{abc} & 0 \\ 0 & R_{FDQ} \end{pmatrix} \begin{pmatrix} i_{abc} \\ i_{FDQ} \end{pmatrix} - \begin{pmatrix} \dot{\Psi}_{abc} \\ \dot{\Psi}_{FDQ} \end{pmatrix} \ . \tag{5.28}$$

The vector u_{FDQ} is defined as

$$u_{FDQ} = (-u_F, 0, 0)^T \ , \tag{5.29}$$

while the other vectors are defined as before. R_{abc} and R_{FDQ} are diagonal 3×3 matrices.

If Equation (5.28) is multiplied by P_{ex} according to Equation (5.17), all quantities are transformed to the dq–system, i.e.

$$\begin{pmatrix} u_{0dq} \\ u_{FDQ} \end{pmatrix} = - \begin{pmatrix} P R_{abc} P^{-1} & 0 \\ 0 & R_{FDQ} \end{pmatrix} \begin{pmatrix} i_{0dq} \\ i_{FDQ} \end{pmatrix} - \begin{pmatrix} P\dot{\Psi}_{abc} \\ \dot{\Psi}_{FDQ} \end{pmatrix} \ . \tag{5.30}$$

The matrix $PR_{abc}P^{-1}$ is denoted R_{0dq}, and if $r_a = r_b = r_c = r$, which in most cases is true,

$$R_{0dq} = R_{abc} = rI \tag{5.31}$$

is valid.

To get Equation (5.30) expressed solely in dq–quantities, also the last term on the right hand side must be expressed in these. Since P is time dependent, it is important to remember that

$$\dot{P} \neq 0 \ , \tag{5.32}$$

which leads to

$$\dot{\Psi}_{0dq} = \frac{d}{dt}(P\Psi_{abc}) = \dot{P}\Psi_{abc} + P\dot{\Psi}_{abc} \ , \tag{5.33}$$

and thus

$$P\dot{\Psi}_{abc} = \dot{\Psi}_{0dq} - \dot{P}\Psi_{abc} = \dot{\Psi}_{0dq} - \dot{P}P^{-1}\Psi_{0dq} \ . \tag{5.34}$$

Equation (5.30) can hence be written as

$$\begin{pmatrix} u_{0dq} \\ u_{FDQ} \end{pmatrix} = -\begin{pmatrix} R_{0dq} & 0 \\ 0 & R_{FDQ} \end{pmatrix}\begin{pmatrix} i_{0dq} \\ i_{FDQ} \end{pmatrix} - \begin{pmatrix} \dot{\Psi}_{0dq} \\ \dot{\Psi}_{FDQ} \end{pmatrix} + \begin{pmatrix} \dot{P}P^{-1}\Psi_{0dq} \\ 0 \end{pmatrix} \ . \tag{5.35}$$

Some trivial computations show that the matrix $\dot{P}P^{-1}$ can be expressed as

$$\dot{P}P^{-1} = \begin{pmatrix} 0 & 0 & 0 \\ 0 & 0 & \omega \\ 0 & -\omega & 0 \end{pmatrix} \ . \tag{5.36}$$

The voltage equations in the dq–system can thus be written in component form as

$$\begin{cases} u_0 = -ri_0 - \dot{\Psi}_0 \ , \\ u_d = -ri_d - \dot{\Psi}_d + \omega\Psi_q \ , \\ u_q = -ri_q - \dot{\Psi}_q - \omega\Psi_d \ , \end{cases} \tag{5.37}$$

and

$$\begin{cases} -u_F = -r_F i_F - \dot{\Psi}_F \ , \\ 0 = -r_D i_D - \dot{\Psi}_D \ , \\ 0 = -r_Q i_Q - \dot{\Psi}_Q \ . \end{cases} \tag{5.38}$$

In the previous section, expressions for the dependencies of the flux linkages on the currents in the different windings were derived. To further simplify the expressions that were obtained, the per unit system for the different windings is now introduced so that all mutual inductances in the d–axis are equal, and all in the q–axis are equal. (In our case, only one damping winding in the q–axis was considered, but in a more general case several damper windings can be considered.) We introduce

$$\begin{aligned} &\sqrt{\tfrac{3}{2}}M_F = \sqrt{\tfrac{3}{2}}M_D = M_R = L_{AD} \ , \\ &\sqrt{\tfrac{3}{2}}M_Q = L_{AQ} \ . \end{aligned} \tag{5.39}$$

The different fluxes can then be written as

$$\begin{cases} \Psi_0 = L_0 i_0 \ , \\ \Psi_d = L_d i_d + L_{AD}(i_F + i_D) \ , \\ \Psi_q = L_q i_q + L_{AQ} i_Q \ , \end{cases} \tag{5.40}$$

and

$$\begin{cases} \Psi_F = L_F i_F + L_{AD}(i_d + i_D) \ , \\ \Psi_D = L_D i_D + L_{AD}(i_d + i_F) \ , \\ \Psi_Q = L_Q i_Q + L_{AQ} i_q \ . \end{cases} \tag{5.41}$$

Equations (5.37) and (5.38) together with Equations (5.40) and (5.41) now describe the electrical dynamics of a synchronous machine completely. These equations together with a description of the external system unequivocally determine the behaviour of the synchronous machine during different disturbances. In Figure 5.4, a graphical description of these equations is given.

In Equation (5.37), we observe that the emf in d– and q–direction consists of two terms: one that is a time derivative of the absolute value of the flux linkage and one that arises because the field winding is rotating. The first of these is usually called stator transient and the other rotational emf. In steady state, the first of these vanishes, and the whole emf is created by the rotation of the field winding. It can be shown that the terms $\dot{\Psi}_d$ and $\dot{\Psi}_q$ are in most applications much smaller than $\omega\Psi_d$ and $\omega\Psi_q$, which justifies that the first ones are often neglected.

5.4 Synchronous, Transient, and Subtransient Inductances

The complete description of the synchronous machine given in the previous section can be simplified and made more understandable from a physical standpoint if a number of new parameters are introduced. These new parameters can be derived from the already defined ones. In steady state or a sufficiently long time after a disturbance, the induced currents in the damper windings and in the field winding vanish. After a disturbance different time intervals can be distinguished, during which different couplings between the circuits in Figure 5.4 prevail. This makes it possible to define new inductances describing the synchronous machine during these time periods, and these inductances will be derived in this section. Further, the time constants that specify how fast the currents in the damper windings decay are derived in the next section. These time constants indicate also the duration of the time intervals, during which the derived inductances determine the behaviour of the synchronous machine.

Earlier, the synchronous inductances L_d and L_q were defined. They are

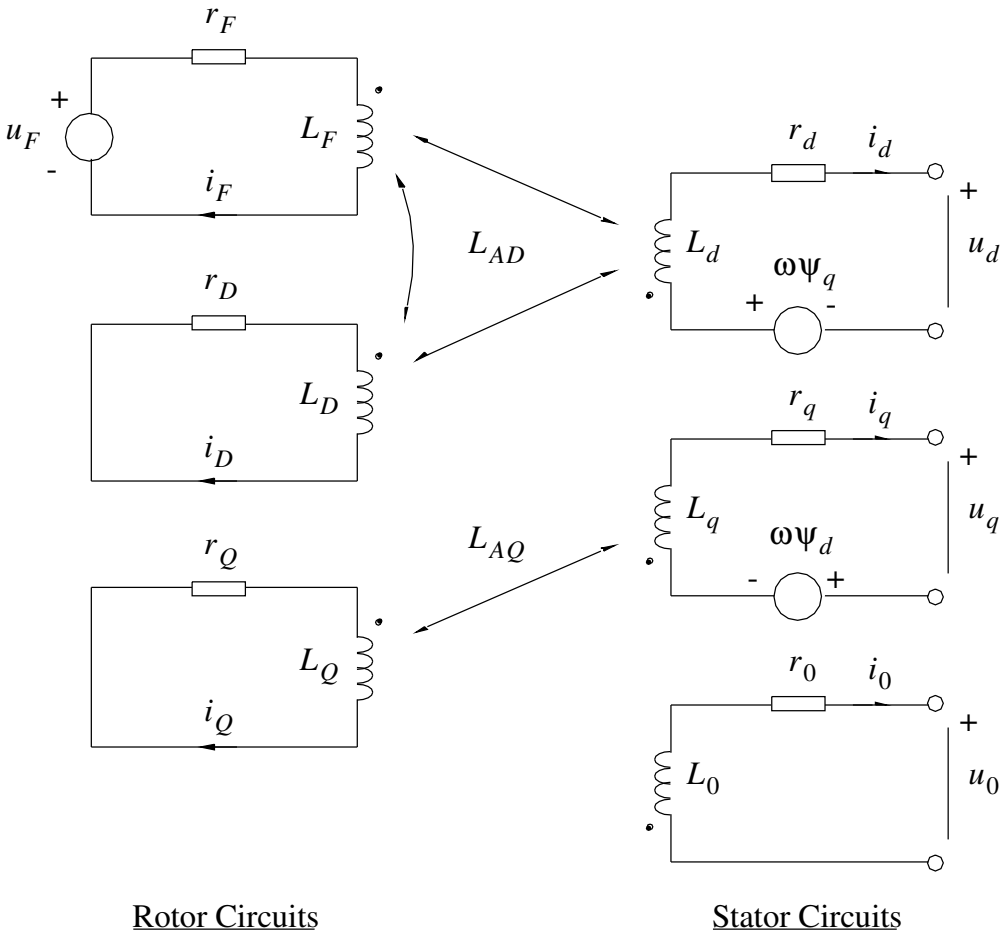

Figure 5.4. Graphical description of the voltage equations and the coupling between the equivalent circuits.

repeated here for completeness.

$$\begin{cases} L_d = L_s + M_s + \frac{3}{2}L_m \\ L_q = L_s + M_s - \frac{3}{2}L_m \end{cases} \tag{5.42}$$

For a synchronous machine with salient poles, like a hydro power generation unit, $L_m > 0$ and thus $L_d > L_q$, while $L_m \approx 0$ for machines with round rotors leading to $L_d \approx L_q$. These inductances describe the synchronous machine in steady state as can be seen from Figure 5.4. In steady state the currents i_D and $i_Q = 0$, so there is no influence from the damper windings on the stator circuits. Since in steady state the rotor current i_F is a pure dc current the only influence from the field current on the stator circuits is through the rotational voltages $\omega\Psi_d$ and $\omega\Psi_q$. From Figure 5.4 it is thus obvious that the inductances seen from the generator terminals are in

steady state L_d and L_q. However, when transients occur, e.g. due to short circuits or other disturbances, there will be couplings between the circuits in Figure 5.4 and this will result in that the equivalent inductances as seen from the terminals will change. These equivalent inductances will be derived in the following.

First, the *subtransient* and *transient* inductances in the d-axis will be derived. It is assumed that the machine is in steady state before the disturbance and a voltage change of the form

$$\begin{pmatrix} \Delta u_a \\ \Delta u_b \\ \Delta u_c \end{pmatrix} = \sqrt{2}\Delta u \begin{pmatrix} \sin(\theta+\alpha) \\ \sin(\theta+\alpha-\frac{2\pi}{3}) \\ \sin(\theta+\alpha-\frac{4\pi}{3}) \end{pmatrix} c(t) \tag{5.43}$$

is superimposed on the terminal voltages. The function $c(t)$ is a step function at $t=0$, i.e. $c(t)=0$ for $t<0$ and $c(t)=1$ for $t>0$. With $\alpha=\pi/2$ the Park–transformed voltage vector in Equation (5.43) becomes

$$\begin{pmatrix} \Delta u_0 \\ \Delta u_d \\ \Delta u_q \end{pmatrix} = \sqrt{3}\Delta u \begin{pmatrix} 0 \\ c(t) \\ 0 \end{pmatrix} \tag{5.44}$$

For $t=0+$, that is, directly after the voltage is applied on the terminals, the flux linkages Ψ_F and Ψ_D are still zero since they cannot change instantaneously. This gives the following equations

$$\begin{cases} \Psi_F(0+) = 0 = L_F\Delta i_F + L_{AD}(\Delta i_d + \Delta i_D) \\ \Psi_D(0+) = 0 = L_D\Delta i_D + L_{AD}(\Delta i_d + \Delta i_F) \end{cases} \tag{5.45}$$

where Δi_f, Δi_d, and Δi_D, with obvious notation, are the currents induced in the circuits due to the step in the voltage. From (5.45) Δi_D and Δi_F can be expressed in Δi_d,

$$\begin{cases} \Delta i_D = -\dfrac{L_F L_{AD} - L_{AD}^2}{L_F L_D - L_{AD}^2}\,\Delta i_d \ , \\ \Delta i_F = -\dfrac{L_D L_{AD} - L_{AD}^2}{L_F L_D - L_{AD}^2}\,\Delta i_d \ . \end{cases} \tag{5.46}$$

These expressions for Δi_D and Δi_F can now be inserted into the expression for $\Delta\Psi_d$ in (5.40) giving

$$\begin{aligned} &\Delta\Psi_d = L_d\Delta i_d + L_{AD}(\Delta i_F + \Delta i_D) = \\ &\left(L_d - \frac{L_D L_{AD}^2 + L_F L_{AD}^2 - 2L_{AD}^3}{L_F L_D - L_{AD}^2}\right)\Delta i_d = L_d''\Delta i_d \ , \end{aligned} \tag{5.47}$$

where the subtransient inductance L_d'' in the d–axis has been defined and it can be rewritten as

$$L_d'' = L_d - \frac{L_D + L_F - 2L_{AD}}{L_F L_D/L_{AD}^2 - 1} \ . \tag{5.48}$$

The time constant of the decay of the current in the damper winding is much smaller that the time constant in the field winding, see next section, which means that after a certain time it can be assumed that the current in the damper winding has decayed to zero, i.e. $\Delta i_D = i_D = 0$. The same assumption regarding i_D can be made if no damper winding is modelled in the d-axis. This assumption gives

$$\Delta\Psi_F = 0 = L_F\Delta i_F + L_{AD}\Delta i_d \tag{5.49}$$

which gives

$$\Delta i_F = -(L_{AD}/L_F)\Delta i_d \tag{5.50}$$

and with use of (5.40) and $i_D = 0$

$$\Delta\Psi_d = \left(L_d - \frac{L_{AD}^2}{L_F}\right)\Delta i_d = L'_d i_d \ , \tag{5.51}$$

The transient inductance in the d–axis, L'_d, is defined in Equation (5.51) as

$$L'_d = L_d - \frac{L_{AD}^2}{L_F} \ . \tag{5.52}$$

The time constant for the decay of the current in the damper winding is derived in the next section.

An equivalent analysis to the one above can be performed for the q–axis, but, since no field winding exists in the q–axis for the model we are considering here, the terminology is somewhat different. For a machine with salient poles and damper winding in the q–axis, the effective inductance after the current in the damper winding has decayed is practically equal to the synchronous inductance. Hence it is sometimes said that, for machines with salient poles, the transient and synchronous inductances in the q–axis are equal.

With $\alpha = \pi$ the Park–transformed voltage vector in Equation (5.43) becomes

$$\begin{pmatrix} \Delta u_0 \\ \Delta u_d \\ \Delta u_q \end{pmatrix} = \sqrt{3}\Delta u \begin{pmatrix} 0 \\ 0 \\ c(t) \end{pmatrix} \tag{5.53}$$

A similar analysis as above will the give the subtransient inductance in q–axis

$$L''_q = L_q - \frac{L_{AQ}^2}{L_Q} \tag{5.54}$$

for a synchronous machine with one damper winding in the q–axis. According to the reasoning above we have

$$L'_q = L_q \ . \tag{5.55}$$

in this case.

If one additional damper winding is modelled into the q–axis, a value of L'_q can be derived that differs from L_q. This derivation is analogous to the one done for the inductances in the d–axis.

In general, for the inductances defined, the following relations hold

$$\begin{aligned} L''_d < L'_d < L_d \ , \\ L''_q < L'_q < L_q \ . \end{aligned} \tag{5.56}$$

The subtransient, transient, and synchronous reactances are defined in an obvious way, e.g. $X_d = \omega_0 L_d$ etc., which most often are expressed in p.u. based on the machine power and voltage ratings, see Table 5.1.

5.5 Time constants

The time constants that determine how fast transients in the rotor and damper windings decay after a disturbance depend on the resistances of these windings and associated inductances. We will here derive the so called open circuit time constants whereby it assumed that the stator circuits are open, i.e. $i_a = i_b = i_c = 0$, or equivalently $i_0 = i_d = i_q = 0$. These time constants are normally denoted by an index o for open, e.g. T''_{do} as explained below. An alternative that also occurs in the literature are the time constants when the stator terminals are short-circuited, which also uniquley determine the winding resistances. The open circuit time constants are normally the ones given by the manufacturer of the generator and can be obtained by measurements.

Thus, suppose now that the stator windings are open and and a step change in the field voltage at the time $t = 0$, i.e. $u_F = u_F(0) + \Delta u_F c(t)$ will be investigated, with $c(t)$ being a step function at $t = 0$. We will here derive the time constants associated with the field winding and the damper winding in the d–axis. The circuit equations describing the currents induced by the step in the field voltage for these two windings are for $t > 0$

$$\begin{cases} r_F \Delta i_F + \Delta \dot{\Psi}_F = \Delta u_F c(t) \\ r_D \Delta i_D + \Delta \dot{\Psi}_D = 0 \end{cases} \tag{5.57}$$

For a synchronous machine $r_D \gg r_F$ and the induced current will consequently decay much faster in the damper winding than in the field winding. (This fact was also used above in the derivation of L''_d and L'_d.) Therefore we will analyze the decay of the current in the damper winding first. Since $i_d = 0$, the fluxes in the field and damper windings can be written as

$$\begin{cases} \Delta \Psi_D = L_D \Delta i_D + L_{AD} \Delta i_F \ , \\ \Delta \Psi_F = L_F \Delta i_F + L_{AD} \Delta i_D \ . \end{cases} \tag{5.58}$$

Taking the time derivative of the lower equation in (5.58) gives

$$\Delta\dot{\Psi}_F = L_F\Delta\dot{i}_F + L_{AD}\Delta\dot{i}_D \ . \tag{5.59}$$

From the upper equation of (5.57) we can replace $\Delta\dot{\Psi}_F$ in (5.59), which after some re-arrangements gives

$$\Delta\dot{i}_F = \frac{\Delta u_F - r_F\Delta i_F - L_{AD}\Delta\dot{i}_D}{L_F} \tag{5.60}$$

Now the time derivative of the upper equation of (5.58) is inserted into the lower equation of (5.57) yielding

$$r_D\Delta i_D + L_D\Delta\dot{i}_D + L_{AD}\Delta\dot{i}_F = 0 \ , \tag{5.61}$$

in which the expression for $\Delta\dot{i}_F$ in (5.60) is inserted giving

$$r_D\Delta i_D + L_D\Delta\dot{i}_D + L_{AD}\frac{\Delta u_F - r_F\Delta i_F - L_{AD}\Delta\dot{i}_D}{L_F} = 0 \ . \tag{5.62}$$

This equation can be rewritten as

$$\Delta\dot{i}_D + \frac{r_D}{L_D - L_{AD}^2/L_F}\Delta i_D = -\Delta u_F\frac{L_{AD}/L_F}{L_D - L_{AD}^2/L_F} + r_F\frac{L_{AD}}{L_F}\Delta i_F \ . \tag{5.63}$$

As pointed out above the current in the damper circuit will decay must faster, which means that the current in the field winding, Δi_F, can be regarded as a constant in Equation (5.63). The time constant of the decay of the damper winding current, Δi_D, is the *subtransient* time constant of the open circuit in the d–axis, T''_{do}, and can now with the above assumptions be identified from Equation (5.63) as

$$T''_{do} = \frac{L_D - L_{AD}^2/L_F}{r_D} \ . \tag{5.64}$$

When i_D has vanished, i.e. when $i_D = 0$, the field current is determined solely by the upper equation in (5.57), and the *transient* time constant of the open circuit, T'_{do}, and together with the lower equation of (5.58) it is easily seen that this time constant is given by

$$T'_{do} = L_F/r_F \ . \tag{5.65}$$

Accordingly, for a synchronous machine with a damper winding in the q–axis,

$$T''_{qo} = L_Q/r_Q \tag{5.66}$$

can be derived.

	Round Rotor	Salient Pole
x_d (p.u.)	1.0 – 2.3	0.6 – 1.5
x_q (p.u.)	1.0 – 2.3	0.4 – 1.0
x'_d (p.u.)	0.15 – 0.4	0.2 – 0.5
x''_d (p.u.)	0.12 – 0.25	0.15 – 0.35
x'_q (p.u.)	0.3 – 1.0	—
x''_q (p.u.)	0.12 – 0.25	0.2 – 0.45
T'_{do} (s)	3.0 – 10.0	1.5 – 9.0
T''_{do} (s)	0.02 – 0.05	0.01 – 0.05
T'_{qo} (s)	0.5 – 2.0	–
T''_{qo} (s)	0.02 – 0.05	0.01 – 0.09
H (s)	3 – 5 ($n = 3000$ rpm) 5 – 8 ($n = 1500$ rpm)	1.5 – 5

Table 5.1. Typical values of some parameters of synchronous machines.

The quantities introduced in this and the previous sections are important parameters of a synchronous machine and are usually given by the manufacturer of the machine. The reasons for this are that they are easily measured by simple tests and that they are introduced in a natural way into the simplified models we will derive in the next section. In Table 5.1, typical values of the discussed parameters for different types and sizes of synchronous machines are given. Reactances instead of inductances are given in Table 5.1, i.e. $x_d = \omega_0 L_d$ etc., with $\omega_0 = 2\pi f_0$. The p.u. base is the power and voltage ratings of the machine.

5.6 Simplified Models of the Synchronous Machine

5.6.1 Derivation of the fourth-order model

A complete and exact model of the synchronous machine, considering the assumptions and approximations made, was presented in sections 5.2 and 5.3. When a synchronous machine is modelled in for example a software package for stability simulations, these are often the equations used to represent the synchronous machine. Nevertheless, it is, for several reasons, often meaningful to use models that comprise more simplifications and approximations than those derived earlier. If a better insight into a problem is wanted or if a problem is analyzed without using computer simulations, simplified representations of the synchronous machine are often the only possibility. Here, such a model will be derived under the following assumptions:

- The stator transients are neglected, i.e. we set $\dot{\Psi}_d = \dot{\Psi}_q = 0$.

- The d–axis contains no damper windings.
- In the q–axis, one damper winding is modelled.

With these assumptions, the synchronous machine is described by the equations

$$\begin{cases} \Psi_d = L_d i_d + L_{AD} i_F \ , \\ \Psi_q = L_q i_q + L_{AQ} i_Q \ , \\ \Psi_F = L_F i_F + L_{AD} i_d \ , \\ \Psi_Q = L_Q i_Q + L_{AQ} i_q \ , \end{cases} \tag{5.67}$$

$$\begin{cases} u_F = r_F i_F + \dot{\Psi}_F \ , \\ 0 = r_Q i_Q + \dot{\Psi}_Q \ , \end{cases} \tag{5.68}$$

$$\begin{cases} u_d = -r i_d + \omega \Psi_q \ , \\ u_q = -r i_q - \omega \Psi_d \ . \end{cases} \tag{5.69}$$

For completeness, some relations defined above are repeated here.

$$\begin{cases} L'_d = L_d - L_{AD}^2 / L_F \\ L''_q = L_q - L_{AQ}^2 / L_Q \end{cases} \tag{5.70}$$

The goal is now to eliminate all quantities with indices F and Q, except for u_F, from the equations above to get a model that can be used to represent the synchronous machine as a component in a system. That means that the only quantities that should be present in the model are stator voltages, the stator current, and u_F, which is a control variable that can be changed by the excitation system as described in Chapter 6.

From the Equations (5.67), i_Q is eliminated, which leads to

$$\Psi_q - \frac{L_{AQ}}{L_Q} \Psi_Q = L''_q i_q \ . \tag{5.71}$$

Now, by defining

$$e'_d = \omega \frac{L_{AQ}}{L_Q} \Psi_Q \ , \tag{5.72}$$

Equation (5.71) can be written as

$$\Psi_q - e'_d / \omega = L''_q i_q \ . \tag{5.73}$$

Equivalent derivations can be done for the rotor circuit in the d–axis, i.e. for the field winding.

$$\Psi_d - \frac{L_{AD}}{L_F} \Psi_F = L'_d i_d \tag{5.74}$$

is obtained, which, using the definition

$$e'_q = -\omega \frac{L_{AD}}{L_F} \Psi_F \ , \tag{5.75}$$

can be written as

$$\Psi_d + e'_q/\omega = L'_d i_d \ . \tag{5.76}$$

Now, the quantities

$$\begin{cases} e_d = \omega L_{AQ} i_Q \ , \\ e_q = -\omega L_{AD} i_F \end{cases} \tag{5.77}$$

are introduced. From the equations above, the relationships

$$\begin{cases} e_d = e'_d - (x_q - x''_q) i_q \ , \\ e_q = e'_q + (x_d - x'_d) i_d \ , \end{cases} \tag{5.78}$$

with $x_d = \omega L_d$ etc. can be obtained.

According to Equations (5.77) and (5.78),

$$i_Q = \frac{e'_d - (x_q - x''_q) i_q}{\omega L_{AQ}} \ . \tag{5.79}$$

Substituting this into the second equation of (5.68), which together with (5.72) give

$$r_Q \frac{e'_d - (x_q - x''_q) i_q}{\omega L_{AQ}} + \frac{L_Q}{\omega L_{AQ}} \dot{e}'_d = 0 \ , \tag{5.80}$$

where it has been assumed that $\dot{\omega} = 0$ or $\omega = \omega_0$. Equation (5.80) can also be written as

$$T''_{qo} \dot{e}'_d + e'_d - (x_q - x''_q) i_q = 0 \ . \tag{5.81}$$

For the rotor circuit in the d–axis, i.e. for the exciter winding, accordingly

$$T'_{do} \dot{e}'_q + e'_q + (x_d - x'_d) i_d = -\frac{\omega L_{AD}}{r_F} u_F \tag{5.82}$$

is obtained, which, using

$$e_F = \frac{\omega L_{AD}}{r_F} u_F \ , \tag{5.83}$$

can be written as

$$T'_{do} \dot{e}'_q + e'_q + (x_d - x'_d) i_d = -e_F \ . \tag{5.84}$$

If Equations (5.81) and (5.84) are Laplace–transformed and the voltage equation (5.69) is rewritten with the introduced quantities, we obtain

$$\begin{pmatrix} \Delta u_d \\ \Delta u_q \end{pmatrix} = \begin{pmatrix} \Delta e'_d \\ \Delta e'_q \end{pmatrix} + \begin{pmatrix} -r_d & x''_q \\ -x'_d & -r_q \end{pmatrix} \begin{pmatrix} \Delta i_d \\ \Delta i_q \end{pmatrix} \ , \tag{5.85}$$

with e'_d given by

$$\Delta e'_d = \frac{(x_q - x''_q) \Delta i_q}{1 + s T''_{qo}} \tag{5.86}$$

and e'_q from

$$\Delta e'_q = -\frac{\Delta e_F + (x_d - x'_d)\Delta i_d}{1 + sT'_{do}} \quad . \tag{5.87}$$

This model, i.e. Equations (5.85)–(5.87), together with the swing equation, are often called the fourth order model. This model of the synchronous machine demands, with the assumptions made here, four state variables: $\Delta e'_d$ and $\Delta e'_q$ and the "mechanical" quantities $\Delta\omega$ and $\Delta\delta$.

Often, also the damper winding in the q–axis can be neglected. That leads to a third order model, which can be written as

$$\begin{pmatrix} \Delta u_d \\ \Delta u_q \end{pmatrix} = \begin{pmatrix} 0 \\ \Delta e'_q \end{pmatrix} + \begin{pmatrix} -r_d & x_q \\ -x'_d & -r_q \end{pmatrix} \begin{pmatrix} \Delta i_d \\ \Delta i_q \end{pmatrix} \quad , \tag{5.88}$$

with $\Delta e'_q$ according to Equation (5.87).

5.6.2 The Heffron-Phillips formulation for stability studies

The third-order model of the synchronous machine derived in the previous section can be formulated as a block diagram. The basis for the model presented here, which was originally proposed by Heffron and Phillips, is the "single machine, infinite bus" (SMIB) setup. By introducing a number of new constants, a very compact notation is achieved. The model shall enable the reader to directly implement a usable representation of an SMIB system, including the mechanical dynamics, field winding, and excitation system. This implementation can be used directly for stability studies. In the present case, a generic simplified representation of the excitation system is used. Detailed descriptions and common variants of these systems can be found in chapter 6.

Background: Low-frequency oscillations in power systems

In large interconnected power systems, low-frequency oscillations can arise spontaneously. Unlike the electro-mechanical oscillations described by the swing equation, these oscillations have a frequency of well below 1 Hz (about 3 – 10 cycles per minute depending on the power system). They are known to either decay slowly or continue to grow, which leads eventually to system separation. The main cause of the oscillations is a lack of damping in the system due to the effect of excitation systems in synchronous machines.

An effective countermeasure to low-frequency oscillations is the usage of Power Systems Stabilizers (PSS). These are automatic controllers acting on the excitation systems, providing an additional damping component which leads to an attenuation of the oscillations. Further details about this system, which can be directly attached to the Heffron-Phillips model derived in this section, will be presented in the chapters 6 and 7.

Block diagram

Figure 5.5 presents the transfer function block diagram of the Heffron-Phillips model. Note that all quantities are presented in per unit. The mechanical system is represented by the system inertia and the damping constant, where the torque balance $\Delta T_m - \Delta T_e$ is considered as an input and the incremental torque angle $\Delta\delta$ as an output. The electrical part of the system consists of three main parts: 1) the composition of the electrical torque (influenced by $\Delta\delta$ over constant K_1 and the internal incremental voltage $\Delta e'_q$ over constant K_2), 2) the effect of the field winding (determined by the field winding constant K_3 and influenced by $\Delta\delta$ over constant K_4), and 3) the effect of the excitation system (influenced by $\Delta\delta$ over constant K_5 and $\Delta e'_q$ over constant K_6). The excitation system itself is modeled by a first-order transfer function including the amplification factor K_A and the time constant T_A.

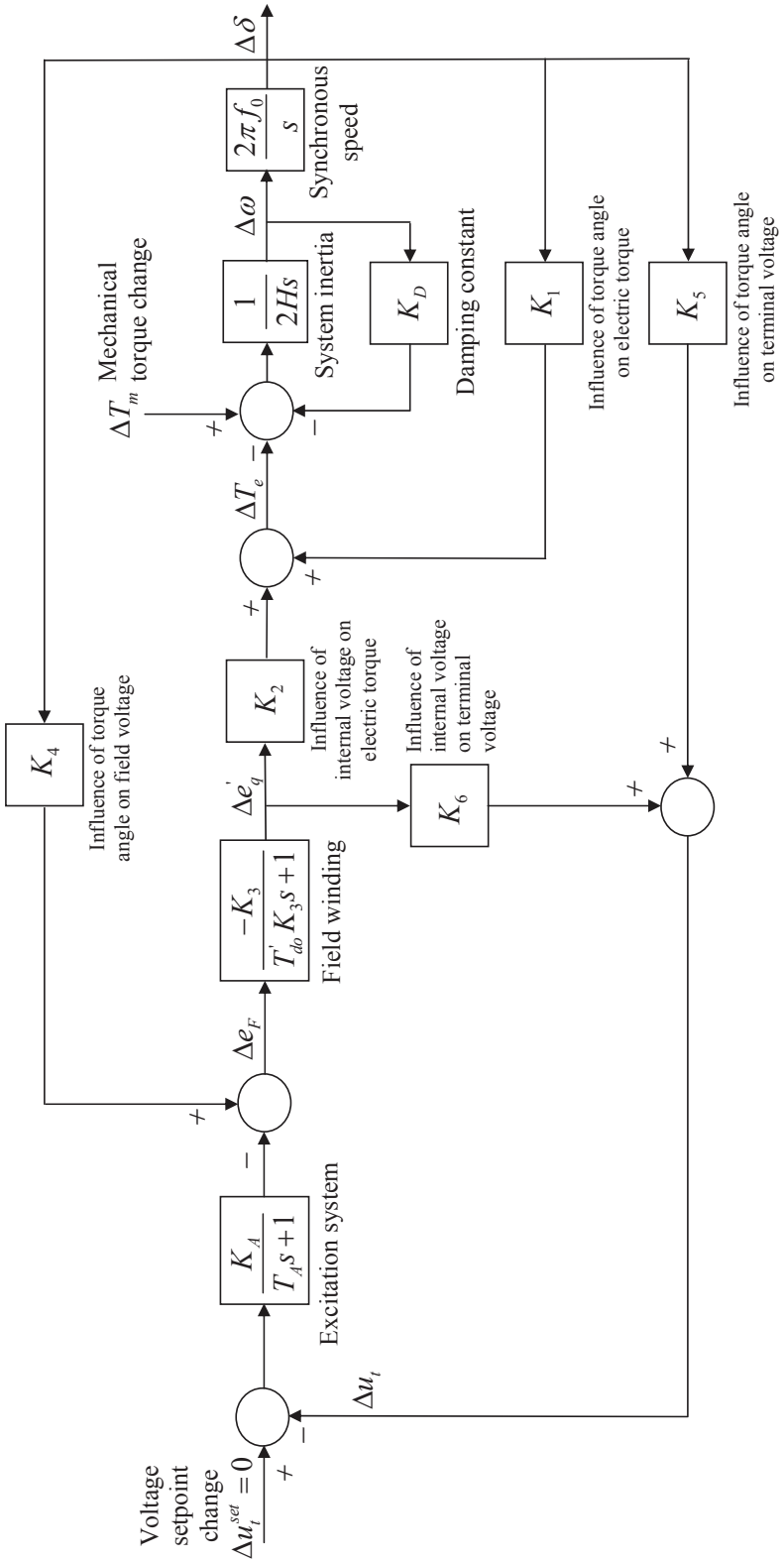

Figure 5.5. Block diagram representing synchonous machine in a SMIB system.

Derivation of constants $K_1 \dots K_6$

The constants $K_1 \dots K_6$ shown in Figure 5.5 describe internal influence factors within the system and can be found by a comparison of coefficients with the equations governing the synchronous machine dynamics. While K_1 and K_2 are derived from the computation of the electric torque, K_3 and K_4 have their origin in the field voltage equation (5.87). K_5 and K_6 come from the equation governing the terminal voltage magnitude. Below we will calculate these constants from the previously presented third-order model.

SMIB system setup: The power system under consideration is a so-called "single machine, infinite bus" (SMIB) system. This means that one synchronous generator is connected via a transmission line (represented by series impedance $Z = R + jX$ and shunt admittance $Y = G + jB$) to an "infinite" bus with constant voltage u_0. The generator has a terminal voltage u_t and injects the armature current i via its terminals. For the calculations below, the armature currents i_d and i_q are assumed to be known.

The current and voltage phasors are defined as shown in Figure 5.6. The torque angle δ is defined as the angle between u_0 and the internal voltage e'_q. The following definitions will be used later in the computations:

$$\begin{gathered} i = i_d + j i_q \quad , \quad v_t = v_d + j v_q \quad , \\ 1 + ZY = C_1 + jC_2 \quad , \\ R_1 = R - C_2 x'_d \quad , \quad X_1 = X + C_1 x_q \quad , \\ X_2 = X + C_1 x'_d \quad , \quad R_2 = R - C_2 x_q \quad , \\ Z_e^2 = R_1 R_2 + X_1 X_2 \quad , \\ Y_d = (C_1 X_1 - C_2 R_2)/Z_e^2 \quad , \quad Y_q = (C_1 R_1 + C_2 X_2)/Z_e^2 \quad , \end{gathered} \tag{5.89}$$

The voltages and current in the SMIB system are related to the admittances and impedances by

$$i = Y u_t + Z^{-1}(u_t - u_0) \quad \text{or} \quad Zi = (1 + ZY)u_t - u_0 \quad . \tag{5.90}$$

This can be separated into real and imaginary parts, which yields

$$\begin{bmatrix} R & -X \\ X & R \end{bmatrix} \begin{bmatrix} i_d \\ i_q \end{bmatrix} = \begin{bmatrix} C_1 & -C_2 \\ C_2 & C_1 \end{bmatrix} \begin{bmatrix} u_d \\ u_q \end{bmatrix} - u_0 \begin{bmatrix} \sin\delta \\ \cos\delta \end{bmatrix} \quad , \tag{5.91}$$

where

$$C_1 = 1 + RG - XB \quad , \quad C_2 = XG + RB \quad . \tag{5.92}$$

Now, Equation (5.88) is taken into account with one further simplification: the armature resistance is neglected, i.e. $r_d = r_q = 0$. This can be inserted into Equation (5.91), which yields

$$\begin{bmatrix} i_d \\ i_q \end{bmatrix} = \begin{bmatrix} Y_d \\ Y_q \end{bmatrix} e'_q - \frac{u_0}{Z_e^2} \begin{bmatrix} R_2 & X_1 \\ -X_2 & R_1 \end{bmatrix} \begin{bmatrix} \sin\delta \\ \cos\delta \end{bmatrix} \quad . \tag{5.93}$$

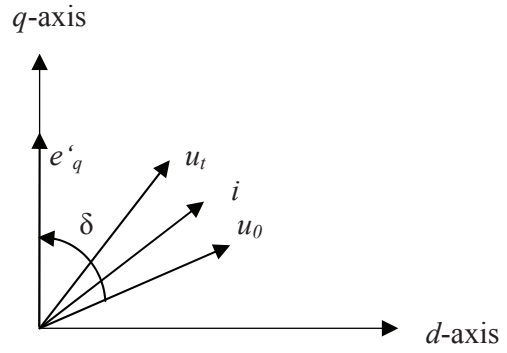

Figure 5.6. Phasor diagram of SMIB system.

This can be linearized again, resulting in

$$\begin{bmatrix} \Delta i_d \\ \Delta i_q \end{bmatrix} = \begin{bmatrix} Y_d \\ Y_q \end{bmatrix} \Delta e'_q + \begin{bmatrix} F_d \\ F_q \end{bmatrix} \Delta\delta \quad , \tag{5.94}$$

with the constants F_d and F_q introduced for abbreviation, which are equal to

$$\begin{bmatrix} F_d \\ F_q \end{bmatrix} = \frac{u_0}{Z_e^2} \begin{bmatrix} -R_2 & X_1 \\ X_2 & R_1 \end{bmatrix} \begin{bmatrix} \cos\delta_0 \\ \sin\delta_0 \end{bmatrix} \quad , \tag{5.95}$$

where δ_0 is the initial torque angle.

Now, the constants $K_1 \ldots K_6$ can be defined in terms of the introduced notation.

K_1 and K_2 from electric torque: The electric torque of a synchronous machine can be approximated by the electric power for small deviations from the synchronous speed. The overall power is the sum of powers in the d- and q-axis:

$$T_e \approx P_e = i_d u_d + i_q u_q \quad . \tag{5.96}$$

Taking into account Equation (5.88) with $r_d = r_q = 0$, Equation (5.96) can be written as

$$T_e = i_q e'_q + (x_q - x'_d) i_d i_q \quad . \tag{5.97}$$

Merging this with Equation (5.94), this yields with one further linearization:

$$\Delta T_e = K_1 \Delta\delta + K_2 \Delta e'_q \quad , \tag{5.98}$$

where the wanted constants K_1 and K_2 are equal to:

$$\begin{bmatrix} K_1 \\ K_2 \end{bmatrix} = \begin{bmatrix} 0 \\ i_{q0} \end{bmatrix} + \begin{bmatrix} F_d & F_q \\ Y_d & Y_q \end{bmatrix} \begin{bmatrix} (x_q - x'_d) i_{q0} \\ e'_{q0} + (x_q - x'_d) i_{d0} \end{bmatrix} \quad . \tag{5.99}$$

K_3 and K_4 from field voltage equation: The field winding circuit voltage equation from (5.84) can be linearized, which yields

$$(1 + s\,T'_{do})\Delta e'_q = -\Delta e_F - (x_d - x'_d)\Delta i_d \quad . \tag{5.100}$$

Substituting Δi_d of Equation (5.94) into this yields

$$(1 + s\,T'_{do}K_3)\Delta e'_q = -K_3(\Delta e_F + K_4\Delta\delta) \tag{5.101}$$

where

$$K_3 = 1/(1 + (x_d - x'_d)Y_d) \tag{5.102}$$
$$K_4 = (x_d - x'_d)F_d \quad . \tag{5.103}$$

K_5 and K_6 from terminal voltage magnitude: The magnitude of the terminal voltage of the generator can be expressed by the d and q components:

$$u_t^2 = u_d^2 + u_q^2 \quad . \tag{5.104}$$

The deviation from a steady state is thus equal to

$$\Delta u_t = (u_{d0}/u_{t0})\Delta u_d + (u_{q0}/u_{t0})\Delta u_q \quad . \tag{5.105}$$

Substituting Equation (5.94) into Equation (5.105) yields

$$\Delta u_t = K_5\Delta\delta + K_6\Delta e'_q \quad , \tag{5.106}$$

where

$$\begin{bmatrix} K_5 \\ K_6 \end{bmatrix} = \begin{bmatrix} 0 \\ u_{q0}/u_{t0} \end{bmatrix} + \begin{bmatrix} F_d & F_q \\ Y_d & Y_q \end{bmatrix} \begin{bmatrix} -x'_d u_{q0}/u_{t0} \\ x_q u_{d0}/u_{t0} \end{bmatrix} \quad . \tag{5.107}$$

Note that all subscripts 0 denote steady-state quantities in this section.

Excitation system parameters: The only missing parameters for the completion of the Heffron-Phillips model are the excitation system parameters K_A and T_A. The corresponding transfer function represents a generic exciter and voltage regulator of the fast-response type. Reasonable values for the parameters are $K_A \approx 50$ and $T_A \approx 0.05$ s.

6
Voltage Control in Power Systems

Having introduced the principal governing equations for the synchronous machine in the previous chapter, this chapter deals with the basics of voltage control in electric power systems. First, the relation between voltage and the reactive power balance is discussed and various influences to this balance are presented. The primary voltage control equipment in the synchronous machine is also discussed and finally a short description of the hierarchical voltage control structure is provided. The following structure is based on [6]

6.1 Relation between voltage and reactive power

As explained in detail in chapters 2 – 4, the active power balance of a power system must be maintained in order to keep the system in steady state. Furthermore, the reactive power balance must be kept in such a way that the voltages are within the acceptable limits. If the active power balance is not kept, the frequency in the system will be influenced, while an improper reactive power balance will result in deviations of the voltages in the system from the desired ones.[1]

Normally the power system is operated such that the voltage drops along the lines are small. The node voltages of the system will then almost be equal (flat voltage profile). In this case the transmission system is effectively used, i.e. primarily for transmission of active power, and not for transmission of reactive power.

Thus, the voltage magnitudes can be controlled to desired values by control of the reactive power. Increased production of reactive power results in higher voltage near the production source, while an increased consumption of reactive power results in lower voltage. While the active power is entirely produced by the generators in the system, there are several sources and sinks of reactive power. On the other hand, the reactive power, in contrast with the active power, cannot be transported over long distances in the system,

[1] The frequency deviation is a consequence of an imbalance between power fed into the system by the prime movers and the electric power consumed by the loads and losses. However, the generated reactive power is always equal to the consumed reactive power, which is a consequence of Kirchhoff's laws. The voltage magnitudes are always adjusted such that this balance is maintained. If the voltages settle at too low values, the reason is that the reactive generation is too small. Vice versa, overvoltages arise when reactive generation is too high. However, this does not mean that the generated and consumed reactive power is not equal as in the case of active power.

since normally $X >> R$ in a power system. Consequently, the reactive power can be regarded as a fairly local quantity.

Important generators of reactive power are:

- Overexcited synchronous machines
- Capacitor banks
- The capacitance of overhead lines and cables
- FACTS devices[2]

Important consumers of reactive power are:

- Inductive static loads
- Underexcited synchronous machines
- Induction motors
- Shunt reactors
- The inductance of overhead lines and cables
- Transformer inductances
- FACTS devices

For some of these, the reactive power is easy to control, while for others it is practically impossible. The reactive power of the synchronous machines is easily controlled by means of the excitation. Switching of shunt capacitors and reactors can also control the reactive power. FACTS devices offer also a possibility to control the reactive power.

It is most effective to compensate the reactive power as close as possible to the reactive load. There are certain high voltage tariffs to encourage large consumers, e.g. industries, and electrical distributions companies to compensate their loads in an effective way. These tariffs are generally designed so that the reactive power is only allowed to reach a certain percentage of the active power. If this percentage is exceeded, the consumer has to pay for the reactive power. The high voltage network is in this way primarily used for transmission of active power.

The reactive losses of power lines and transformers depend on the size of the reactance. For overhead-transmission lines the reactance can be slightly reduced by the use of multiple conductors. The only possibility to radically reduce the total reactance of a transmission line s to connect a series capacitor or a series FACTS device.

[2]FACTS = *Flexible AC Transmission Systems*. FACTS devices are power electronics devices equipped with fast control that can often can be used for reactive power control. They can normally be used both as reactive power sources and sinks. Further discussion of FACTS devices is given in the Section 6.3.4.

6.2 Voltage Control Mechanisms

The following factors influence primarily the voltages in a power system:

- Terminal voltages of synchronous machines
- Impedances of lines
- Transmitted reactive and active power
- Turns ratio of transformers

A suitable use of these leads to the desired voltage profile.

The generators are often operated at constant voltage, by using an automatic voltage regulator (AVR). The output from this controls the excitation of the machine via the electric field exciter. In that way, the voltage can be kept equal to the set value. The voltage drop caused by the generator transformer is sometimes compensated totally or partly by this means, and the voltage can consequently be kept constant on the high voltage side of the transformer. Synchronous compensators can also be installed for voltage control. These are synchronous machines without turbine or mechanical load, which can produce and consume reactive power by controlling the excitation. Nowadays new installations of synchronous compensators are very rare, and power electronics based solutions are preferred if fast voltage control is needed.

The reactive power transmitted over a line has a great impact on the voltage profile. Large reactive transmissions cause large voltage drops, thus these should be avoided. Instead, the production of reactive power should be as close as possible to the reactive loads. This can be made by the excitation of the synchronous machines, as described above. However, there are often no synchronous machines close to the load, so the most cost-effective way is to use shunt capacitors which are switched according to the load variations. A power electronics based device can be economically motivated if fast response or accuracy in the regulation is required. Shunt reactors must sometimes be installed to limit the voltages to reasonable levels. In networks which contain a lot of cables this is also necessary, since the reactive generation from these is much larger than from overhead lines. (C is much larger and X is smaller.)

6.3 Primary Voltage Control

The task of the primary voltage control is to control the reactive output from a device so that the voltage magnitude is kept at or close to the set value of the controller. Usually the node of the controlled voltage is at the same or very close to the node of the reactive device, since reactive power is a fairly local quantity. The set values for the voltage controllers are selected so that the desired voltage profile of the system is obtained. The selection of set values is the task of the secondary voltage control, which is briefly summarized in section 6.4.

In the following the most important devices for reactive power and voltage control are described.

6.3.1 Synchronous Machine Excitation System and AVR

The reactive power output of synchronous machine can for a given active power level be adjusted within the limits of the capability curve by the excitation system. This offers a very efficient and fast way to control the terminal voltage of the machine, which in most power system is the most important voltage control.

The main purpose of the excitation system is to feed the field winding of the synchronous machine with direct current so that the main flux in the rotor is generated. Further, the terminal voltage of the synchronous machine is controlled by the excitation system, which also performs a number of protection and control tasks. A schematic picture of a generator with excitation system is depicted in Figure 6.1. Below, a short description of the functions of the different blocks in Figure 6.1 is given:

- **The exciter** supplies the field winding with direct current and thus comprises the "power part" of the excitation system.

- **The controller** treats and amplifies the input signals to a level and form that is suited for the control of the exciter. Input signals are pure control signals as well as functions for stabilizing the exciter system.

- **The voltage measurement and load compensation unit** measures the terminal voltage of the generator and rectifies and filters it. Further, load compensation can be implemented if the voltage in a point apart from the generator terminals, such as in a fictional point inside the generator's transformer, should be kept constant.

- **The power system stabilizer, PSS**, gives a signal that increases the damping to the controller, cf. Chapter 7. Usual input signals for the PSS are deviations in rotor speed, accelerating power, or voltage frequency.

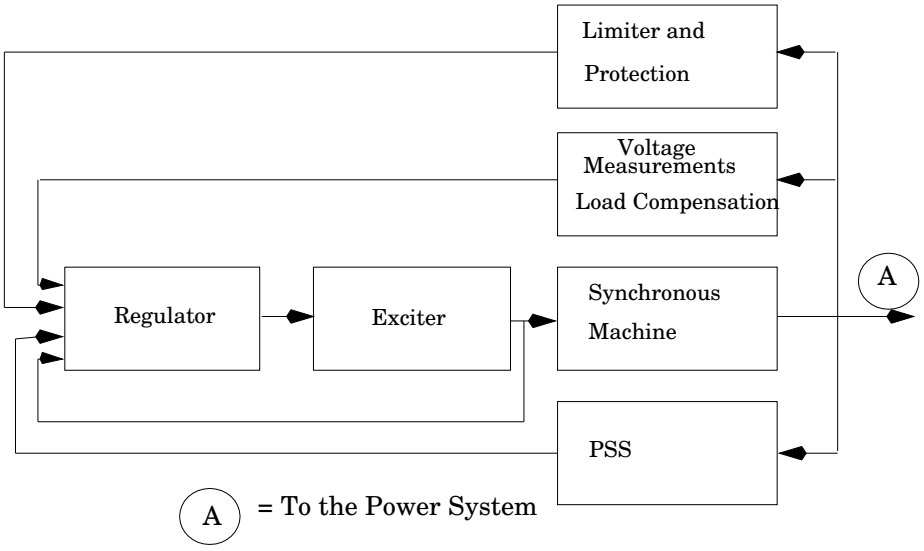

Figure 6.1. Schematic picture of a synchronous machine with excitation system with several control, protection, and supervisory functions.

- **The limiter and protection** can contain a large number of functions that ensure that different physical and thermal limits, which generator and exciter have, are not exceeded. Usual functions are current limiters, over–excitation protection, and under–excitation protection. Many of these ensure that the synchronous machine does not produce or absorb reactive power outside of the limits it is designed for.

Today, a large number of different types of exciter systems is used. Three main types can be distinguished:

- **DC excitation system**, where the exciter is a DC generator, often on the same axis as the rotor of the synchronous machine.

- **AC excitation system**, where the exciter is an AC machine with rectifier.

- **Static excitation system**, where the exciting current is fed from a controlled rectifier that gets its power either directly from the generator terminals or from the power plant's auxiliary power system, normally containing batteries. In the latter case, the synchronous machine can be started against an unenergised net, "black start". The batteries are usually charged from the net.

Below, a more comprehensive treatment of some of the functions described above is given.

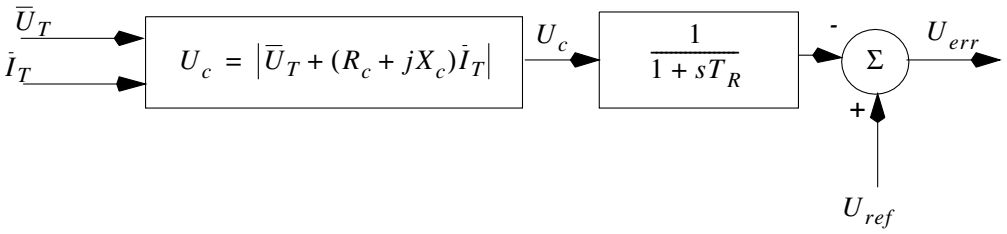

Figure 6.2. Block diagram of compensating circuit.

Load Compensation Equipment

Figure 6.2 shows the block diagram of a compensation circuit, consisting of a converter for measured values, a filter, and a comparator.

There are several reasons for the use of compensation in voltage control of synchronous machines. If two or more generators are connected to the same bus, the compensation equipment can be used to create an artificial impedance between those. That is necessary to distribute the reactive power in an appropriate way between the machines. The voltage is measured "somewhat inside" the generator, corresponding to positive values of R_c and X_c in Figure 6.2. If a machine is connected with a comparatively large impedance to the system, which usually is the case since the generator's transformer normally has an impedance in the order of magnitude of 10% on basis of the machine, it can be desirable to compensate a part of this impedance by controlling the voltage "somewhat inside" of that impedance. This then corresponds to negative values of R_c and X_c. As a rule, X_c is much larger than R_c.

DC Excitation Systems

Today, hardly any DC excitation systems are being installed, but many of these systems are still in operation. Generally, it can be said that there is a large number of variants of the different excitation systems listed above. Every manufacturer uses its own design, and demands that depend on the application often lead to considerable differences in the detailed models of the devices in each group. Here, typical examples for models will be given. In reality, the models given by the manufacturers and power suppliers must be used. One example of a DC excitation system, the IEEE type DC1 system, is given in Figure 6.3. The input signal for the controller is the voltage error U_{err} from the compensation equipment. The stabilizing feedback U_F is subtracted, and sometimes a signal from the PSS is added. Both these signals vanish in steady state. The controller is mainly described by the dominating time constant T_A and the amplification K_A. The limits can represent saturation effects or limitations of the power supply. The time

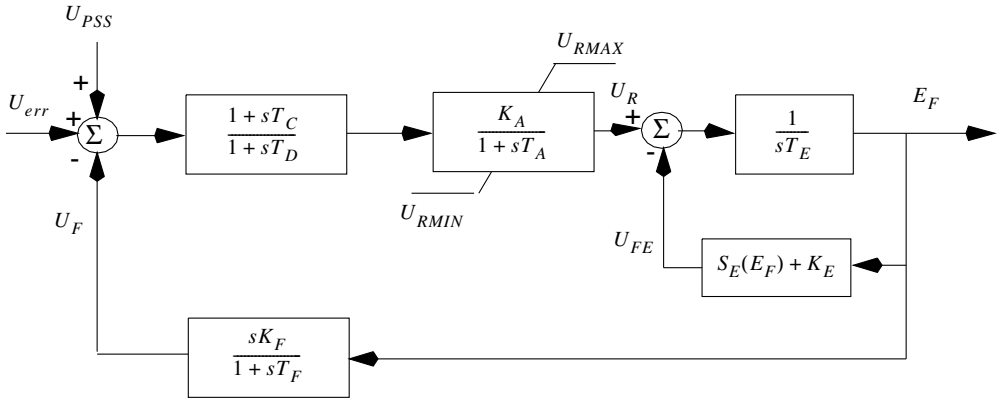

Figure 6.3. Model of DC exciter system (IEEE Type DC1).

constants T_C and T_D can be used to model internal time constants in the controller. These are often small and can then usually be neglected.

The output signal from the voltage controller, U_R, controls the exciter. The exciter consists of a DC machine that can be excited independently or shunt excited. For shunt excited machines, the parameter K_E models the setting of the field regulator. The term S_E represents the saturation of the exciter and is a function of the exciter's output voltage, E_F. If saturation is neglected, that is $S_E = 0$, the effective time constant of the exciter becomes T_E/K_E, and its effective amplification is $1/K_E$.

AC Excitation Systems

For AC excitation systems, the exciter consists of a smaller synchronous machine that feeds the exciter winding through a rectifier. The output voltage of the exciter is in this case influenced by the loading. To represent these effects, the exciter current is used as an input signal in the model. In Figure 6.4, an example of a model of AC exciter systems is shown (IEEE type AC1). The structure of the model is basically the same as for the DC excitation system. Some functions have been added. The rectifier of the exciter prevents (for most exciters) the exciter current from being negative. The feedback with the constant K_D represents the reduction of the flux caused by a rising field current I_F. That constant depends on the synchronous and transient reactances of the exciter. The voltage drop inside the rectifier is described by the constant K_C, and its characteristic is described by F_{EX}, which is a function of the load current.

DC and AC excitation systems are sometimes called rotating exciters, since they contain rotating machines. That distinguishes them from static excitation systems, which are described in the sequel.

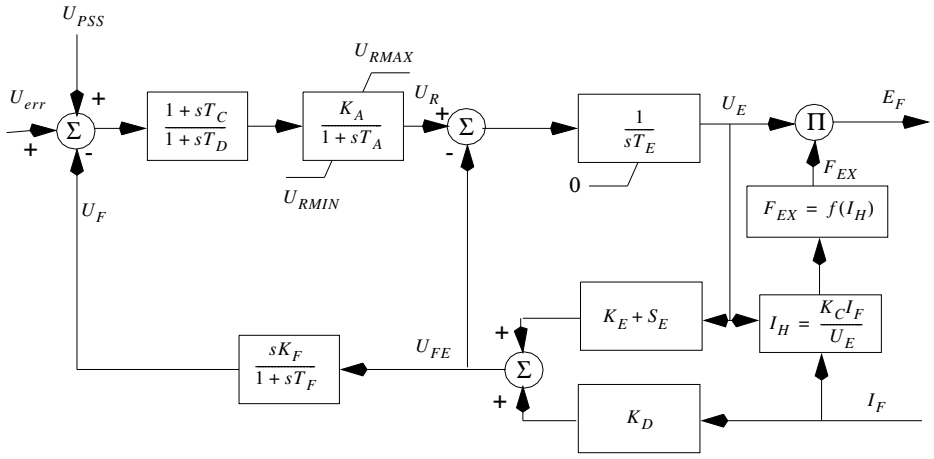

Figure 6.4. Model of an AC exciter system (IEEE Type AC1).

Static Excitation Systems

In static excitation systems, the exciter winding is fed through a transformer and a controlled rectifier. By far most exciter systems installed today are of that type, and a large number of variants exists. The primary voltage source can be a voltage transformer that is connected to the generator terminals, but even a combination of voltage and current transformers can be found. With the latter arrangement, an exciter current can be obtained even if the voltage at the generator terminals is low, for example during a ground fault in or near the power plant. Sometimes, it is possible to supplement these voltage sources by using the auxiliary power of the power plant as voltage source. That makes it possible to start the generator in an unenergised net. An example of a model of a static exciter system is shown in Figure 6.5.

Static excitation systems can often deliver negative field voltage and even negative field current. However, the maximum negative field current is usually considerably lower than the maximum positive field current.

The time constants are often so small that a stabilizing feedback is not needed. The constant K_F can then be set to zero. Since the exciter system is normally supplied directly from the generator bus, the maximum exciter voltage depends on the generator's output voltage (and possibly its current). This is modelled by the dependency of the limitations of the exciter output on the generator's output voltage. The constant K_C represents the relative voltage drop in the rectifier.

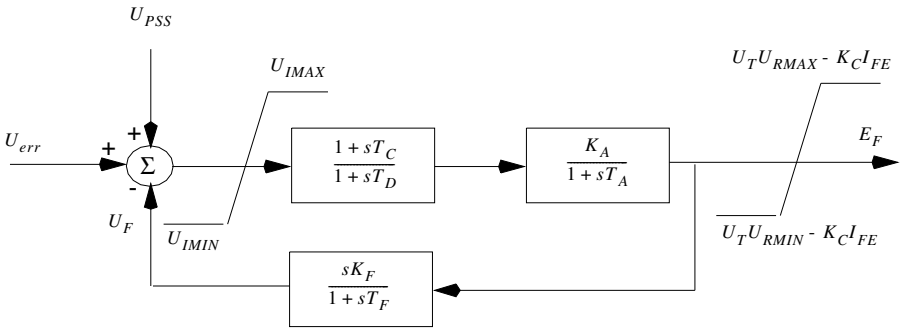

Figure 6.5. Model of a static exciter system.

6.3.2 Reactive Shunt Devices

In many systems, the reactive control capabilities of the synchronous machines are not sufficient to keep the voltage magnitudes within prescribed limits at all loading conditions. The varied loading condition of the system during low and peak load situations implies that the reactive power needed to keep the desired voltage magnitudes vary significantly. It is impossible and also unwise to use the reactive power capabilities of synchronous machines to compensate for this, since many synchronous machines will be driven to their capability limits, and the fast and continuous reactive power control offered by the synchronous machine will not be available. Therefore, in most systems, breaker-switched shunt capacitor banks and shunt reactors are used for a coarse control of reactive power, so that the synchronous generators can be used for the fast and continuous control.

Generally shunt capacitors are switched on during high-load conditions, when the reactive consumption from loads and line reactances is the highest. Since these load variations are rather slow and predictable, no fast control is needed and the capacitor banks can be breaker switched. In systems with long high-voltage lines, the reactive power generation of these lines can be very high during light load conditions. To keep the voltages at acceptable levels, shunt reactors might be needed. The sizes of the reactive shunt elements determine how accurate the control can be. Capacitor banks, in particular, can often be switched in smaller units, while shunt reactors are most often installed in one single unit, because of high costs. A factor limiting the element size is the transient voltage change resulting from switching. The fundamental frequency voltage change in pu caused by switching a shunt element can be estimated as $\Delta V = Q_{\text{shunt}}/S_{\text{sc}}$, where Q_{shunt} is the size of the shunt element and S_{sc} is the short-circuit power at the node.

Reactive shunt elements are also used for reactive power and voltage control at HVDC terminal stations. Since typically a line commutated HVDC converter station consumes about 50% as much reactive power as active

power transmitted, reactive compensation is needed. Part of the reactive compensation is usually provided by harmonic filters needed to limit the harmonic current injection into the ac networks. These filters are almost purely capacitive at fundamental frequency.

6.3.3 Transformer Tap Changer Control

An important method for controlling the voltage in power systems is by changing the turns ratio of transformers. Certain transformers are equipped with a number of taps on one of the windings. Voltage control can be obtained by switching between these taps, as illustrated in Figure 6.6. Switching during operation by means of tap changers is very effective and useful for voltage control. Normally, the taps are placed on the high-voltage winding (the upper side), since then lower currents needs to be switched.

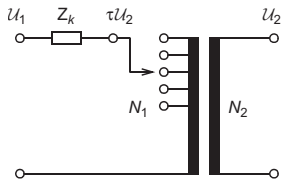

Figure 6.6. Transformer with a variable turns ratio (tap changer).

If N_1 is the number of turns on the high-voltage side and N_2 is the number of turns on the low-voltage side, the turns ratio of transformer is defined as

$$\tau = \frac{N_1}{N_2} \quad . \tag{6.1}$$

Then, the relation between the voltage phasors on the high-voltage side U_1 and on the low-voltage side U_2, at no load, is

$$U_2 = \frac{U_1}{\tau} \quad . \tag{6.2}$$

If the voltage decreases on the high-voltage side, the voltage on the lower side can be kept constant by decreasing, that is, by switching out a number of windings on the high-voltage side. When the transformer is loaded, equation (6.2) is of course incorrect, since the load current yields a voltage drop over the leakage reactance of the transformer Z_k , but the same principle can still be applied for voltage control.

Transformers with automatic tap changer control are often used for voltage control in distribution networks. The voltage at the consumer side can therefore be kept fairly constant even though voltage variations occur on the high-voltage network. Time constants in these regulators are typically in the

order of tenths of seconds. In some transformers, the turns ratio cannot be changed during operation, but just manually when the transformer is unloaded. In this case, voltage variations in the network cannot be controlled, with voltage levels changing in large steps.

6.3.4 FACTS Controllers

As previously mentioned, power electronics-based equipment, usually referred to as FACTS controllers or devices, can be used for fast voltage and reactive power control. The first devices introduced were based on thyristors as active elements, but more recently, devices using voltage source converters have been introduced; with the latter, a faster and more powerful control can be achieved. FACTS devices used for voltage control are connected in shunt. Two such devices are discussed here: the Static var compensator (SVC), and the STATic synchronous COMpensator (STATCOM). The SVC is based on thyristors, while the STATCOM is based on a voltage source converter. There are also series-connected FACTS devices that in principle can be used for voltage control, but the main reason for installing these devices is to control active power, which indirectly influences voltages. Among these devices, the unified power flow controller (UPFC) is equipped with a shunt part for voltage control, which basically operates as a STATCOM.

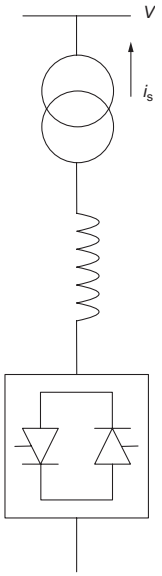

Figure 6.7. Thyristor controlled reactor.

Static Var Compensator

The SVC may be composed of two different shunt elements, that is, a thyristor controlled reactor (TCR) and thyristor switched capacitor (TSC) banks. If fast switching of the capacitor banks is not needed, one can also use breaker-switched capacitors. The TCR is depicted in Figure 6.7 by delaying the firing of the thyristors, a continuous control of the current through the reactor can be obtained, with the reactive power consumption varying between 0 and V^2/X, where X is the reactance of the reactor. By combining the TCR with a suitable number of capacitor banks, a continuous control of the reactive power can be achieved by a combination of capacitor bank switching and control of the reactor current. Usually, the TCR and TSC are connected to the high-voltage grid through a transformer, as shown in Figure 6.8. The control system of the SVC controls the reactive output so that the voltage magnitude of the controlled node is kept constant. Usually, a certain slope is introduced in the control, as shown in Figure 6.9, which shows the reactive current as a function of the voltage. In the (almost) horizontal part of the curve, around the voltage set point, the SVC control is active. When the SVC has reached its maximum or minimum reactive output, the voltage cannot be controlled, and the device will behave as a pure reactor or pure capacitor; thus, in extreme voltage situations, the SVC behaves as a reactor or capacitor bank. The control of the reactor current is based on thyristors, which limits the bandwidth of the voltage control. If a fast control is needed to compensate for flicker and voltage dips, one has to use technologies based on voltage source converters.

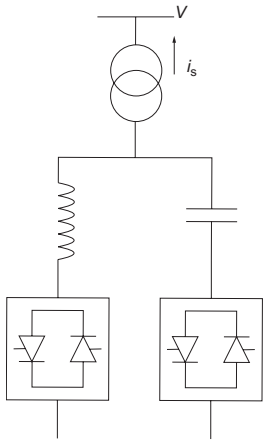

Figure 6.8. Static var compensator.

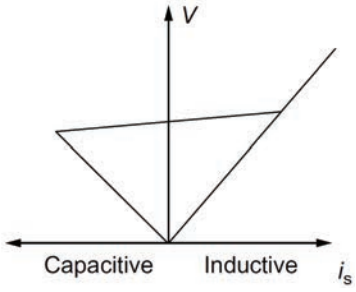

Figure 6.9. Static var compensator control.

STATCOM

The STATCOM is a device which is based on a voltage source converter. The device is connected in shunt and consists of a capacitor charged with a dc voltage, which provides the input voltage for a voltage source converter, as illustrated in Figure 6.10. The converter feeds a reactive current into the network, and by controlling this reactive current, voltage control is achieved. Since a voltage source converter needs semiconductor elements with current interrupting capabilities, thyristors cannot be used; instead, elements such as GTOs or IGBTs have to be used.

In comparison with the SVC, the STATCOM offers two advantages. First, the STATCOM's output reactive current is not limited at low- or high-voltage conditions; rather, the output current is only limited by the converter ratings and is not dependent on the system voltage. This means that the reactive support during extreme voltage situations is much better with respect to the SVC, as shown in Figure 6.11. Second, the control response is much faster, since it is limited by the switching frequency of the voltage source converter (usually around 1 kHz). The STATCOM can hence be used to reduce flicker and other fast voltage variations effectively. The dc capacitor of the voltage source converter constitutes an active power storage; hence, an active current can also be injected into the network. The STATCOM can thus also be used for active power control (example, to damp power oscillations). However, the energy stored in the dc capacitor is fairly small; therefore, to truly control the active power output, a battery must be installed on the dc side.

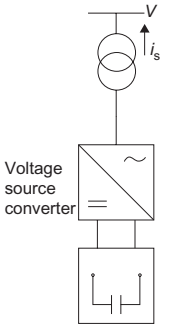

Figure 6.10. STATCOM.

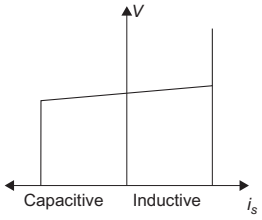

Figure 6.11. Voltage control and reactive capability of a STATCOM.

6.4 Secondary Voltage Control

As previously discussed, balancing the reactive power via AVRs and other devices can be considered a local control action. Hence in case of a disturbance, the devices electrically nearby will try to compensate the reactive power needs. This may result in unacceptable voltage values and an uneven reactive power distribution over the generators. This creates the need of a coordinated adjustment of the setpoints of the reactive power suppliers.

Secondary Voltage Regulation (SVR) has been developed to address the above mentioned situation. SVR is a hierarchical, centralized voltage control scheme that supervises the generator AVRs and other reactive power sources in a given network zone so as to enhance voltage stability of the grid. Figure 6.12 illustrates the basic setup. In each zone, a 'pilot' node is selected and controlled typically by the participating generators so as to maintain the voltage of the pilot node at a specific value, by delivering the reactive power proportionally to their own capabilities.

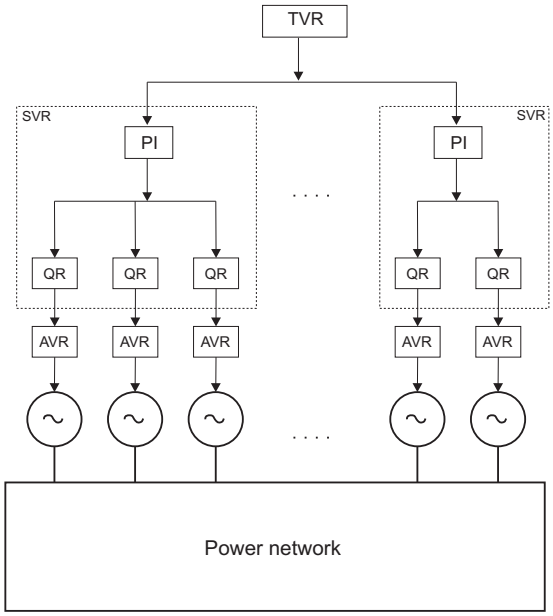

Figure 6.12. Structure of the voltage regulation.

Therefore the AVR is enhanced with two additional control levels. The higher level is responsible for the voltage control of the 'pilot' node. The voltage error serves as input to a proportional-integral controller (PI) and the generated signal is then used by each generator at a lower control level. The latter corresponds to a local reactive power regulator (QR) that adjusts the input of the AVR with respect to the generator capability. A similar hierarchy applies also in the time constants of each control level in order to

avoid any interaction among them. The AVR time constant is in the order of 0.5 sec, the QR time constant is in the order of 5 sec, whereas the time constant of the PI controller is in the order of 50 sec.

The scheme can be further enhanced with the use of Tertiary Voltage Regulation (TVR) which, based on an overall system economic optimization, will determine the setpoints of the above mentioned PI controller in a time scale of 15 minutes.

The described secondary closed-loop control scheme is already implemented in some European power grids, particularly in France and in Italy (since the early 1980's). Other countries still follow an open-loop strategy, in which the operator adjusts the setpoints manually with an expected performance degradation.

7
Stability of Power Systems

In this chapter, factors influencing the stability of electric power systems are discussed. First, a short introduction to damping in a power system is given. Different sources of positive and negative damping are discussed, and methods to improve the damping are given. Furthermore, the effect of the loads on system stability is regarded in the second part of this chapter.

7.1 Damping in Power Systems

7.1.1 General

What damping in the context of electro–mechanical oscillations in a power system means is quite self–evident. Normally, two different kinds of electrical torques appear at a generator rotor that is oscillating: a synchronizing torque ΔT_s and a damping torque ΔT_d. The synchronizing torque ΔT_s is in phase with the deviation in rotor angle $\Delta\theta$, whereas the damping torque ΔT_d is in phase with the deviation in rotor speed $\Delta\omega$. The synchronizing torque, also called the synchronizing power, strives, if it is positive, to bring the rotor back to the stable equilibrium in which the mechanical power is equal to the electrical power. When the generator has reached an operating point where the synchronizing power no longer can return the system to the stable equilibrium, the generator will fall out of phase. The variation of the synchronizing torque with the rotor angle determines, together with the machine's moment of inertia, the frequency of rotor oscillations. The partitioning into synchronizing and damping torque is shown in Figure 7.1.

Damping is neglected in the classical model. Therefore, the system will, after a disturbance, either fall out of phase (instability) or oscillate with unchanged amplitude. This is not realistic, since real systems contain damping. The damping torque depends on the time derivative of the rotor angle in such a way that the oscillation is damped. Normally, the damping torque is rather small and thus influences the oscillation frequency only marginally. It mainly influences the amplitude. In a synchronous machine, the main contributors to damping are the damper windings and the field winding.

If the modes of oscillation in a system are determined by computing the eigenvalues of the linearised system's Jacobian matrix, changes in the synchronizing and damping torques will become apparent as follows: An increase of the synchronizing torque moves the eigenvalue parallel to the

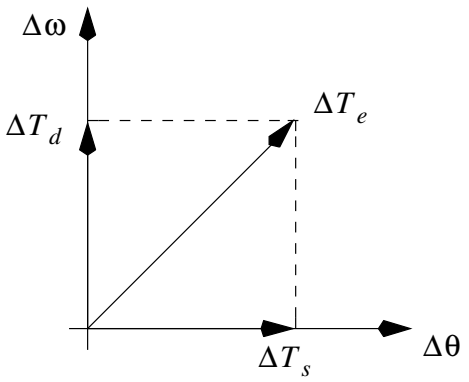

Figure 7.1. Partitioning of electrical torque in synchronizing and damping components.

imaginary axis towards larger values. This corresponds to an increase in the spring constant in a mechanical analogy. If the damping torque is increased instead, the eigenvalue will move parallel to the real axis to the left. In the classical model, all eigenvalues will be situated on the imaginary axis. Necessary for stability is that no eigenvalues are situated in the right half plane. This corresponds to positive ΔT_s as well as positive ΔT_d in Figure 7.1.

7.1.2 Causes of Damping

As mentioned earlier, the internal damping of a generator comes from the windings in the rotor circuit. That damping is determined by phases and amplitudes of the oscillating torques caused by induced currents in exciter winding and damping windings. Further, some loads contribute with positive damping. These contributions originate from the frequency dependency of the loads, but also their voltage dependency contributes.

Generally, the inner damping of the generators decreases with decreasing frequency of the oscillations. The currents in the damping windings decay, and hence, for very slow oscillations, their contribution is small.

Low or negative damping in a power system can lead to spontaneous appearance of large power oscillations. This can, in the worst case, necessitate tripping of lines and it must be avoided. That type of instability is called small signal instability or instability caused by low damping. (Earlier, that type of instability was called dynamic instability.)

A common reason for low damping is the use of voltage controllers with high gain. That was experienced in generators feeding a strong net through a line. Such a configuration can also be analyzed comparably easily. It can be shown that an eigenvalue with positive real part can occur when large amounts of power are transmitted and voltage controllers with high gains are used. Before the reason behind this phenomenon was known, the problem was solved by operating the generator with manual voltage control, or by

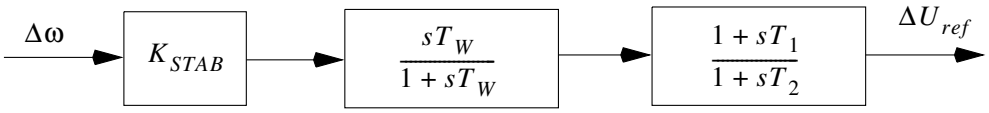

Figure 7.2. Block Diagram of a simple PSS.

making the voltage controller slower or decreasing its gain.

To explain that mechanism in detail is beyond the scope of this compendium, but in summary, it can be said that the rotor angle influences the generator voltage, which through the voltage controller influences the transient emf, which influences the electrical torque. Now it turns out that, when the load on the machine is high, the phase angle can be such that a contribution with negative damping is obtained. If the amplification in the voltage controller is high, that negative contribution can be significant.

7.1.3 Methods to Increase Damping

Several methods for increasing the damping in a power system are available. The simplest and usually cheapest way is the installation of power system stabilizers, PSS, in the generators. The operating principle for these is very simple. To increase the damping in the system, a signal is added to the reference voltage of the generator's voltage controller. The phase of this signal should of course be such that it results in a positive contribution to the damping. Thus, the same physical mechanism in the system of generator and voltage controller that above resulted in negative damping is used to obtain positive damping.

Such a power system stabilizer usually utilizes the rotor deviation from the synchronous frequency $\Delta\omega$ as input signal. Sometimes, other signals that contain the same information can be used, like P_e or T_e. A diagram illustrating the principle mode of operation of a PSS is given in Figure 7.2. The input signal, in this case $\Delta\omega$, first passes a high–pass filter to ensure that permanent frequency deviations do not contribute. The next filter shifts the phase appropriately for the critical oscillation frequency so that a positive contribution to damping is obtained. The constant K_{stab} determines the size of that contribution. That constant should of course not be chosen larger than necessary to obtain the needed damping, since this could lead to undesired side effects.

Other possibilities for increasing the damping in a system are different types of controllable equipment that may be installed in the system, such as HVDC (High Voltage Direct Current) or SVC (Static Voltage Condensers). These components can often give large contributions to damping, but they are usually too expensive to install them only to increase the damping, and the existing equipment is not always located optimally for damping purposes.

7.2 Load Modelling

Since, neglecting losses, an equal amount of power is consumed in the loads in the system as is generated in the generators, the load characteristics are on principle just as important for the system properties as the generators. That is, however, not reflected in the level of detail and the accuracy usually used in load models for analyzing system stability. This chapter discusses briefly how load characteristics influence the system stability and which problems arise in the derivation of appropriate load models. The most common load models are presented.

7.2.1 The Importance of the Loads for System Stability

The characteristics of the loads influence the system stability and dynamics in many different ways. The voltage characteristics of the loads have a direct influence on the accelerating power for generators nearby and are thus very important for the behaviour during the first oscillation after a fault. It has been shown in section 2.1.2 that the frequency dependency of the loads influences directly how large the frequency deviation after different system disturbances will become. The frequency dependency of the loads also influences the system damping. The same is true for their voltage dependency since it influences the voltage control.

This compendium concentrates on what is usually called angular stability, or synchronous stability, that is, the ability of the generators to stay synchronized after disturbances. Another important property of a power system is the ability to keep the voltages in the system within acceptable limits during disturbances. This is a measure for the voltage stability of the system. Voltage stability is highly dependent on the balance of reactive power in the system, but also the active power has some influence here. It is obvious that the voltage dependency of the loads is of high importance for the system's voltage stability.

It is for several reasons difficult to derive good load models. (Of course, deriving models for single load objects is formally not very difficult. Loads here are, however, lumped loads as they are perceived from a bus in the high voltage grid.) First, it is difficult to estimate the composition of the loads, since it varies during the day as well as during the year. Further, this composition varies from bus to bus. Thus, sometimes different load models have to be used at different buses, depending on the composition of the loads, for example industrial loads, domestic loads, and rural loads.

7.2.2 Load Models

For studies of angular stability, loads are usually modelled with static models. Sometimes, large induction motors have to be represented individually

by special models to obtain the correct dynamic behaviour. Dynamic load models for lumped loads have begun to be used during the last few years, especially for studying voltage stability, but those are expected to be used in the future more widely and even for other types of studies.

Static Load Models

For traditional stability studies, where the investigated time frame is at most around 10 s after the disturbance, the most commonly used model types are static models. They are called static since they describe the load using only algebraic equations. The modelled load dynamics are in these cases so fast that they can be considered instantaneous compared with other phenomena, like rotor oscillations, that are modelled. The most common model for voltage dependency is

$$\begin{aligned} P &= P_0 \left(\frac{U}{U_0}\right)^{\alpha} \quad , \\ Q &= Q_0 \left(\frac{U}{U_0}\right)^{\beta} \quad . \end{aligned} \tag{7.1}$$

However, the load can also be modelled as an arbitrary polynomial in (U/U_0),

$$P = P_0 \sum_i k_i \left(\frac{U}{U_0}\right)^{\alpha_i} \quad . \tag{7.2}$$

In Equations (7.1) and (7.2), U_0 is the nominal voltage at nominal load, P_0 and Q_0. In Equations (7.1), the voltage exponents α and β are often different.

If $\alpha = 0$, the load is called constant power load; if $\alpha = 1$, it is called constant current load; and if $\alpha = 2$, it is a constant impedance load. It is very common to model the (active) load for stability studies as consisting of these three parts. Usually, a somewhat larger voltage exponent is used for the reactive load.

Some examples for the voltage exponents of different loads are:
Electric heating: $\alpha = 2$, $Q = 0$.
Light bulbs: $\alpha \approx 1,6$, $Q = 0$.
Fluorescent tubes: $\alpha \approx 0,9$, $\beta \approx 2$.
To be able to include active and reactive losses in the underlying distribution grid, the above models have to be modified.

A load model often used is the so called *ZIP–Model*. The ZIP-Model is a special case of the model in Equation (7.2), which contains three terms with:

- $\alpha_1 = 2$, i.e. constant impedance (Z) load

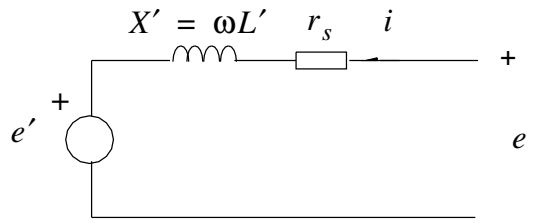

Figure 7.3. Representation of induction motor.

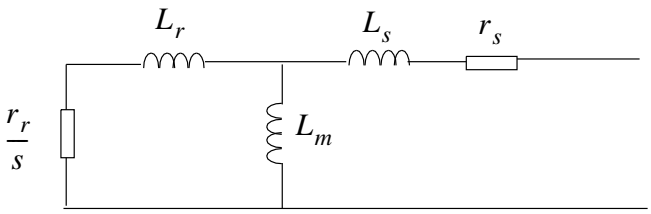

Figure 7.4. Equivalent circuit for induction motor.

- $\alpha_2 = 1$, i.e. constant current (I) load
- $\alpha_3 = 0$, constant power (P) load

Motor Loads

Around half of all electric power used by the industry is used for operation of motors. Sometimes, the load in certain nodes is dominated by electric motors. It can then be justified to model those explicitly.

For small changes in voltage, a motor load behaves approximately like a constant power load. For larger voltage changes, it can be necessary to use a more accurate representation. Synchronous machines are then modelled according to the models derived in Chapter 5, with the mechanical part P_m depending on the characteristic of the mechanical load. A large part of the motor load consists of induction motors that can be modelled as follows: An induction motor is basically a synchronous machine with short–circuited exciter coil. If the exciter coil rotates with an angular speed different from the rotating fluxes generated by the three phase coils, a current that generates a flux is induced in the exciter coil. Between the rotating synchronous flux generated in the phase windings and the flux from the exciter winding, energy is exchanged. This is the basis for the function of the induction motor.

The induction motor can, according to Figure 7.3, be described by a voltage source behind an impedance. The value of L' can be obtained from the equivalent circuit of the induction motor shown in Figure 7.4.

In Figure 7.4
r_s and L_s are the stator resistance and inductance,
L_m is the magnetizing inductance,
r_r and L_r are rotor resistance and inductance.

The slip s is defined by

$$s = \frac{\omega_0 - \omega}{\omega_0} \tag{7.3}$$

and thus L' is given by

$$L' = L_s + \frac{L_m L_r}{L_m + L_r} \ . \tag{7.4}$$

The dynamics are described by

$$\frac{de'}{dt} + \frac{1}{\tau'_0}(e' + j\omega_0(L_s + L_m - L')i) + j\omega_0 s e' = 0 \ , \tag{7.5}$$

$$i = \frac{e - e'}{r_s + j\omega_0 L'} \ , \tag{7.6}$$

$$\frac{d\omega}{dt} = \frac{1}{2H_m}(T_e - T_l) \ , \tag{7.7}$$

$$T_e = \Re(e' \cdot i^*) \ . \tag{7.8}$$

Here,
ω is the machine's angular speed,
ω_0 is the system's angular speed,
T_l is the load torque,
$\tau'_0 = (L_r + L_m)/r_r$ are no load operation constants.

Equivalent Dynamic Loads

The load models presented above are, as mentioned, valid for studying phenomena that do not last longer than about ten seconds after a disturbance. If phenomena taking place in a longer time frame should be studied, slow dynamics in the system have to be accounted for. These dynamics originate mainly from two different sources: The tap changers installed at lower voltage levels that try to restore the voltage to the desired value and the controllers installed at the loads.

The control of tap changers can be done in several different ways, but common to most systems are that tap changers are stepped, typically in intervals of some tens of seconds, until the voltage is restored . Since this control exists at different voltage levels (cascade coupled controllers), undesirable overshoots in the control can occur if the control loops are not coordinated. Generally, the control has to be slower the lower the voltage level is.

In Sweden, a large part of the load, at least in winter, consists in many areas of heating loads. The changes in this type of load are determined by thermostats. Hence, it takes some time until, for example, a voltage drop becomes apparent. That time is determined by the thermal time constants for what is heated, such as houses, and by the design of the thermostats.

Summarizing, it can be said that the dynamics determined by tap–changer control and load dynamics are highly complicated. Measurements are needed to get reliable results. Measurements of load characteristics have during the last few years become very important, and much work is being done in many utilities to investigate load characteristics under different loading conditions.

A typical example of a load behaviour after a voltage drop is shown in Figure 7.5. It is clearly visible how the load drops momentarily, as described by the load models from Section 7.2.2, to recover later to a considerably higher level. A rather general description is given by

$$T_p \frac{dP_r}{dt} + P_r = P_s(U) - P_t(U) \ , \tag{7.9}$$

$$P_l(t) = P_r + P_t(U) \ , \tag{7.10}$$

where
$P_r(t)$ is a state variable,
$P_s(U)$ is a static model for the long term load behaviour,
$P_t(U)$ is a static model for the transient load behaviour,
$P_l(t)$ is the value of the active load at the time t.
Of course, $U = U(t)$ in the equations above.

For the reactive load, similar behaviour and equations are valid.

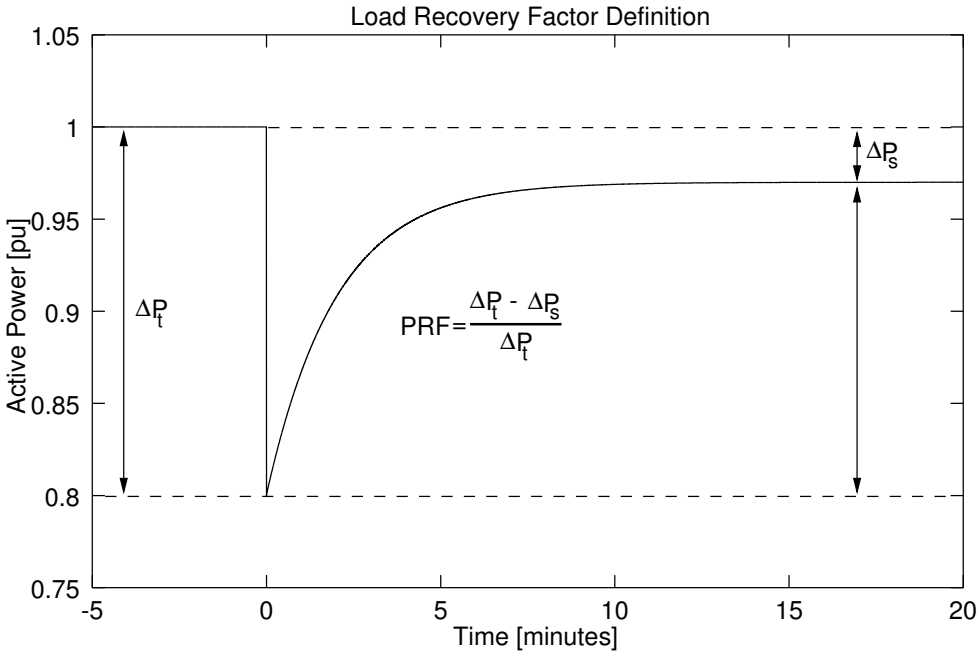

Figure 7.5. The Transient Behaviour of the Load in Equations (7.9) and (7.10) after a Step in the Voltage.

References

[1] P. Kundur: Power System Stability and Control, McGraw-Hill Inc., New York, 1994 (ISBN 0-07-035958-X).

[2] Dynamic Models for Steam and Hydro Turbines in Power System Studies, *IEEE Trans. Power Appar. Syst.* 1904-1915, Nov./Dec. 1973.

[3] G. Andersson: Modelling and Analysis of Electric Power Systems, *ETH Zurich*, 2009.

[4] W.G. Heffron and P.A. Phillips: Effect of modern aplidyne voltage regulator on under-excited operation of large turbine generators, *Trans. Am. Inst. Electr. Eng.*, Part 3, 71, 692 – 697, 1952. As cited in: Yao-Nan Yu, Electric Power System Dynamics, *Academic Press*, 1983.

[5] A.R. Bergen and V. Vittal: Power System Analysis, Second Edition, *Prentice Hall*, 2000.

[6] A. Gomez-Exposito, A. J. Conejo and C. Canizares: Electric Energy Systems: Analysis and Operation, *CRC Press*, 2009.

Appendix A
Connection between per unit and SI Units for the Swing Equation

If nothing else is given after a quantity, that quantity is in SI–units. If a quantity is expressed in per unit, p.u. is given in brackets after the quantity (p.u.). For simplicity, it is assumed that the nominal electrical and mechanical frequencies are equal, (rad/s).

In SI–units,

$$J\,\frac{d^2\theta}{dt^2} = \Delta T \quad , \tag{A.1}$$

with
J = moment of inertia for rotor turbine (kgm^2),
θ = angle (rad),
ω = angular velocity (rad/s),
ΔT = effective torque on the rotor turbine (Nm).

When using electrical degrees, Equation (A.1) is usually written as

$$\frac{M}{\omega_0}\cdot\frac{d^2\theta}{dt^2} = \Delta T \quad , \tag{A.2}$$

with
M = moment of inertia = $J\omega_0\frac{180}{\pi}$ (Js/el°).
The H-factor, or constant of inertia, for synchronous machine i is defined by

$$H_i = \frac{\frac{1}{2}J\omega_0^2}{S_i} \quad , \tag{A.3}$$

with
H_i = constant of inertia for synchronous machine i (s),
S_i = rated power of synchronous machine.
The per unit base for torques at synchronous machine i, $T_{bas,i}$, is given by

$$T_{bas,i} = \frac{S_i}{\omega_0} \quad , \tag{A.4}$$

leading to

$$\Delta T = \Delta T(p.u.)\frac{S_i}{\omega_0} \quad . \tag{A.5}$$

Using (A.3) and (A.5), (A.1) can be written as

$$\frac{2H_iS_i}{\omega_0^2}\cdot\frac{d^2\theta}{dt^2} = \frac{S_i}{\omega_0}\,\Delta T(p.u) \quad , \tag{A.6}$$

or

$$\frac{d^2\theta}{dt^2} = \frac{\omega_0}{2H_i}\,\Delta T(p.u) \quad . \tag{A.7}$$

Equation (A.7) can also be written as

$$\frac{d}{dt}(\dot{\theta}) = \frac{\omega_0}{2H_i}\Delta T(p.u) \quad , \tag{A.8}$$

which is the same as

$$\frac{d}{dt}(\omega) = \frac{\omega_0}{2H_i}\Delta T(p.u) \quad , \tag{A.9}$$

or

$$\frac{d}{dt}(\omega(p.u.)) = \frac{\Delta T(p.u)}{2H_i} \quad . \tag{A.10}$$

Generally,

$$P = T\omega_m \quad , \tag{A.11}$$

with the actual mechanical angular speed of the rotor ω_m that, according to the assumptions, is equal to the electrical angular speed ω. With the equations above, this gives

$$P(p.u) = T(p.u)\,\omega(p.u) \quad . \tag{A.12}$$

Equation (A.10) now becomes

$$\dot{\omega}(p.u.) = \frac{\Delta P(p.u.)}{2H_i} \cdot \frac{1}{\omega(p.u.)} \quad . \tag{A.13}$$

For rotor oscillations, $\omega(p.u.) \approx 1$ and (A.13) can be approximated by

$$\dot{\omega}(p.u.) = \frac{\Delta P(p.u.)}{2H_i} \quad , \tag{A.14}$$

or

$$\dot{\omega} = \frac{\omega_0}{2H_i}\Delta P(p.u.) \quad . \tag{A.15}$$

The most common equations in literature are (A.9), (A.10), (A.14), and (A.15). Of these, (A.9) and (A.10) are exact if ω is the actual angular frequency. Equations (A.14) and (A.15) are good approximations as long as $\omega \approx \omega_0$. That is valid for "normal" oscillations in power systems.

Appendix B
Influence of Rotor Oscillations on the Curve Shape

If the relative movement between the field winding of a synchronous machine and its phase windings is a purely rotating motion with constant angular speed, the resulting induced voltages in the phase windings will be shaped ideally like a sinusoid. From now on, it is assumed that the field winding is in the rotor, while the phase windings are on the stator, but since the relative motion determines the voltage in the phase windings, it is even possible to think of stationary field windings and rotating phase windings. In all modern larger synchronous machines, the field winding is on the rotor, so the assumption above does have a practical background. However, almost all relationships and conclusions are independent of this assumption.

For simplicity, consider a single phase synchronous machine according to Figure B.1. A three phase machine has two more phase windings shifted $\pm 120^\circ$ relative to the phase winding in the figure. The phase winding and the exciter winding are arranged so that the flux linkage through the phase winding is sinusoidally shaped as a function of the angle θ_m in Figure B.1:

$$\Phi(t) = \Phi_0 \cos\theta_m = \Phi_0 \cos\omega_0 t \quad , \tag{B.1}$$

with the angular speed of the rotor ω_0 according to the system's electrical frequency. That flux induces a voltage in the phase winding that is given by

$$U(t) = \frac{d\Phi}{dt} = -\Phi_0\,\omega_0 \sin\omega_0 t = -\hat{U}\sin\omega_0 t \quad . \tag{B.2}$$

Now, we shall study how the flux linkage through the phase windings will be influenced when rotor oscillations appear in the system. If the balance between power into the generator and power from the generator, i.e. between mechanical torque and electrical power, is disturbed, the rotor will start to oscillate relative to an undisturbed reference rotor that continues to rotate with the angular speed ω_0. The rotor position can generally be described by

$$\theta_m(t) = \omega_0 t + \theta(t) \quad , \tag{B.3}$$

where $\theta(t)$ is a solution of the swing equation. It has earlier been mentioned that stable solutions of the swing equation for a synchronous machine connected to a strong grid consist of oscillations that are nearly sinusoidal with frequencies on the order of magnitude of some tenths of a Hertz to some

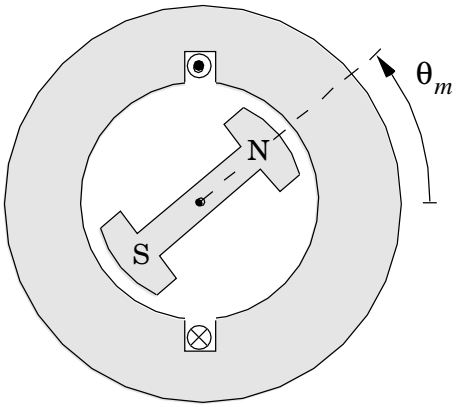

Figure B.1. Schematic picture of single phase synchronous machine.

Hertz. To investigate how the linked flux, and thus the voltage and the current, look during an oscillatory movement, a rotor motion according to

$$\theta_m(t) = \omega_0 t + \mu \sin(\omega_r t + \theta_r) \ , \tag{B.4}$$

with the angular speed ω_r corresponding to the oscillation frequency and the amplitude of the oscillatory movement μ, is assumed. The flux linkage can now be written as

$$\Phi(t) = \Phi_0 \cos\theta_m(t) = \Phi_0 \cos(\omega_0 t + \mu \sin(\omega_r t + \theta_r)) \ , \tag{B.5}$$

which implies that the oscillatory movement contains a phase–angle modulation of the flux linkage. The momentary angular frequency, $\Omega(t)$, is defined for $\Psi(t)$ as

$$\Omega(t) = \frac{d}{dt}(\omega_0 t + \mu \sin(\omega_r t + \theta_r)) \tag{B.6}$$

and varies between $\omega_0 + \mu\omega_r$ and $\omega_0 - \mu\omega_r$. It can be shown (cf. text books on modulation theory) that Equation (B.5) can be written as

$$\Phi(t) = \Phi_0 \sum_{n=-\infty}^{n=\infty} J_n(\mu) \cos((\omega_0 + n\omega_r)t + n\theta_r) \ . \tag{B.7}$$

$J_n(\mu)$ is a Bessel function of the first kind with the argument μ and degree n, as given by

$$J_n(\mu) = \frac{1}{\pi} \int_{-\pi}^{\pi} \cos(\mu \sin x - nx) dx \ . \tag{B.8}$$

An important property of $J_n(\mu)$ that will be used later is

$$J_{-n}(\mu) = (-1)^n J_n(\mu) \ . \tag{B.9}$$

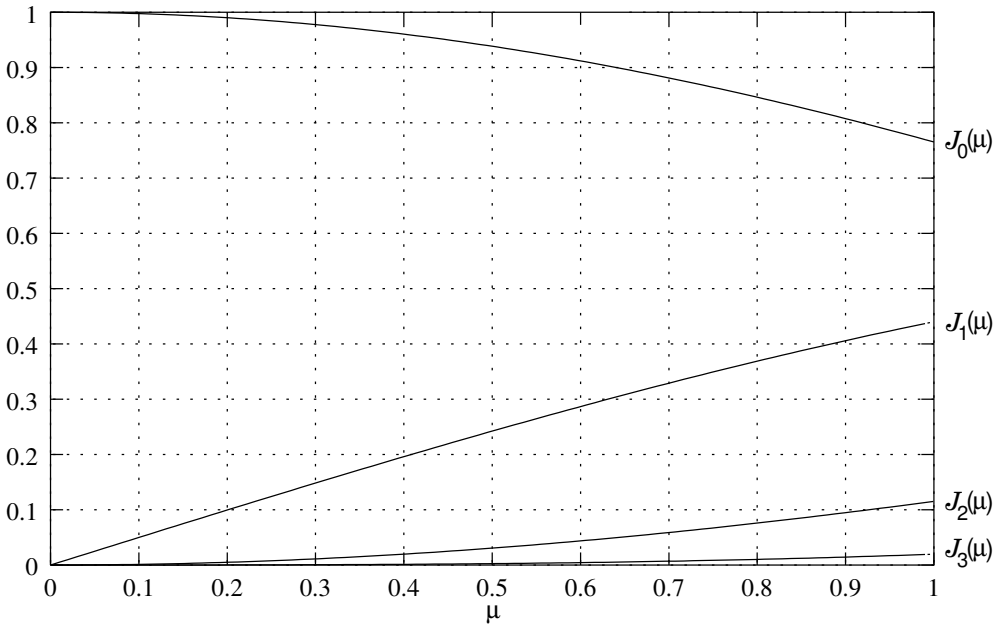

Figure B.2. Bessel functions of the first kind of order 0 to 3.

From Equation (B.7) follows that, in spite of that the momentary angular frequency for $\Phi(t)$ is between $\omega_0+\mu\omega_r$ and $\omega_0-\mu\omega_r$, $\Phi(t)$ will have infinitely many side bands with the frequencies $\omega_0 \pm n\omega_r$ beside the fundamental frequency ω_0. A relevant question is how large the amplitudes of these side bands are. Generally, the coefficients $J_n(\mu)$ decay rapidly when the order n becomes larger than the argument μ. In Figure B.2, values for the first four Bessel functions are shown for the argument μ between 0 and 1. It should be observed that μ is measured in radians, so that 1 corresponds to approximately 57°, which in this context is quite a large amplitude. Figure B.2 shows that side bands with $n = 3$ and larger can be neglected even for amplitudes as large as $\mu = 1$. $\Phi(t)$ can thus be approximated quite accurately by

$$\Phi(t) \approx \Phi_0 \sum_{n=-2}^{n=2} J_n(\mu) \cos((\omega_0 + n\omega_r)t + n\theta_r) \quad . \tag{B.10}$$

Typical oscillation frequencies are, in most cases considerably, lower than 3 Hz, so that practically the whole energy spectrum for $\Phi(t)$ lies in the frequency area $f_0 \pm 6$ Hz, i.e. 50(60) $\pm$ 6 Hz. This justifies the usual representation of the grid with the traditional phasor model with a constant frequency corresponding to f_0.

If the amplitude is very small, say less than $\mu \approx 0.2$, corresponding to an amplitude of approximately 10°, side bands with $n = 2$ and higher can

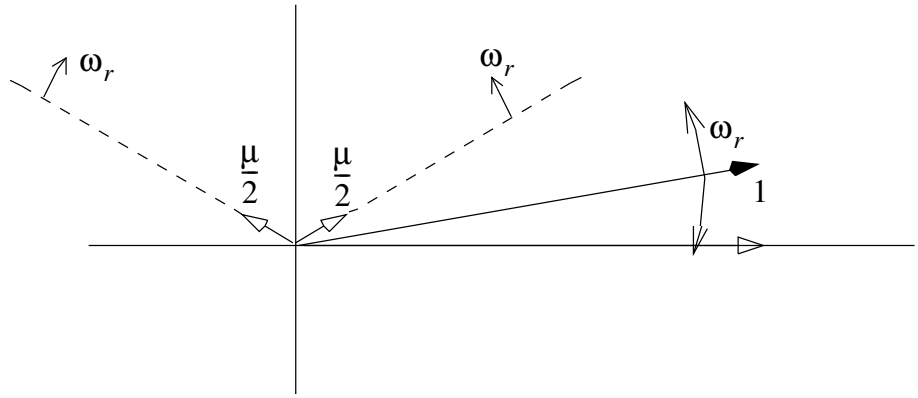

Figure B.3. Vector with superimposed oscillation, according to the text.

be neglected, see Figure B.2. Further, it can be shown that, if μ is small,

$$\begin{aligned} J_0(\mu) &\approx 1 - \frac{\mu^2}{4} \ , \\ J_1(\mu) &\approx \frac{\mu}{2} \ , \end{aligned} \tag{B.11}$$

are valid, and $\Phi(t)$ can be written as

$$\Phi(t) \approx \Phi_0((1-\frac{\mu^2}{4})\cos\omega_0 t + \frac{\mu}{2}\cos((\omega_0+\omega_r)t+\theta_r) - \frac{\mu}{2}\cos((\omega_0-\omega_r)t-\theta_r)) \ . \tag{B.12}$$

Equation (B.9) has here been used. That approximation is used even in a context of power system analysis other than rotor oscillations, namely when studying so–called subsynchronous oscillations, SSO. If there is a resonance phenomenon at a subsynchronous frequency it is called subsynchronous resonance, SSR. The most common cause of SSO are torsional oscillations on the axis connecting the turbine(s) and the generator rotor. The frequencies of the natural oscillations on that axis are typically 5 Hz and higher. (For an axis with n distinct "masses", including generator rotor and, maybe, exciter, there are $n-1$ different eigenfrequencies.) For the side band in Equation (B.12), i.e. for $\omega_0 \pm \omega_r$, the frequency can deviate significantly from the nominal frequency, so that it is normally not possible to look only at the component with nominal frequency. Since the electrical damping for the lower side band, the subsynchronous frequency, can be negative, due to, for example, series compensation, the partitioning according to Equation (B.12) has to be kept. The damping in the upper side band, the supersynchronous frequency, is almost always positive.

To increase the understanding for the partitioning in Equation (B.12), a more intuitive derivation than the stringent mathematical one using Bessel

functions can be given. Consider a vector with amplitude 1 that performs small oscillations with an angular frequency ω_r and amplitude μ. This can be illustrated geometrically according to Figure B.3. The vector with filled arrowhead oscillates symmetrically around the horizontal axis with the frequency ω_r and the amplitude μ. That vector can now be partitioned into the three vectors with unfilled arrowheads. One vector does not move and lies along the horizontal axis. Two vectors with amplitude $\mu/2$ rotate with the angular frequency $\pm\omega_r$ according to Figure B.3. It is easily observed that the sum of the vectors with hollow arrowhead is at all times equal to the vector with filled arrowhead. Since the vectors rotate with the angular frequency ω_0 with respect to a stationary system, Equation (B.12) is obtained directly from the projection of the vectors on to the horizontal axis, with the modification that the factor for the fundamental frequency is one.